



NTNU – Trondheim
Norwegian University of
Science and Technology

Sequence Stratigraphic Correlation of the Tor Field

Trygve Andreas Elind

Earth Sciences and Petroleum Engineering

Submission date: June 2012

Supervisor: Mai Britt E. Mørk, IGB

Co-supervisor: Lutz Seiffert, TOTAL E&P NORGE AS

Norwegian University of Science and Technology
Department of Geology and Mineral Resources Engineering

Abstract

A new sequence stratigraphic correlation of the Tor Field has been created in this MSc thesis.

The lithostratigraphic correlation currently used by the Tor Field operator ConocoPhillips for reservoir characterization, has been criticized by Total E&P Norge because: (a) it is mainly based on the porosity curve derived from wireline logs (b) it displays random thickness variations, which can not be explained with faults visible on seismic.

The presented correlation of the Tor Field is based on the principle of sequence stratigraphic correlation. Six Tor Field wells were previously correlated as a part of a regional study by Gennaro et al. (2011) and became the principle reference for the new correlation. Other previous correlations of the Tor Field were also reviewed and considered. The new correlation used composite logs instead of just the derived porosity log. In addition, a biostratigraphic study of two Tor Field wells by Lottaroli and Catrullo (2000) was included to support the new correlation.

The new correlation proved to be more uniform in terms of interval thickness and the remaining thickness changes could be better explained, compared to the lithostratigraphic correlation. The interval thickness trends that are found in new correlation are more consistent than earlier. A repeated section in well 2/5-2 was identified with the help of the biostratigraphy from Lottaroli and Catrullo (2000) and the affected markers were modified.

This new sequence stratigraphic correlation will be tested by Total E&P Norge in a revision of their reservoir characterization model and dynamic simulation model.

Sammendrag

En ny sekvensstratigrafisk korrelasjon av Tor feltet har blitt utført i denne Masteroppgaven.

Den litostratigrafiske korrelasjonen som for øyeblikket benyttes av operatørselskapet ConocoPhillips til å beskrive reservoaret, har blitt kritisert fordi: (a) den hovedsaklig baserer seg på porositets logger (b) de ulike enhetende har tilsynelatende tilfeldige variasjoner i tykkelse, som ikke kan forklares med forkastninger som er synlige på seismikken.

Den presenterte korrelasjonen av Tor feltet er basert på prinsippene om sekvensstratigrafisk korrelasjon. En tidligere korrelasjon av seks brønner på Tor feltet, fra en regional studie av Gennaro et al. (2011), ble brukt som et utgangspunkt for den nye korrelasjonen. Flere andre tidligere korrelasjoner av Tor feltet ble også nøye gjennomgått og vurdert. Den nye korrelasjonen benyttet ”orginale” kompositt logger, istedenfor utregnete porositets logger. Itillegg ble en biostratigrafisk studie av to brønner (Lottaroli og Catrullo, 2000) inkludert for å støtte opp den nye korrelasjonen.

Den nye korrelasjonen viste seg å ha en mer ensartet tykkelse av reseroarintervallene, samtidig som gjenværende variasjoner i tykkelse kunne forklares bedre, sammenlignet med dagens litostratigrafiske korrelasjon. I den nye korrelasjonen er trendene av intervaltykkelse mer konsekvente enn tidligere. Biostratigrafien fra Lottaroli og Catrullo (2000) gjorde det mulig å identifisere en repetert seksjon i brønn 2/5-2 og endre de berørte markørene.

Denne nye sekvensstratigrafiske korrelasjonen skal bli testet av Total E&P Norge i en ny utgave av deres statiske og dynamiske reservoar modell.

Acknowledgments

I would like to thank my main advisor Dr. Mai Britt Engeness Mørk at the Department of Geology and Mineral Resources Engineering at NTNU for providing literature, reviewing my work and giving me helpful advice. Thank you for your positive attitude and for believing in me.

A very special thanks to my advisor in Total E&P Norge, Senior-geologist Lutz Seiffert. Thank you for creating and planning this project, and for all your help and feedback. You always took the time to help and to check in on me, even though you were extremely busy. This thesis would not have been made without you, thank you. I also want to thank Total E&P Norge for giving me the opportunity to write my MSc thesis for the company in the Stavanger office, for providing me with accommodation and for offering me a trainee-position in the company after finishing my MSc degree. I am truly grateful.

Thanks to Dr. Matteo Gennaro (ConocoPhillips Norge), who took the time to answer my questions and give me very helpful advice regarding the correlation.

Thanks to all my fellow students, colleagues and friends at both NTNU and Total E&P Norge for making my time as an university student truly memorable. I would like to thank my family for always supporting and encouraging me. To my dear Thea, thank you for all your love, support and patience.

List of Figures

2.1	Illustration of the earth at the time boundary between the Cretaceous and Tertiary (K-T), 65 million years ago.	3
2.2	SEM image of a coccosphere.	5
2.3	Illustration of chalk depositional systems.	6
2.4	Table with cyclic sequence types and their corresponding durations.	7
2.5	Picture of 3 core sections with different facies from well 2/4-7 at the Tor Field.	8
2.6	Illustration of chalk resedimentation mechanisms and depositional fabrics. .	10
2.7	Map of the Central Graben displaying the main oilfields, the main structural elements and zones.	11
2.8	Map of the the Tor Fm. in the Central Graben displaying the main oilfields, the main structural elements, Facies distribution and sediment transport directions.	12
2.9	Map of the the Lower Ekofisk Member in the Central Graben displaying the main oilfields, the main structural elements, Facies distribution and sediment transport directions.	13
2.10	3D view of the Tor Field seen from the South-SouthWest.	14
3.1	Lithostratigraphic subdivision of the Upper Cretaceous - Lower Paleocene strata in the Norwegian Central North Sea with two different nomenclatures, and corresponding sea-level curve.	17
3.2	The lithostratigraphic markers used in the current reservoir correlation at the Tor Field.	18
3.3	Table of the stratigraphic markers used in this well correlation.	19
3.4	Different classifications of bio-zonation with corresponding age and biostratigraphy in well 2/5-2.	20
4.1	Map with the position of the wells at the Tor Field.	22
4.2	Well 2/4-8, with all sequence stratigraphic markers.	23
4.3	Log signature, top Ekofisk marker, well 2/4-7.	24
4.4	Isochore map of the Ekofisk interval	25
4.5	Log signature, Eko 90 marker, well 2/4-E-10.	26
4.6	Log signature, Eko 90 marker, well 2/4-E-12 T2.	26
4.7	Isochore map of the Eko 90 interval	27
4.8	Log signature, Eko 80 marker, well 2/4-E-10.	28
4.9	Isochore map of the Eko 80 interval	29
4.10	Log signature, Eko 70 marker, well 2/4-E-10.	30
4.11	Log signature, Eko 70 marker, well 2/4-8.	30
4.12	Isochore map of the Eko 70 interval	31
4.13	Log signature, Eko 60 marker, well 2/4-E-14.	32
4.14	Isochore map of the Eko 60 interval	33
4.15	Log signature, Eko 50 marker, well 2/4-8.	34

4.16	Isochore map of the Eko 50 interval	35
4.17	Log signature, Eko 40 marker, well 2/4-E-10.	36
4.18	Log signature, Eko 40 marker, well 2/4-E-2 A.	36
4.19	Isochore map of the Eko 40 interval	37
4.20	Log signature, Eko 30 marker, well 2/5-1.	38
4.21	Log signature, Eko 30 marker, well 2/4-E-14.	38
4.22	Isochore map of the Eko 30 interval	39
4.23	Log signature, Eko 20 marker, well 2/4-8.	40
4.24	Log signature, Eko 20 marker, well 2/4-7.	40
4.25	Isochore map of the Eko 20 interval	41
4.26	Log signature, Eko 10 marker, well 2/4-7.	42
4.27	Isochore map of the Eko 10 interval	43
4.28	Log signature, Eko 5 marker, well 2/4-E-14.	44
4.29	Isochore map of the Eko 5 interval	45
4.30	Log signature, Tor marker, well 2/4-8.	46
4.31	Log signature, Tor marker, well 2/4-E-14.	46
4.32	Isochore map of the Tor interval	47
4.33	Log signature, Tor 05 marker, well 2/4-E-10.	48
4.34	Log signature, Tor 05 marker, well 2/5-2.	48
4.35	Isochore map of the Tor 05 interval	49
4.36	Log signature, Tor 10 marker, well 2/4-E-10.	50
4.37	Log signature, Tor 10 marker, well 2/4-8.	50
4.38	Isochore map of the Tor 10 interval	51
4.39	Log signature, Tor 15 marker, well 2/4-E-10.	52
4.40	Log signature, Tor 15 marker, well 2/4-E-2.	52
4.41	Isochore map of the Tor 15 interval	53
4.42	Log signature, Tor 20 marker, well 2/4-8.	54
4.43	Log signature, Tor 20 marker, well 2/4-E-2.	54
4.44	Isochore map of the Tor 20 interval	55
4.45	Log signature, Tor 30 marker, well 2/4-8.	56
4.46	Log signature, Tor 30 marker, well 2/4-7.	56
4.47	Isochore map of the Tor 30 interval	57
4.48	Log signature, Tor 40 marker, well 2/5-1.	58
4.49	Log signature, Tor 40 marker, well 2/4-E-14 A.	58
4.50	Isochore map of the Tor 40 interval	59
4.51	Log signature, Tor 50 marker, well 2/4-8.	60
4.52	Isochore map of the Tor 50 interval	61
4.53	Log signature, Tor 60 marker, well 2/4-8.	62
4.54	Log signature, Tor 60 marker, well 2/5-1.	62
4.55	Isochore map of the Tor 60 interval	63
4.56	Log signature, Tor 70 marker, well 2/4-8.	64
4.57	Log signature, Tor 70 marker, well 2/4-E-5.	64
4.58	Map displaying the path of the well section with the "type wells".	65

4.59	Map displaying the path of 3 well sections, crossing the Tor Field from West to East.	67
4.60	Map displaying the path of the 4 well sections, crossing the Tor Field from North to South.	69
5.1	Log display of Type Well 2/4-E-14, before and after the Eko 90 marker was modified.	71
5.2	Log display of Type Well 2/5-2, before and after re-interpretation of the Upper Ekofisk Formation.	72
5.3	Log display of a large interval in well 2/4-8, with stratigraphic markers from both the new correlation and the currently used lithostratigraphic correlation	74
5.4	Log display of the Eko 50 (equivalent of EM4-EL2) interval in well 2/4-8 .	75
5.5	Comparison of isochore maps (example from the Ekofisk Formation). . . .	76
5.6	Log display of the Tor 10 (equivalent of TM3a-TM4) interval in well 2/4-E-10	77
5.7	Comparison of isochore maps (example from the Tor Formation).	78
A.1	Well section, West-East, with correlation of the Type Wells. A3 Foldout. .	III
A.2	Well section, West-East across the Middle of the Tor Field, with correlation of the wells. A3 Foldout.	V
A.3	Well section, West-East across the Southern part of the Tor Field, with correlation of the wells. A3 Foldout.	VII
A.4	Well section, West-East across the Northern part of the Tor Field, with correlation of the wells. A3 Foldout.	IX
A.5	Well section, North-South across the Western part of the Tor Field, with correlation of the wells. A3 Foldout.	XI
A.6	Well section, North-South across the middle part of the Tor Field, with correlation of the wells. A3 Foldout.	XIII
A.7	Well section, North-South across the Eastern part of the central Tor Field, with correlation of the wells. A3 Foldout.	XV
A.8	Well section, North-South across the Eastern-most part of the Tor Field, with correlation of the wells. A3 Foldout.	XVII

Contents

Abstract	i
Acknowledgements	iii
List of Figures	vii
1 Objective of the project	1
2 Introduction	3
2.1 Geological Setting	3
2.2 Composition of the Chalk	4
2.3 Depositional processes of Chalk	6
2.3.1 Primary pelagic sedimentation, autochthonous chalk	7
2.3.2 Resedimentation, allochthonous chalk	8
2.4 Structural evolution and the influence of local tectonics on the chalk distribution	10
2.5 The Tor Field	14
3 Methodology	17
3.1 Lithostratigraphy	17
3.2 Sequence Stratigraphy	18
3.3 Biostratigraphy	20
4 Observations and Results	21
4.1 The sequence stratigraphic markers	21
4.1.1 Top Ekofisk	24
4.1.2 Eko 90	26
4.1.3 Eko 80	28
4.1.4 Eko 70	30
4.1.5 Eko 60	32
4.1.6 Eko 50	34
4.1.7 Eko 40	36
4.1.8 Eko 30	38
4.1.9 Eko 20	40
4.1.10 Eko 10	42
4.1.11 Eko 5	44
4.1.12 Top Tor	46
4.1.13 Tor 05	48
4.1.14 Tor 10	50
4.1.15 Tor 15	52
4.1.16 Tor 20	54
4.1.17 Tor 30	56
4.1.18 Tor 40	58
4.1.19 Tor 50	60

4.1.20	Tor 60	62
4.1.21	Tor 70	64
4.2	Well sections	65
4.2.1	Type wells, West - East well section	65
4.2.2	Middle of the Tor Field, West - East well section	66
4.2.3	Southern part of the Tor Field, West - East well section	66
4.2.4	Northern part of the Tor Field, West - East well section	66
4.2.5	Western part of the Tor Field, North - South well section	68
4.2.6	Middle part of the Tor Field, North - South well section	68
4.2.7	Central-Eastern part of the Tor Field, North - South well section	68
4.2.8	Eastern part of the Tor Field, North - South well section	68
5	Discussion	71
6	Conclusion	79
	References	80
A	Appendices	I

1 Objective of the project

This MSc Thesis is written by Trygve A. Elind during the Spring-semester of 2012, for the Norwegian University of Science & Technology, in cooperation with Total E&P Norge.

A major redevelopment plan (Tor II) for the Tor Field, with the purpose of increasing the recovery of the remaining resources, is currently being evaluated. The objective of this MSc thesis is to create a new and improved correlation of the reservoir units in the Tor Field, which might replace the current subdivision. At the moment, a lithostratigraphic correlation based mainly on porosity derived from wireline data, is being used to correlate the different flow units within the chalk reservoir.

In this project, the author will conduct a sequence stratigraphic correlation of the Ekofisk and Tor formations in all the wells of the Tor Field. The correlation will be based on a regional sequence stratigraphic correlation of the Central Graben, from a PhD thesis by Gennaro et al. (2011) . In addition, a biostratigraphic study by ENI-Agip (Lottaroli and Catrullo, 2000) will be integrated into the new correlation.

During the autumn of 2011, the author conducted a literature study on the Chalk in the Norwegian sector of the Central North Sea as a preparation project to this MSc Thesis, focusing on depositional environments, structural evolution and reservoir quality (Elind, 2011). Selected sections of the literature study are included in Chapter 2 of this thesis.

2 Introduction

2.1 Geological Setting

The name of the time-period Cretaceous is derived from the Latin word "creta", which denotes a white fine-grained limestone, i.e. chalk (Brekke and Olaussen, 2006). During the Cretaceous, the continued break-up of the Supercontinent Pangea went from being predominantly caused by rifting into being more influenced by ocean floor spreading. The rifting activity in the Central Graben decreased, but the continued extension and creation of new oceanic crust further West led to the birth of the Atlantic Ocean. Although it was little tectonic activity in the northern Europe during the Late Cretaceous, there were some pulses of compression and inversion related to the Laramide, Alpine and Pyrenean Orogeny as well as halokinetic movement of Permian salt (Bramwell et al., 1999; Surlyk et al., 2003). These movements in the subsurface influenced the chalk deposition and structural evolution in the central North Sea.

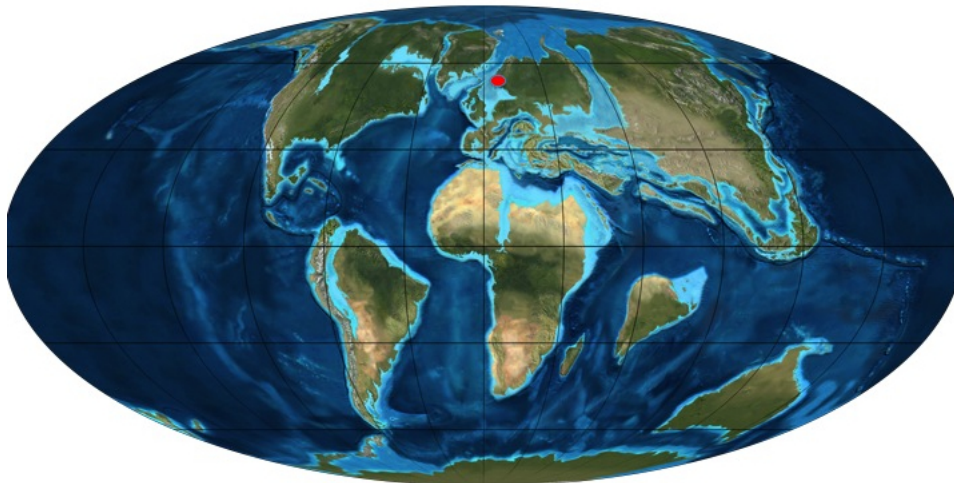


Figure 2.1: *Illustration of the earth at the time boundary between the Cretaceous and Tertiary (K-T), 65 million years ago. The light blue color represents continental shelves and dark blue oceanic crust. Norway is marked with a red dot. Illustration by R. Blakley from <http://jan.ucc.nau.edu/rcb7/65moll.jpg>.*

In the Late Cretaceous, the earth went through a "greenhouse" phase. Estimations suggests that the global average paleo-temperature was approximately 10°C higher than today and the paleo-sea level in western Europe could have been almost 350m higher than what it is today (Schatzinger et al., 1985; Brekke and Olaussen, 2006). This made the ocean cover much of the continental surface in the North Sea area at the time (Figure 2.1), creating large shallow paleo-continental shelves with favorable living conditions for algae. Long distances from terrigenous sediment sources at the time led to deposition of calcareous sediment, which filled in the rift basins and evened out the sea floor relief (Surlyk et al., 2003; Brekke and Olaussen, 2006).

The Central Graben is the southernmost branch of the North Sea triple rift system and was formed by rifting in the North Sea area from the Late Permian/Early Triassic until the Early Cretaceous (Friedman, 1996). Throughout the Cretaceous and Tertiary, the rapid subsidence continued and several thousand meter of sediments were deposited in the basins (D’Heur, 1984). Within this thick sequence of sediments, the chalks of the Chalk Group and the reservoirs of many Norwegian oilfields are located.

Deposition of chalk in the North Sea took place during late Cretaceous and the early Paleocene. The succession of deposits from that period in the Central Graben, is dominated by chalk with maximum thickness exceeding 1500m. Further north than 59°N, a mudstone-dominated succession with maximum thickness around 2000m were deposited during the same period of time (Spencer et al., 1996; Surlyk et al., 2003). The chalk deposition in the North Sea region ended with a tectonic event, related to the opening of the Norwegian - Greenland Sea (63-60 million years ago), which altered the oceanic circulation and the clastic sediment influx (Schatzinger et al., 1985).

2.2 Composition of the Chalk

The generally accepted definition of Chalk according to Kennedy (1985) is *friable to well-cemented biomicrites built up mainly of the debris of planktonic haptophycean algae known as coccolithophorids*. The micron scaled debris consists mainly of low magnesian calcite platelets (0.25-1.0 μ m in diameter) arranged as oval disks (2-20 μ m in diameter) with a hole in the center, called coccoliths (Kennedy, 1985; Friedman, 1996; Brekke and Olaussen, 2006). Multiple coccoliths were originally attached to the membrane of the algae, forming a protective spherical skeleton called a coccosphere (Figure 2.2) (Kennedy, 1985; Brekke and Olaussen, 2006). Coccoliths were produced throughout the life of each alga and they may have been shed periodically (Kennedy, 1985). When the coccolithophorid died, the coccoliths detached from the alga membrane and sunk to the sea floor (Brekke and Olaussen, 2006). Due to the small size of the coccoliths, it is suggested that in order to reach the sea floor by gravitational settling, the coccoliths were eaten by marine plankton feeders and reached the seabed in fecal pellets.(Kennedy, 1980, 1985).

Micropaleontological analysis of cores clearly shows a distinct break in the coccolith flora at the Maastrichtian-Danian boundary and that extensive resedimentation of coccoliths occurred during the Paleocene (Ofstad, 1980). The reason for the distinct break in the coccolith flora was the Cretaceous-Tertiary mass extinction, which only a few species of coccolithophorids survived (Surlyk et al., 2003). These species had coccoliths consisting of smaller platelets than before the extinction, which resulted in smaller pore-throats and lower matrix permeability in the Danian chalks than in the Upper Cretaceous chalks (Kennedy, 1985).

In addition to the coccoliths, chalks in the Chalk Group contain subordinate carbonate debris from calcispheres, single celled foraminifers and larger bioclasts, as well as non-carbonate material such as authigenic minerals, siliceous organisms and terrigenous

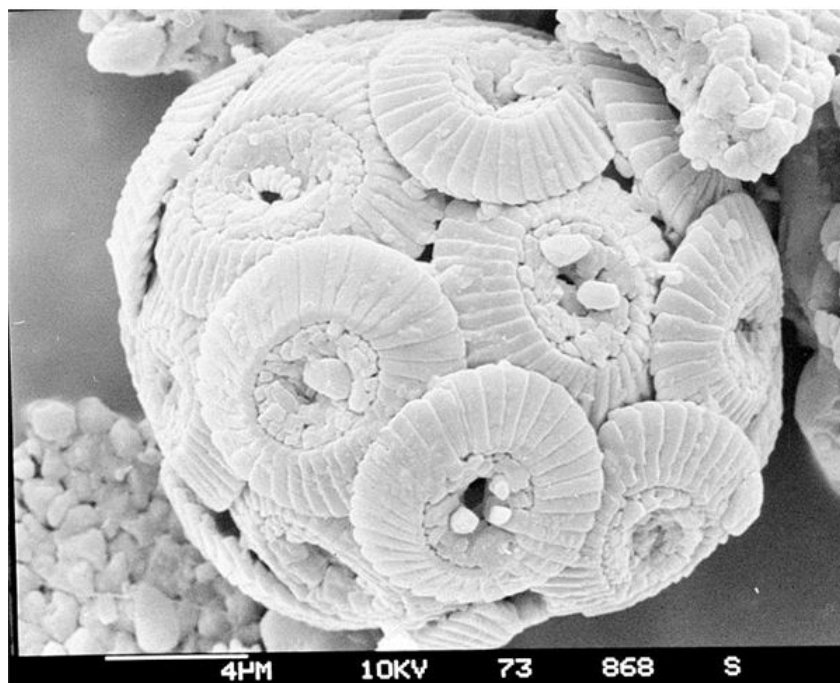


Figure 2.2: *SEM image of a skeleton from a coccolithophorid algae. The overlapping coccolith disks make up the coccosphere. Image from [http : //images.brighthouse.com/43/b43baad625ed78d96fd3acb13b5ca9d6c89046882_large.jpg](http://images.brighthouse.com/43/b43baad625ed78d96fd3acb13b5ca9d6c89046882_large.jpg).*

minerals (Surlyk et al., 2003; Gale, 2011; Kennedy, 1985). Non-carbonate components of biogenic origin, e.g. radiolarians and sponges spicules, are often dissolved after deposition (Surlyk et al., 2003). Variable amounts of terrigenous clay occur throughout the Chalk Group in the Central Graben area. The composition can vary from pure chalk and limestone to marly chalk, marl and calcareous shale (Surlyk et al., 2003). The clay content in some parts of the Plenius Marls (Blodøks), Middle Hod and Lower Ekofisk Formation is so substantial that it grades towards shale or calcareous mudstone (Kennedy, 1985; Surlyk et al., 2003). According to D'Heur (1984), the non-carbonate fraction can reach 20% locally in the Ekofisk Formation and 40% in the Hod Formation.

Flint nodules occur at many levels in the Chalk Group (Surlyk et al., 2003), and it is suggested that the flint formation took place in burrowed zones by mixing of the breakdown products of organic matter via sulphate reduction and the breakdown products of siliceous organisms (Wray and Gale, 2006). They can cover large horizons in the chalk, forming flint bands, which roughly follow the bedding surfaces.

Color alternations in the chalk can reflect changes in terrigenous clay content (Kennedy, 1985). Non-diluted chalk has a light color, and with increasing percentage of clay content

the rock gets darker colors (Gale, 2011).

Scanning electron microscopy of samples from the Central Trough have shown that the porosity is primary (Ofstad, 1980). Chalk contains both inter- and intra-granular porosity (Lucia, 1995).

2.3 Depositional processes of Chalk

There are commonly two main types of chalk deposits from the Upper Cretaceous and the Early Paleocene. The primary pelagic autochthonous chalk deposited from suspension as an unconsolidated ooze of coccolith debris and variable amounts of other carbonate and non-carbonate material, and the allochthonous reworked chalk caused by resedimentation (i.e. slumps, slides, debris flows and turbidity currents) of the primary pelagic chalk (Figure 2.3) (Kennedy, 1985).

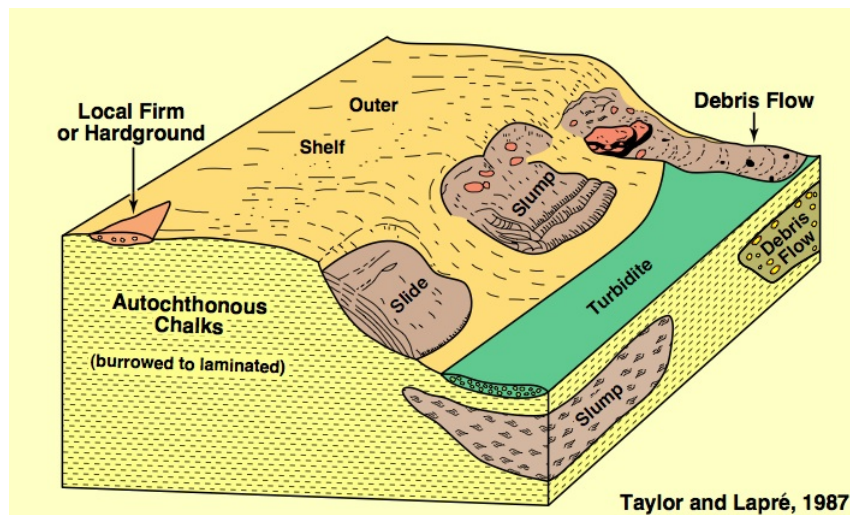


Figure 2.3: *Illustration of chalk depositional systems. The illustration displays examples of different gravitational transport mechanisms for the reworked chalk, as well as hardground development on local highs. Illustration from Moore (2001).*

According to Kennedy (1985), the early works done on characterizing the Chalk Group generally considered all the chalks in the Central Graben to be deposited as a slow pelagic "rain" of coccolith debris, similar to the chalks that they saw in onshore outcrops at the time. Later, the recognition of extensive redeposition inside the chalk sequence in the Central Graben, has led to the general understanding of the large presence and importance of allochthonous chalk, regarding the thicknesses of the Chalk Group and especially its reservoir qualities (D'Heur, 1984). Allochthonous chalk intervals are common in the core samples from the Central Graben, but they can be difficult to recognize and correlate from well to well (Schatzinger et al., 1985).

2.3.1 Primary pelagic sedimentation, autochthonous chalk

The chalk in the Chalk Group was initially deposited at the seafloor as an unconsolidated ooze of coccolith debris and variable amounts of other carbonate and non-carbonate material, which later lithified through diagenesis (Friedman, 1996; Surlyk et al., 2003). This pelagic chalk, deposited from suspension in the water column, is characterized by rhythmic bedding of limestone and marl (periodite facies), as well as intense bioturbation (Figure 2.5.A)(Kennedy, 1985; Hatton, 1986). The rhythmic bedding in the chalk is interpreted to reflect climatic changes within the Milankovich frequency band, and can be used for dating and correlation purposes (Surlyk et al., 2003). Milankovich Cycles are repeating cycles of fluctuation in solar radiation received at a given latitude, due to variations in the Earth's orbit, axial tilt and precession (Figure 2.4). Although the cyclic periodite facies is indicative of pelagic (autochthonous) deposition, the facies can also be allochthonous as a part of a bigger resedimented unit, e.g. in a mass slump or slide (Kennedy, 1985; Surlyk et al., 2003).

Duration (m.y.)	Sequence Type
200-500	Global supercontinent cycle (1st-order cycle)
10-100	Supercycles (2nd-order cycle)
2-10	Regional to local cycles (3rd-order cycle)
0,01-2 •0,1-0,4 •0,041 •0,021	Milankovitch cycles (4th- and 5th-order cycles) •Orbital periods of eccentricity •Orbital periods of obliquity •Orbital periods of precession

Figure 2.4: Table with cyclic sequence types and their corresponding durations. Information in the table is taken from Mabesoone and Neumann (2005).

If the chalk is not subjected to any post-depositional resedimentation it is called autochthonous pelagic chalk (Friedman, 1996).

Initial porosity in a chalk deposited as a watery unconsolidated ooze (Soapground - Softground), could be as high as 70-80% (Surlyk et al., 2003). The relatively slow deposition-rate of pelagic chalk led to intense bioturbation in the sediments at the seafloor by burrowing benthic invertebrates, which caused early dewatering, compaction and cementation (D'Heur, 1984).

2.3.2 Resedimentation, allochthonous chalk

In the Central Graben of the North Sea, redeposition of chalk was dominantly the results of mass-gravity transport processes, triggered by a complex interplay of halokinesis, local tectonics and erosion (Brewster and Dangerfield, 1984). According to Surlyk et al. (2003), the allochthonous chalk facies is rarely observed in the onshore chalk, but is frequently seen in core samples taken from the reservoirs in the Central Graben. It is evident that reworked chalk is the major component of the reservoirs in the area (Lottaroli and Catrullo, 2000). The importance of redeposited chalk was first documented by Perch-Nielsen et al. (1979), who identified a substantial sequence of "Maastrichtian chalk" overlaying the Danian "tight zone" in the Ekofisk field (well 2/4-A8) (D'Heur, 1984).

The redeposited chalk is generally known for having a better reservoir quality than autochthonous chalk, because the argillaceous minerals have been winnowed out of the chalk, it is better sorted with regard to particle and pore size, it has a much higher preserved porosity and the rapid deposition only allowed bioturbation at the top of each deposition sequence (D'Heur, 1984).

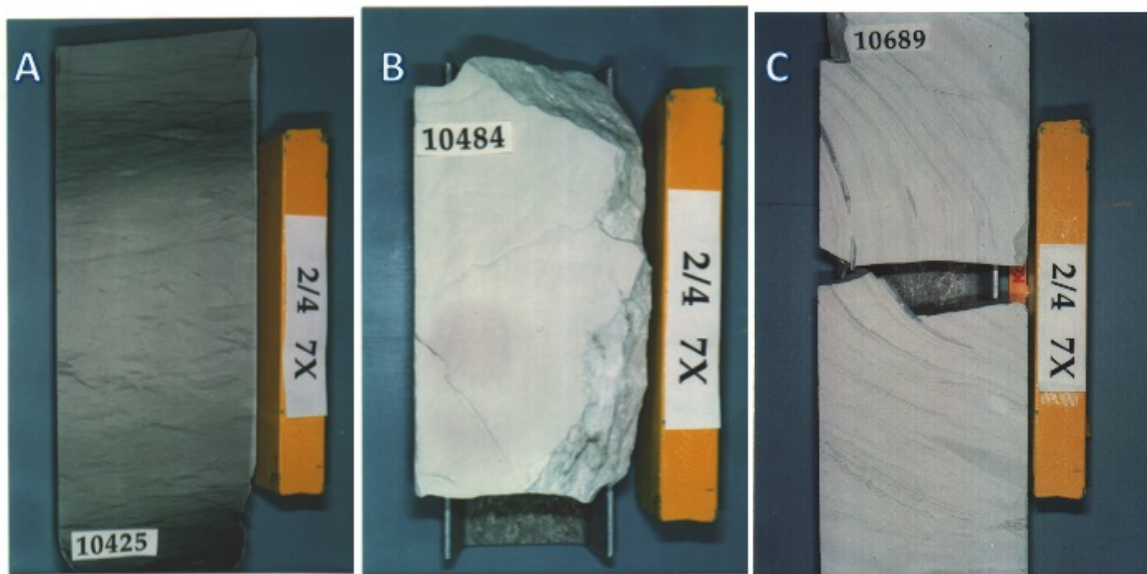


Figure 2.5: *Picture of 3 core sections with different facies from well 2/4-7 at the Tor Field. A) burrowed argillaceous chalk, typically autochthonous B) homogeneous chalk, probably allochthonous C) deformed laminated chalk, typically allochthonous. Depths are in feet. Pictures are taken from Caldwell and Siemers (1993).*

Depositional processes of allochthonous chalk (Figure 2.3 & 2.6) in the Central Graben, summarized from D'Heur (1984); Kennedy (1985); Schatzinger et al. (1985); Hatton (1986); Kennedy (1987) and Surlyk et al. (2003):

- **Slides and Slump deposits** are characterized by downslope movement of semi-

consolidated sediment packages, along a basal sheer plane. The internal coherence and bedding can remain relatively intact in the slides, which can make it difficult to recognize in cores if the basal shear zone is absent. Slump deposits have a more chaotic internal structure than the slides, with slump folds on a cm to m scale (Figure 2.5.C), faults and detachment planes. Both slides and slump deposits could have had movement along a basal shear zone beneath a substantial overburden. According to Kennedy (1980), micropaleontological investigations of the Tor Field showed that the Ekofisk Formation most likely contains slumping on a massive scale.

- **Debris-flows** are mass-flows caused by reduction of shear stress within an entire sediment package and are common sights in cores from the Central Graben. They often contain varying amounts of chalk clasts, floating in a finer matrix. According to Kennedy (1985) and Schatzinger et al. (1985), poorly cemented chalk clasts are destroyed during transport with a debris flow, producing a homogeneous, shredded rock fabric without bedding. According to D'Heur (1984), debris flows generally constitute the best reservoirs in the Chalk Group.
- **Turbidites** occur in all divisions of the Chalk Group. The basal product of the turbidity flows is calcarenite that fines upwards with a general grain size from sand- to silt-size. Turbidite packstones are not the most common depositional packages within the chalk in the Central Graben, but one of the most distinctive. Generally, they tend to be well cemented and therefore constitute vertical permeability barriers or baffles. At the Tor Field, several meters of thick turbidite packstones have been seen in the Tor Formation and lower part of the Ekofisk Formation. Low-density turbidites will produce fine laminated chalk deposits.
- **Laminated Chalk** is often interpreted as deposits from low-density turbidites. The lamination could also be caused by winnowing of pelagic chalk at local highs, followed by redeposition in deeper water. In cores from the Central Graben, laminated and bioturbated intervals commonly alternate, which could indicate changes in the level of dissolved oxygen at the seafloor (Kennedy, 1985).
- **Homogeneous Chalk** is a depositional product with little or none internal structure (Figure 2.5.B). In cores, it is normally difficult to recognize which depositional process caused a homogeneous interval. Homogeneous intervals could be the product of base-absent turbidites, submarine mudflows or debris flows in which the clasts have been totally destroyed.

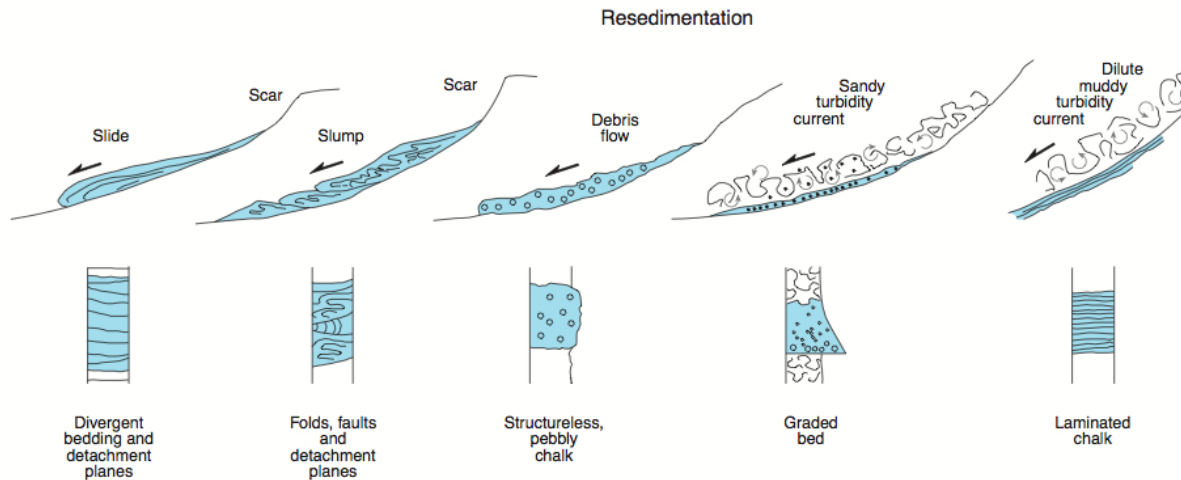


Figure 2.6: *Illustration of chalk resedimentation mechanisms and depositional fabrics. Illustration modified from Surlyk et al. (2003).*

2.4 Structural evolution and the influence of local tectonics on the chalk distribution

The Central Graben is located in the central part of the North Sea (Figure 2.7), and is a part of a riftsystem with a relatively complex framework (Gowers and Sæbøe, 1985). The reason for the structural complexity is that the tectonic evolution has happened in many phases and has been influenced by halokinesis of underlying Permian salt (Caillet et al., 1996). Syndepositional tectonic movements were responsible for the variety of allochthonous facies within the Chalk Group (Kennedy, 1980; Caillet et al., 1996).

Most of the differential tectonic movements related to rifting within the Central Graben took place in pre-Cretaceous times (Gowers and Sæbøe, 1985).

The extension and faulting started to develop during the Late Permian - Early Triassic (Gowers and Sæbøe, 1985; Knott et al., 1993). Simultaneously, in the late Permian, deposition of the Zechstein evaporites took place in two large shallow marine paleo-basins commonly known as the Zechstein-basins (Larsen et al., 2006). Parts of the northern Permian Zechstein basin are located beneath the chalk in the Central Graben (Gowers and Sæbøe, 1985).

The halokinetic movements of the Zechstein salt are composed of several phases (D'Heur, 1984; Surlyk et al., 2003; Larsen et al., 2006). According to Surlyk et al. (2003), the movement of the salt started in the Triassic, while D'Heur (1984) believed the movement begun in the Late Jurassic. In addition, D'Heur (1984) suggested that the halokinesis had created nearly all the discovered oil and gas traps in the chinks of the Norwegian Central Trough and caused significant fracturing, which has been essential for the migration and production of hydrocarbons.

The main tectonic extension contributing to the development of the rift systems in the

North Sea, happened during the Late Jurassic - Early Cretaceous (Surlyk et al., 2003). In the Cretaceous, the rifting in the North Sea decreased, while the continued extensional tectonics and creation of the North Atlantic Ocean were caused by ocean floor spreading further to the west. When the rifting in the North Sea ended, the rapid subsidence continued throughout the Cretaceous and Tertiary times (D'Heur, 1984). During the Late Cretaceous, there was relatively little tectonic activity in the Central Graben area, except for some very important pulses of compression related to the early phases of the Alpine Orogeny that resulted in fault inversion in the basins (Surlyk et al., 2003).

An initial phase of compressional tectonic and inversion occurred in the Mid-Turonian and continued to occur in pulses through to the Danian (Caillet et al., 1996). In this period the shape of the basin and the sediment distribution were mostly controlled by the formation of major inversion structures, such as the Lindesnes Ridge (Caillet et al., 1996). Syn-depositional tectonic movement and halokinesis were responsible for triggering the massive redeposition of chalk from the local heights and graben margins towards the basin depocenters (Gowers and Sæbøe, 1985). Thus, the subsurface movements had a large impact on the facies distribution of the reworked chalk (Caillet et al., 1996).

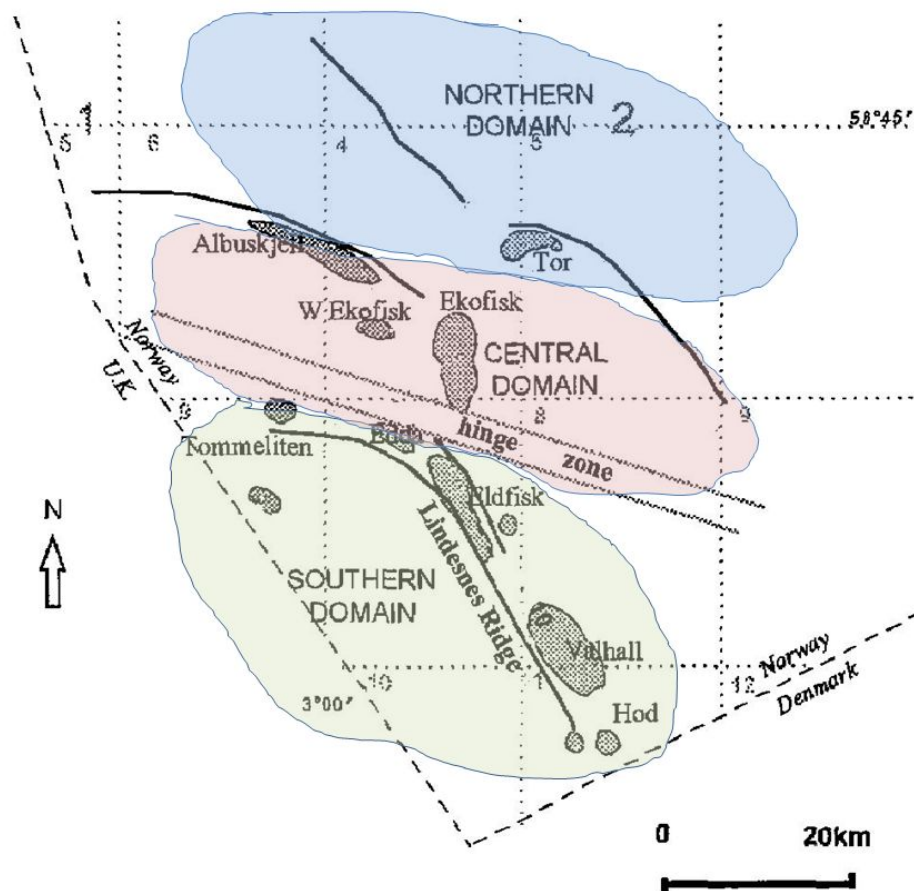


Figure 2.7: Map of the Central Graben displaying the main oilfields, the main structural elements and zones. Modified from Caillet et al. (1996).

The Norwegian part of the Central Graben can be sub-divided into 3 main zones (Figure 2.7), with different structural and faulting styles (Caillet et al., 1996):

1. A Northern zone with NNW-SSE trending ridges and local salt diapirism. The Tor Field structure belongs to this Northern zone.
2. A Southern zone dominated by the Lindesnes ridge trending NNW-SSE.
3. A Central area, dominated by well-developed salt diapirism, serves as a transfer zone between north and south,

A regional compressional phase, early in the Late Cretaceous, caused anticlinal folding and rebound tectonism in the Tor Field. In the Campanian, corresponding to the Upper Hod Formation, the Tor structure emerged along WNW lineaments (Caillet et al., 1996).

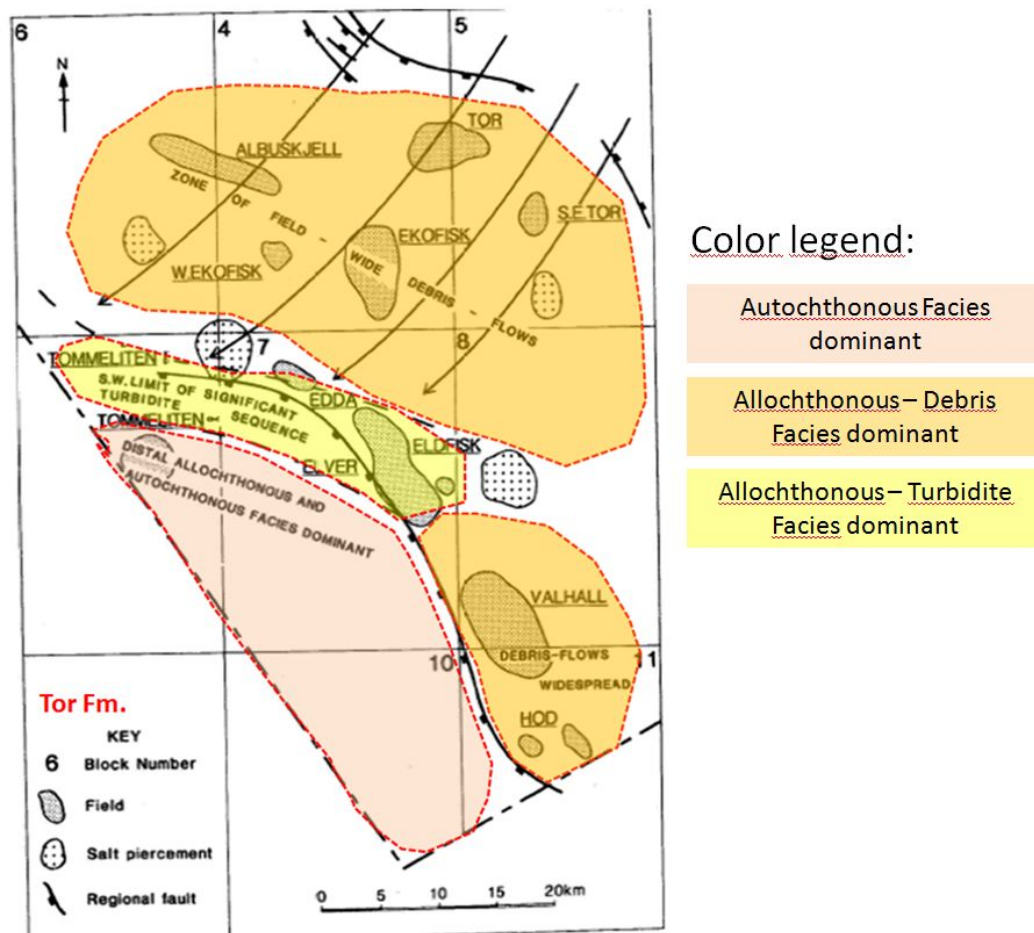


Figure 2.8: Map of the the Tor Fm. in the Central Graben displaying the main oilfields, the main structural elements, Facies distribution and sediment transport directions. Modified from Kennedy (1987).

As mentioned previously in Chapter 2.3.2 , tectonics and halokinesis have, in addition to creating structural highs and lows, triggered the downslope resedimentation from struc-

2.4 Structural evolution and the influence of local tectonics on the chalk distribution 13

tural highs as well as graben margins. Since the redeposition had multiple sources and occurred in pulses, the distribution of the different chalk facies in the Central Graben is highly complex.

Figure 2.8 and Figure 2.9 illustrates how Kennedy (1987) interpreted the regional facies distribution of the Tor and Ekofisk Formation, within the Central Graben. Notice the similarity between the structural zones (Figure 2.7) and the Facies distribution. This is an interpretation at a very large scale and the detailed distribution of facies is far more complex, with facies changes on a decimeter scale.

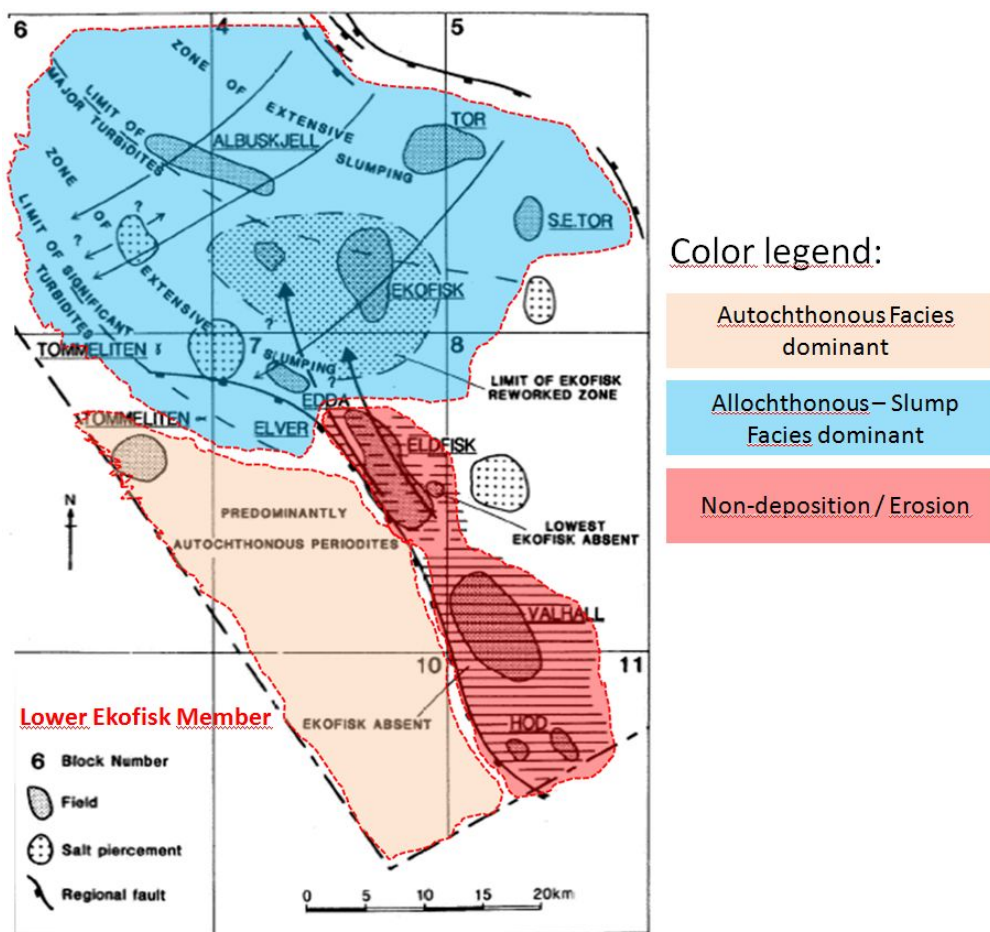


Figure 2.9: Map of the the Lower Ekofisk Member in the Central Graben displaying the main oilfields, the main structural elements, Facies distribution and sediment transport directions. Modified from Kennedy (1987).

2.5 The Tor Field

On the border between block 2/4 and 2/5 in the Norwegian North Sea, at a depth just exceeding 3000m, the Tor Field was discovered in 1970 by Amoco's well 2/5-1X. The oilfield is named after one of the principal Gods of Norse mythology, Tor, son of Odin and the God of thunder. Later, the name was also given to the Maastrichtian Chalk Formation by Deegan and Scull (1977).

The production started in 1978 and today a total of 22 development wells and 4 exploration wells have been drilled (NPD, 2012). The Tor Field initially held an estimated 770 MMSTB of oil, split between the Ekofisk Fm. (30%) and the Tor Fm. (70%) (Bergfjord, 2007). At the end of 2010, a cumulative total of 148,4 MMSTB with oil had been produced from the Tor Field, and the remaining recoverable reserves were thought to be around 5 MMSTB (NPD, 2012). It has been estimated that 95% of the produced oil has come from the Tor Formation. Without any new attempts to increase the recovery, the production from the Tor Field is estimated to end in the near future on an ultimate recovery of approximately 20% (TorCh-project, 2007).

At the moment, a major redevelopment plan (Tor II) for the Tor Field is being evaluated. The goal is to increase the recovery of the remaining resources (NPD, 2012).

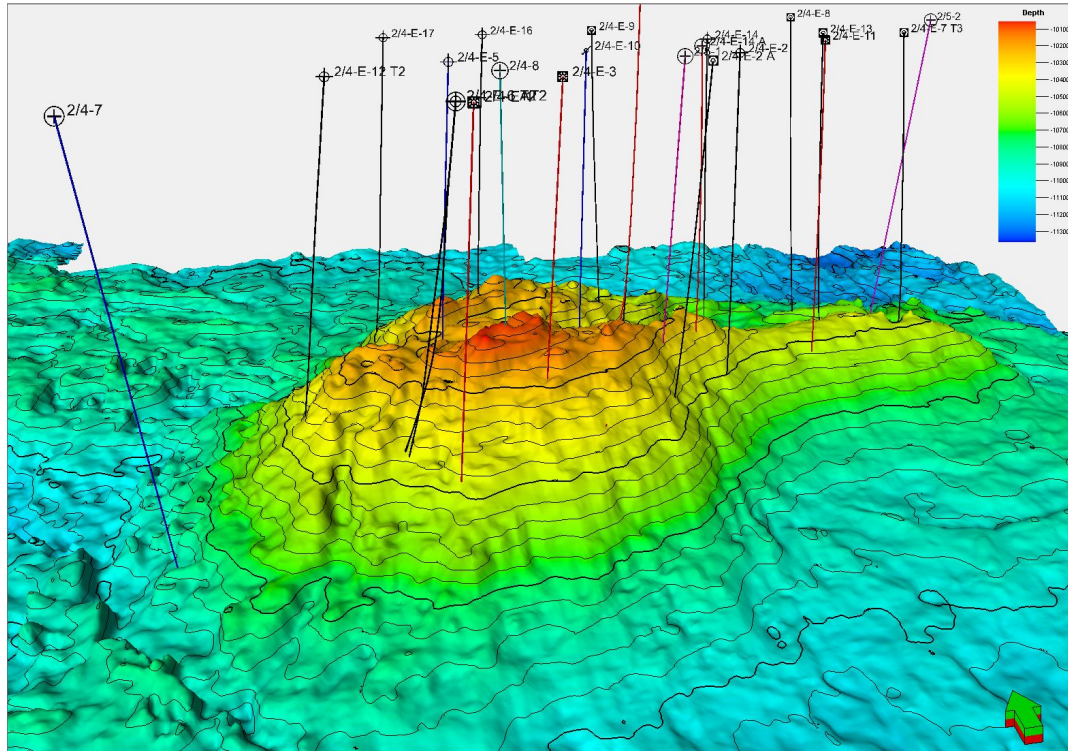


Figure 2.10: 3D view of the Tor Field seen from the South-South West.

The Tor Field is part of the Upper Cretaceous - Lower Paleocene Chalk play in the Central Graben, North Sea. The field has a structural trap, a dome structure above a salt swell

and a seal of Tertiary shale preventing further vertical migration (D’Heur, 1987). The Tor Field is situated in a structurally complex area and is, according to Surlyk et al. (2003), the result of Late Jurassic transtension that developed into a transpressional flower structures in the Early Cretaceous. During the Late Cretaceous to Cenozoic times, the transpression was reactivated in pulses (Surlyk et al., 2003). The transpressional tectonics combined with the halokinetic uplift have caused intense faulting in addition to some zones where the chalk has collapsed at the crest of the field (D’Heur, 1987).

According to D’Heur (1987), geochemical analyses of the hydrocarbons have shown that the source rock is an organic rich Upper Jurassic shale, called Mandal Formation in this particular area of the North Sea. From the well 2/5-1, it is evident that the thickness of the Upper Jurassic shale is at least 120m. Studies done by Phillips Petroleum conclude that peak oil generation in the area of the Tor Field, occurred during Miocene times (D’Heur, 1987). The hydrocarbons could have been generated and migrated from more distal and deeper parts to the Tor Field, as early as the Paleocene (D’Heur, 1987). In general, the timing of the oil migration and early hydrocarbon-charging of the chalk is very important since it is preventing the chemical compaction and subsequently preserve the porosity during burial and diagenesis (D’Heur, 1984; Surlyk et al., 2003).

The chalk intervals containing oil in the Tor Field belong to the Ekofisk and Tor formations (Figure 3.1). With respect to production of hydrocarbons, the Tor Formation is the most important of the two formations due to its superior reservoir quality (NPD, 2012).

3 Methodology

3.1 Lithostratigraphy

A lithostratigraphic unit is a rock unit defined by its physical properties such as composition, texture, color and sedimentary structures (Boggs, 1995).

The Chalk Group in the central part of the North Sea was originally subdivided into the Hydra, Plenus Marl, Hod, Tor and Ekofisk formations by Deegan and Scull (1977). In the Norwegian North Sea, Isaksen and Tonstad (1989) included the chalk succession in the siliciclastic Shetland Group, removed the Plenus Marl and created a new formation called the Blodøks Formation. They subdivided the Hod, Tor and Ekofisk formations into Lower, Middle and Upper members (The Ekofisk Formation was only subdivided into Lower and Upper members). In addition, Isaksen and Tonstad (1989) included the strata corresponding with the UK Herring Formation (Deegan and Scull, 1977) in the Blodøks and lower Hod formations (Surlyk et al., 2003). In a chalk study by Bailey et al. (1999), an alternative subdivision of the Turonian-Campanian Chalk succession (Hod Fm.) was proposed, dividing the Hod Formation into three new formations: Narve, Thud and Magne (Figure 3.1).

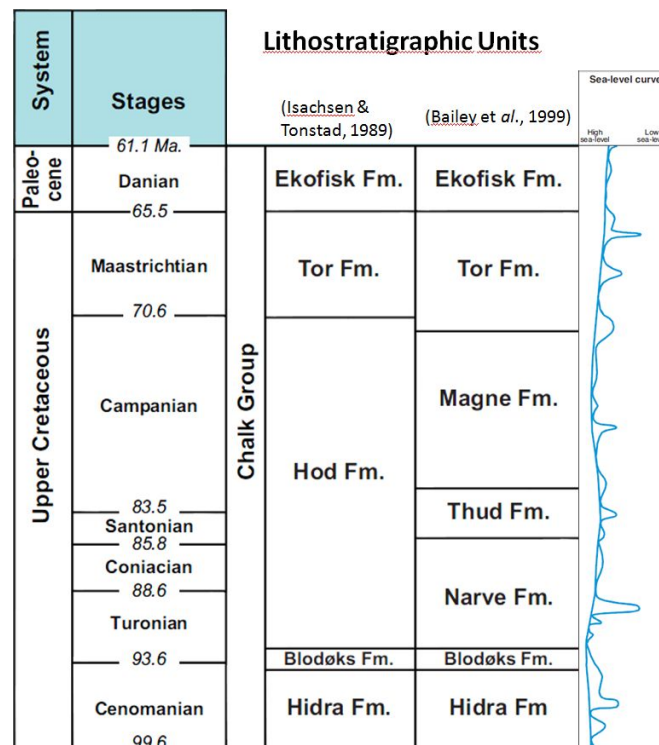


Figure 3.1: Lithostratigraphic subdivision of the Chalk Group (considered Shetland Group by Isaksen and Tonstad (1989)), Upper Cretaceous - Lower Paleocene strata, in the Norwegian Central North Sea with nomenclature from Isaksen and Tonstad (1989) and Bailey et al. (1999), and the corresponding sea-level curve from Surlyk et al. (2003). Figure modified from Gennaro et al. (2011).

The focus of this study are the hydrocarbon bearing Tor and Ekofisk formations.

At the moment, a lithostratigraphic correlation of the Tor Field is being used for the purpose of reservoir characterization (TorCh-project, 2007). In order to characterize the reservoir properly, the Tor and Ekofisk Formation are divided into three and four main units. Furthermore, the Tor Formation is subdivided into 14 minor units and the Ekofisk Formation into 11 minor units (Figure 3.2). The correlation is done mainly by comparison of the porosity logs, which locally displays random thickness variations.

Formation	Lithostratigraphic units	
Ekofisk Fm	EU	1,2,3
	EM	1,2,3,4
	EL	1,2,3
	ET	
Tor Fm.	TU	1,2
	TM	1,2,3,3a,4,4a,5,5a
	TL	1,2,3,4

Figure 3.2: *The lithostratigraphic markers used in the current reservoir correlation at the Tor Field. The markers are picked and correlated based mainly on porosity derived from wireline logs.*

3.2 Sequence Stratigraphy

According to Wagoner et al. (1990), *sequence stratigraphy is the study of genetically related facies within a framework of chrono-stratigraphically significant surfaces*. In other words, sequence stratigraphy is the correlation of sediments of the same age. A sequence is built up by parasequences and parasequence sets, and it is bounded by unconformities or their correlative conformities.

Sequences and especially parasequences are generally more difficult to recognize and interpret in the North Sea Chalk, than in shallower carbonate and clastic depositional environments. The paleo-bathymetry in the Central Graben area, during the Maastrichtian and Danian were approximately 300-600 meter (Kennedy, 1987). Thus, the chalk of the Central Graben was never subjected to subareal exposure and erosion caused by changes in relative sea level. Another difference from other "shallower" depositional environments, is that an increase of shale content in non-reworked chalk can be explained by a reduction in relative sea level, due to reduced distances to clastic sediment sources (e.g. the Ekofisk "tight zone" at the K-T boundary), rather than an elevated relative sea level.

Climatic changes and fluctuations in the relative sea level can have caused changes in the depositional environment, by controlling the influx of clastic material and the rate of coccolith sedimentation (Kennedy, 1987). A reduction in coccolithophorid productivity and coccolith sedimentation, would normally lead to intense bioturbation of the sea floor ooze and subsequently dewatering, cementation and hardground development. Hardground

development normally occurred on structural highs, due to lower sedimentation rates and more bioturbation (Surlyk et al., 2003). With a high content of biogenic silica in the water at the vicinity of a bioturbated seafloor, it was possible for flint nodules and bands to be formed diagenetically in the chalk (Wray and Gale, 2006). An increase in the terrigenous clay content would normally make the chalk more susceptible to both mechanical and chemical compaction (Kennedy, 1987). These dense zones are recognizable and can be used for correlation purposes.

This presented correlation of the Tor Field, builds upon a regional correlation of the chalk in the Central Graben, by Gennaro et al. (2011). The regional correlation was based on the principles of sequence stratigraphy, initiated by Gerard Sambet (Total E&P Norge) for the chalks in the Embla sector and continued by study Tonje Dahl (summer student Total E&P Norge, 2004) in a coarse regional seismic correlation. In 2005, G. Sambet ordered A. Roumagnac and B. Caline (Total E&P Geosciences Technologies) to conduct the first phase of a more refined correlation study of 21 wells in the Tor Field. The study was never continued after its first phase.

In this correlation, the Tor and Ekofisk Formation are subdivided into sequences and parasequences by 21 well markers (Figure 3.3). Of the 26 wells on Tor Field, the regional sequence stratigraphic correlation by Gennaro et al. (2011) included 6 of the Tor Field wells. These 6 wells became the "type wells" for the correlation of the remaining Tor Field wells. In Chapter 4 (page 21), all the markers from the correlation will be presented in text and figures.

CORRELATION MARKERS			
EKOFISK FM.	Ekofisk	TOR FM.	Tor
	Eko 90		Tor 05
	Eko 80		Tor 10
	Eko 70		Tor 15
	Eko 60		Tor 20
	Eko 50		Tor 30
	Eko 40		Tor 40
	Eko 30		Tor 50
	Eko 20		Tor 60
	Eko 10		Tor 70
	Eko 5		

Figure 3.3: Table of the stratigraphic markers used in the well correlation in this thesis and in the regional correlation by Gennaro et al. (2011).

3.3 Biostratigraphy

In biostratigraphy the strata are divided based on the fossil content. The division of strata is based on the principal that organisms have undergone a gradual and non-reversible evolution through time (Boggs, 1995). Locally, biostratigraphic boundaries normally serve as time boundaries. Different periods of occurrence for certain species can vary in different places, but there have not been any evidence of restricted habitat of planktonic algae within the Central Graben.

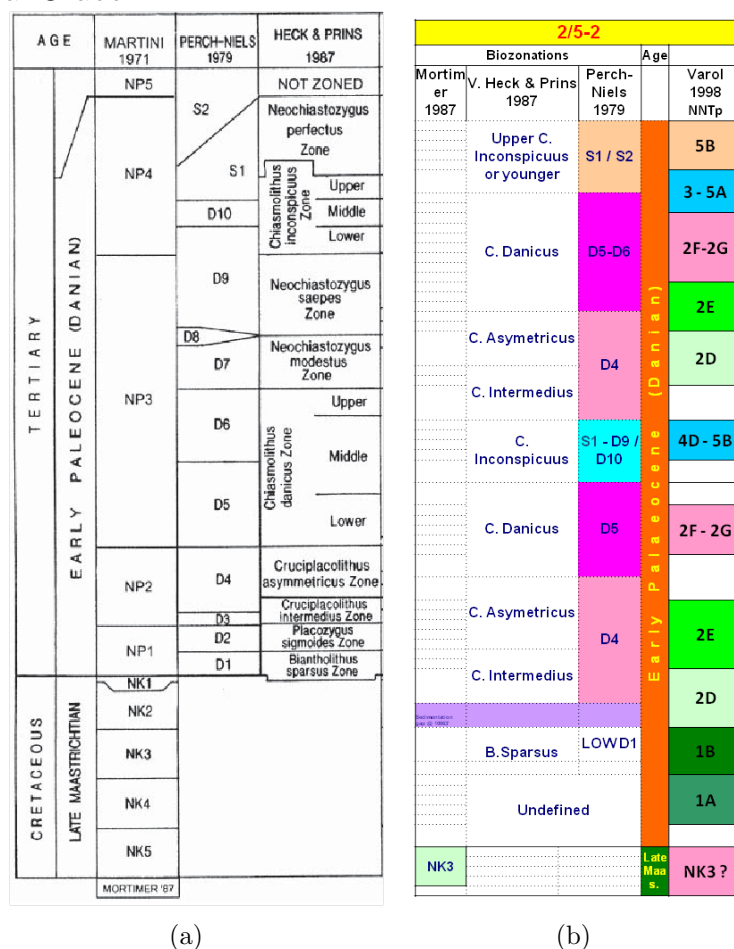


Figure 3.4: a) Different classifications of bio-zonation with corresponding age, from Lottaroli and Catrullo (2000), b) Bio-zones in well 2/5-2, based on Lottaroli and Catrullo (2000). Depths are not shown in the figure.

A biostratigraphic study of cored Maastrichtian and Danian chalk from 10 wells in the Greater Ekofisk area (Central North Sea) was conducted by Lottaroli and Catrullo in 1995 and published in 2000. Four of these wells were from the Tor Field, but the publication by Lottaroli and Catrullo (2000) only included nannofossil data for two of the wells (2/4-8 and 2/5-2). This nannofossil data was classified according to the zonation by Heck and Prins (1987) and Varol (1998) (Figure 3.4). The biostratigraphic interpretations were utilized while conducting the new presented sequence stratigraphic correlation of the Tor Field.

4 Observations and Results

As mentioned in Chapter 3.2, the sequence stratigraphic correlation of all 26 wells in the Tor Field is based on wireline log signatures from the six type wells that were interpreted as a part of a regional correlation of the chalk by Gennaro et al. (2011).

The six type wells are : **2/4-7, 2/4-8, 2/5-1, 2/5-2, 2/4-E-10, 2/4-E-14** .

These type wells are marked with stars in Figure 4.1. A foldout well section displaying all the type wells can be found in the Appendix (Figure A.1).

The following wireline logs were primarily used for the correlation:

- Gamma Ray (GR)
- Bulk Density (RHOB)
- Sonic / P-wave Slowness (DT)

The wireline logs were displayed with a white to black color fill template. This was primarily done to make the GR log fill reflect the shale content in the chalk by having a darker color, the higher the GR reading. At times, the microresistivity log (MSFL) was used to support the correlation. However, not all of the mentioned electrical logs were available for all of the wells. Porosity logs were not used during this correlation, contrary to the lithostratigraphic correlation currently used by the Tor Field operator ConocoPhillips Norge. Biostratigraphic interpretation of two wells by Lottaroli and Catrullo (2000), displayed as bio-zones, were also used in the correlation.

In general, the correlated markers in the Ekofisk Formation correspond to zones of higher GR log readings than the surrounding "cleaner" chalk. In the Tor Formation there is generally little variation in the GR readings, and the markers were often correlated based on the RHOB and DT log signatures. The key markers in this correlation, which were the easiest markers to recognize in all the wells, were the top Ekofisk marker and the markers subdividing the Ekofisk "Tight Zone", the Eko 10, Eko 5 and top Tor (Figure 3.3).

4.1 The sequence stratigraphic markers

In total, this correlation of the Tor Field has 21 sequence stratigraphic markers (Figure 3.3 and 4.2). 11 markers have been defined for the Ekofisk Formation and 10 markers for the Tor Formation. Not all 21 markers have been identified in all the Tor Field wells, because of missing log data. In the following section the different markers are described and presented in figures. The figures will show wireline log response around different markers. In addition, isochore maps have been generated by interpolating the true vertical thicknesses between the stratigraphic markers in the wells (not to be confused with isopachs, which refers to the stratigraphical thickness). For practical uses, all the markers in the well sections figures contain the prefix TAE (initials of the author).

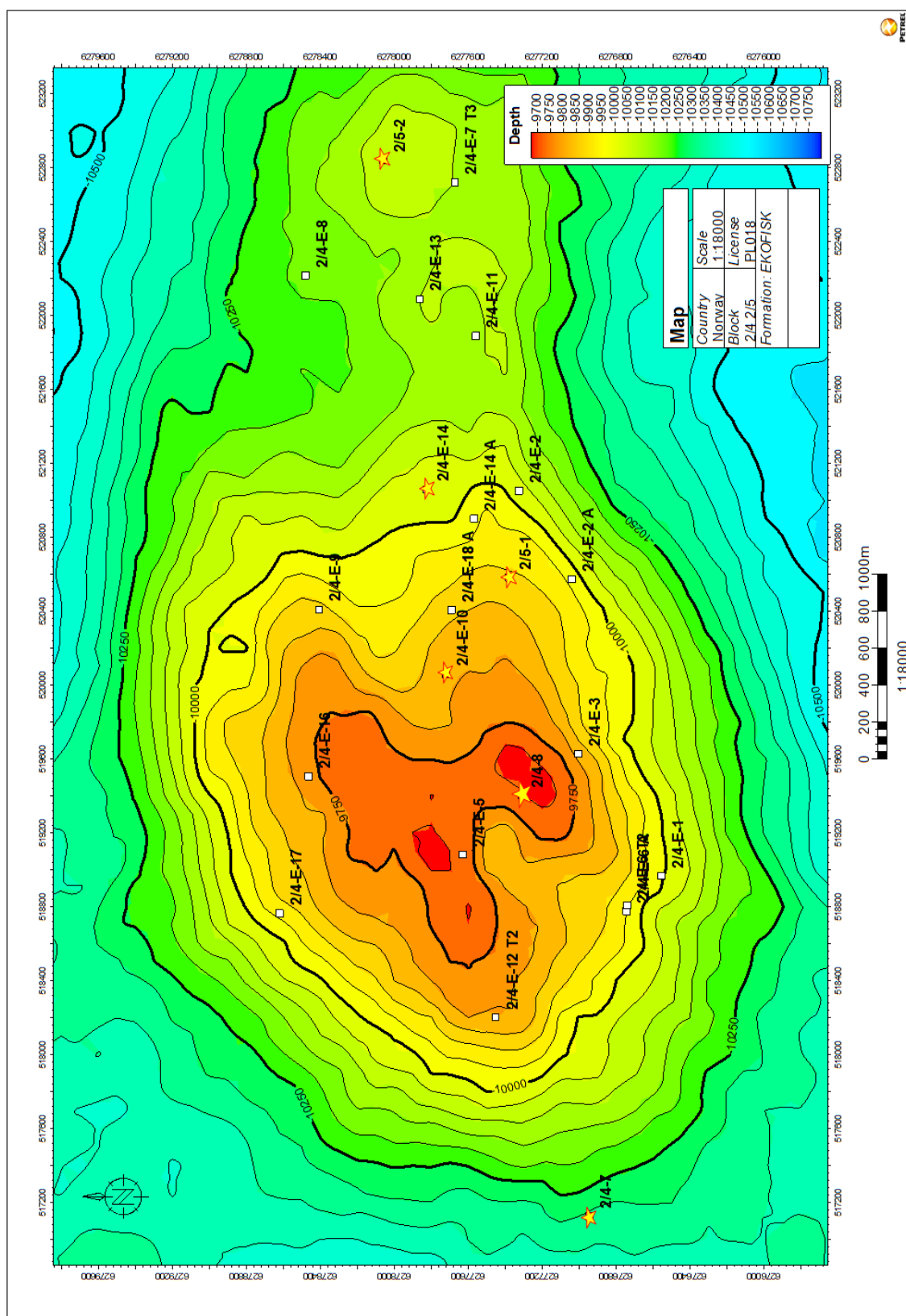


Figure 4.1: Map with the position of the wells at the Tor Field. The type wells are marked with stars on the map. The background is the surface of top Ekofisk Fm.

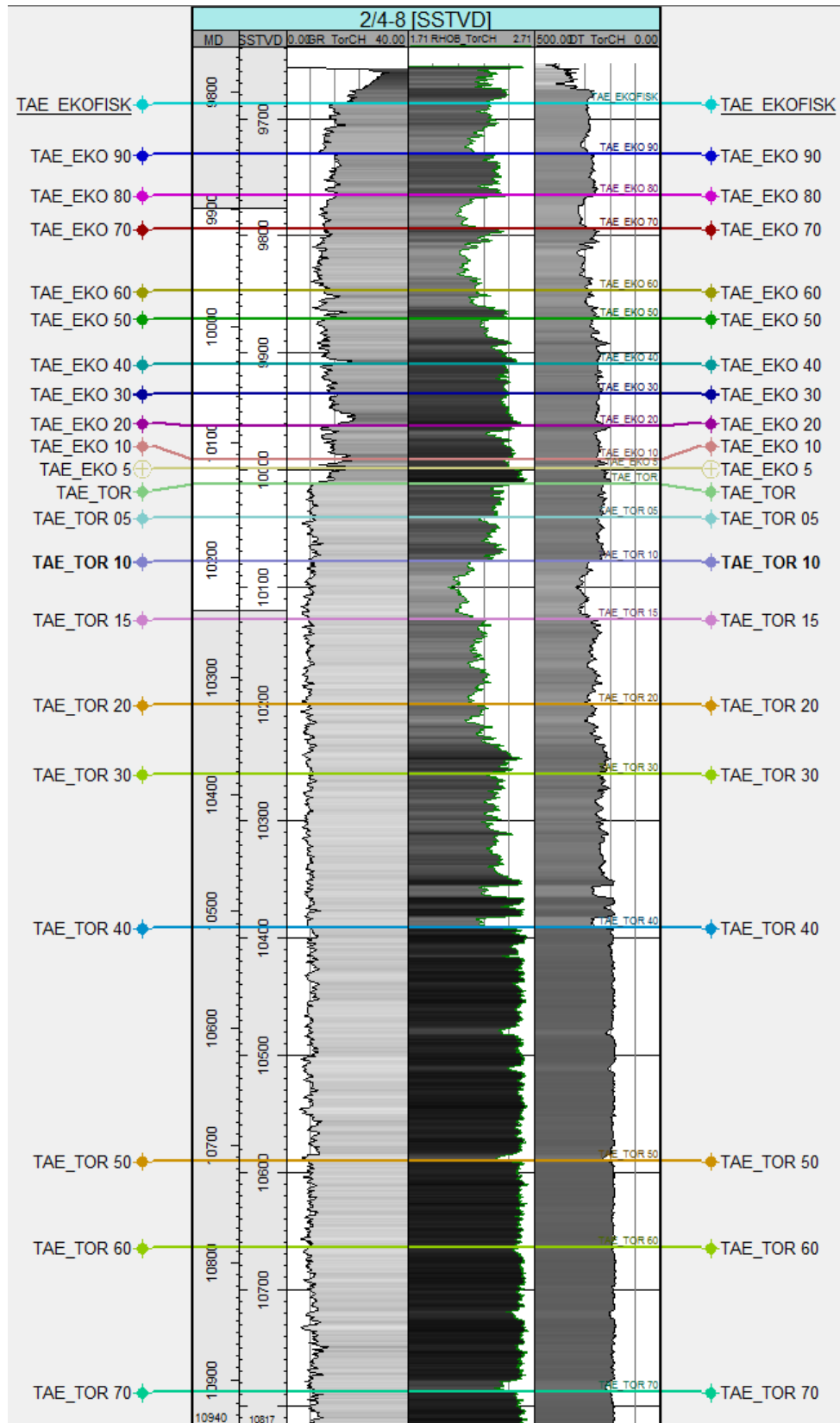


Figure 4.2: Well 2/4-8, with all sequence stratigraphic markers, as defined by Gennaro et al. (2011).

4.1.1 Top Ekofisk

Observation and interpretation of the type wells (Gennaro et al., 2011)

The top Ekofisk marker is positioned at the boundary between the chalk succession and the overlying shale. The marker is placed at the uppermost limit of clean chalk below a sharp GR decrease indicating the overlying shale of the Våle Formation (Figure 4.3). The sonic log (DT) is increasing sharply at this limit.

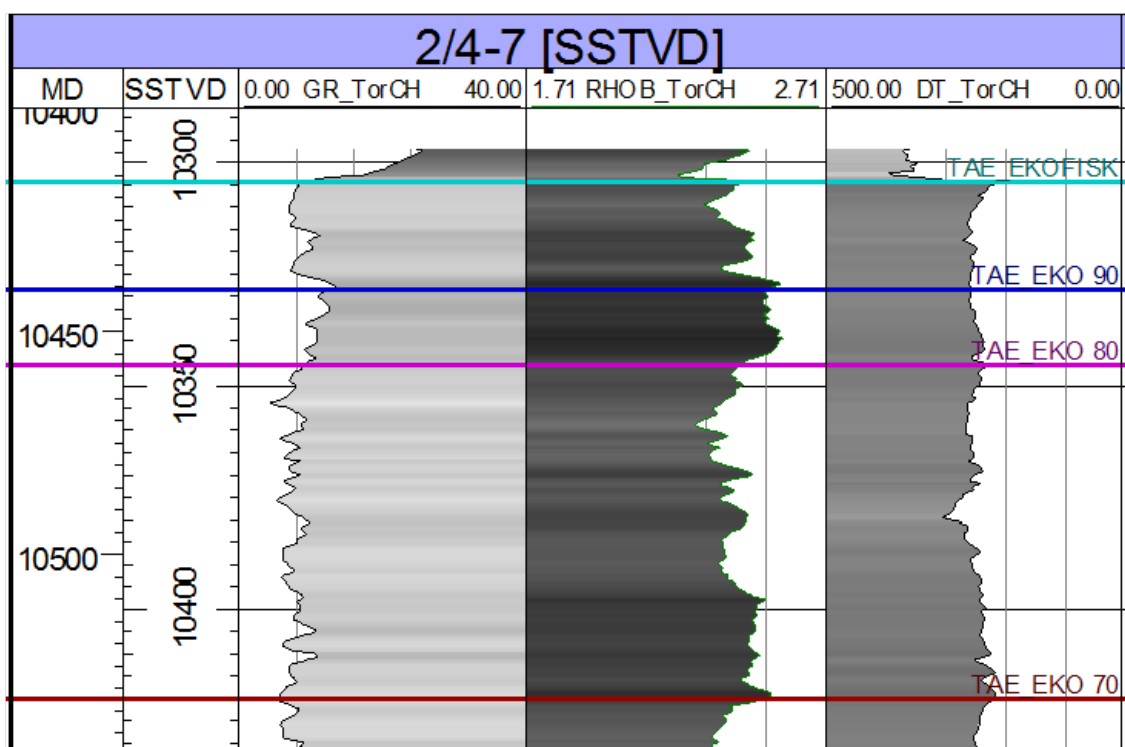


Figure 4.3: Log signature at the top Ekofisk marker (light blue) in well 2/4-7.

New correlation

The wireline log response at the Ekofisk marker is generally the same in all the wells on the Tor Field (Figure 4.3). In some of the wells the log signature is disturbed by the casing shoe.

The thickness between the top Ekofisk and Eko 90 markers vary significantly across the Tor Field (Figure 4.4). The greatest thickness has been interpreted in well 2/4-E-3. In terms of the biostratigraphy from the nannofossil data (wells 2/4-8 and 2/5-2) from Lottaroli and Catrullo (2000), classified after Heck and Prins (1987), the stratigraphic marker is placed in the S1 - S2 biostratigraphic zone (Late Danian / Early Selandian).

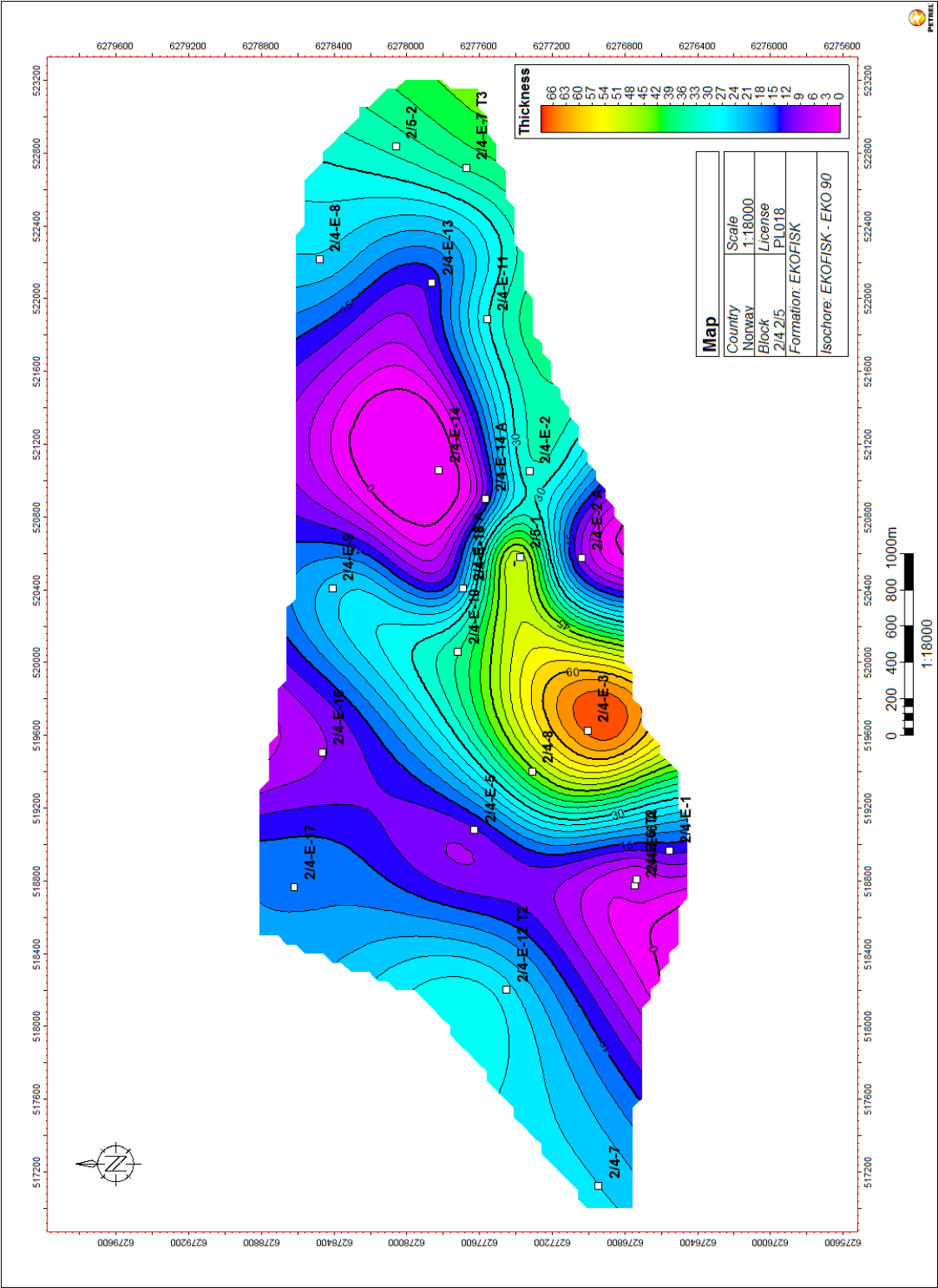


Figure 4.4: isochore map of the Ekofisk interval

4.1.2 Eko 90

Observation and interpretation of the type wells (Gennaro et al., 2011)

The Eko 90 marker was typically placed at an abrupt downhole increase in GR (Figure 4.5). Below the marker, the GR log values decreases towards the Eko 80 marker.

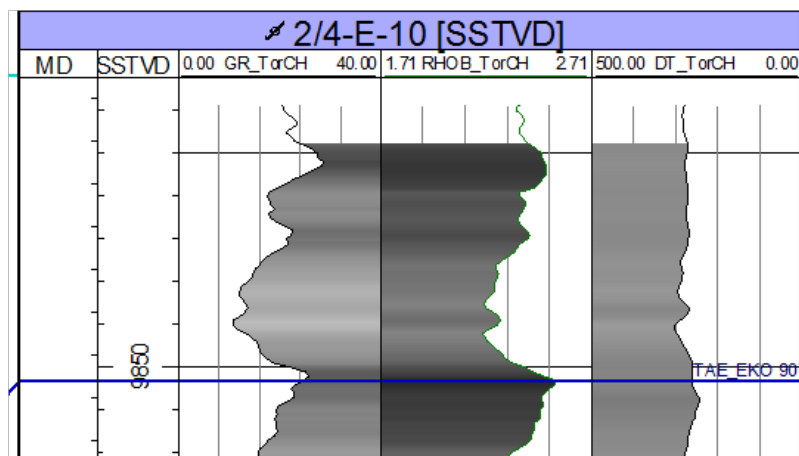


Figure 4.5: Log signature at the Eko 90 marker in well 2/4-E-10.

New correlation

An increase or a high value in the RHO_B log and similar decrease in the DT log, can often be observed at the marker (Figure 4.6).

The interval between Eko 90 and Eko 80 has a relatively similar log response in most wells. Significant thickness changes can be observed, with a maximum thickness of more than 60 feet in well 2/4-E-14 (Figure 4.7). The Eko 90 marker is not present in well 2/5-2, although it was originally included in the regional correlation by Gennaro et al. (2011). The reason for this, will be reviewed in the Discussion (page 71).

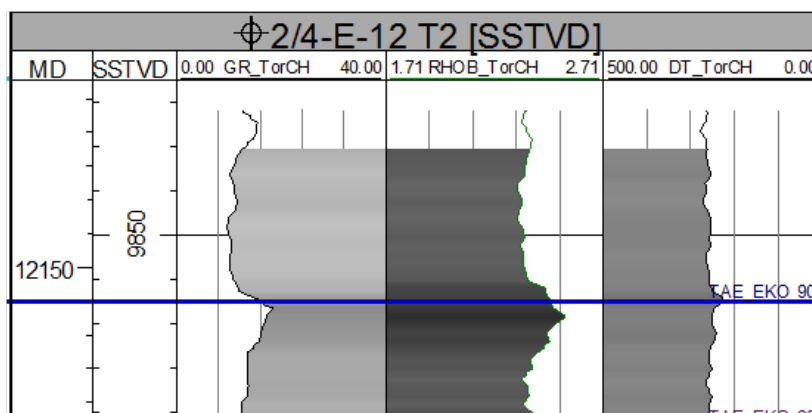


Figure 4.6: Log signature at the Eko 90 marker in well 2/4-E-12 T2.

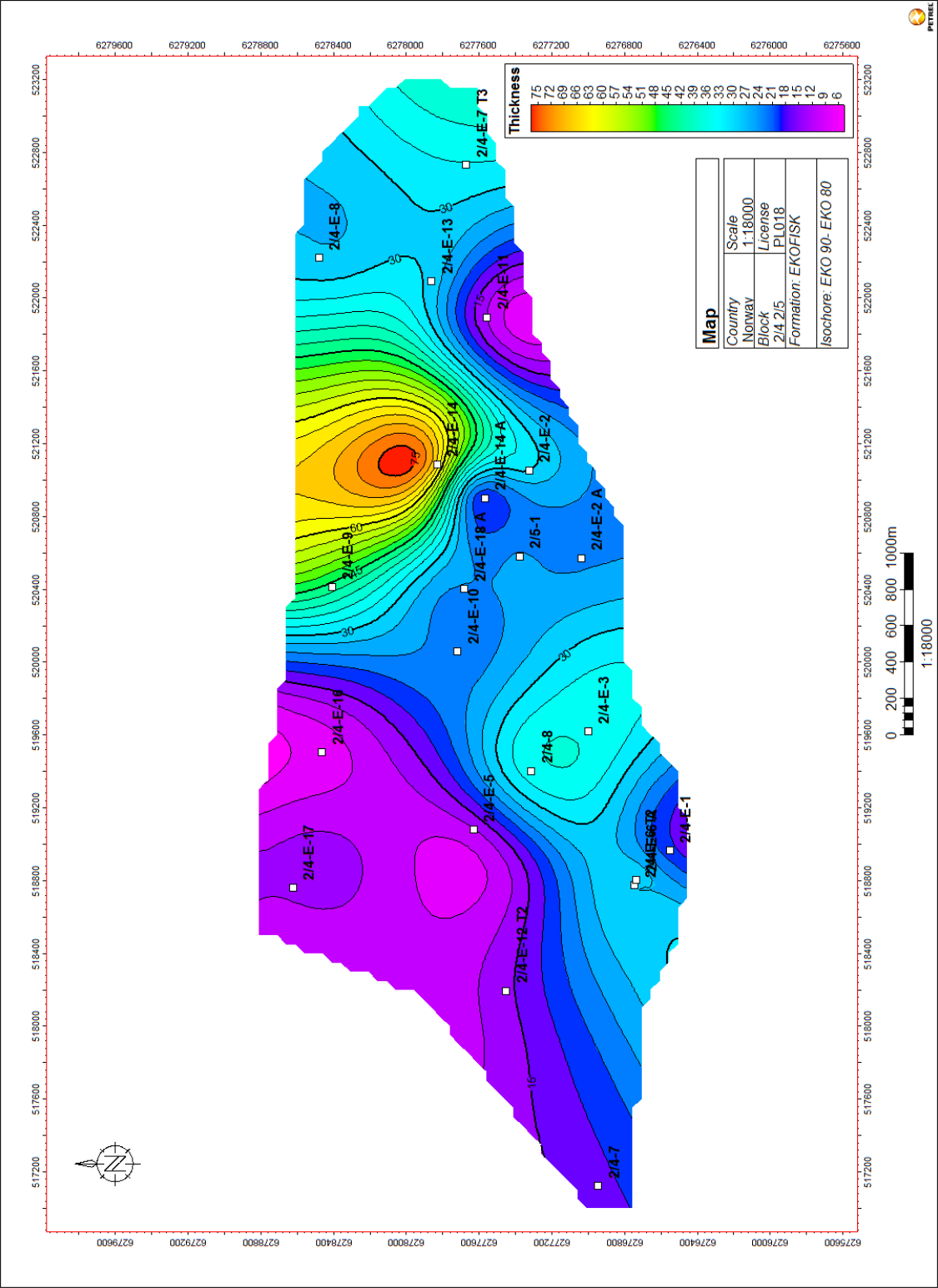


Figure 4.7: Isochore map of the Eko 90 interval

4.1.3 Eko 80

Observation and interpretation of the type wells (Gennaro et al., 2011)

In the type wells the Eko 80 marker was placed on a the lower limit of a density peak, a local GR peak and occasionally in the DT log (Figure 4.8), with a relatively abrupt downhole decrease in GR and RHOB and an increase in the DT log.

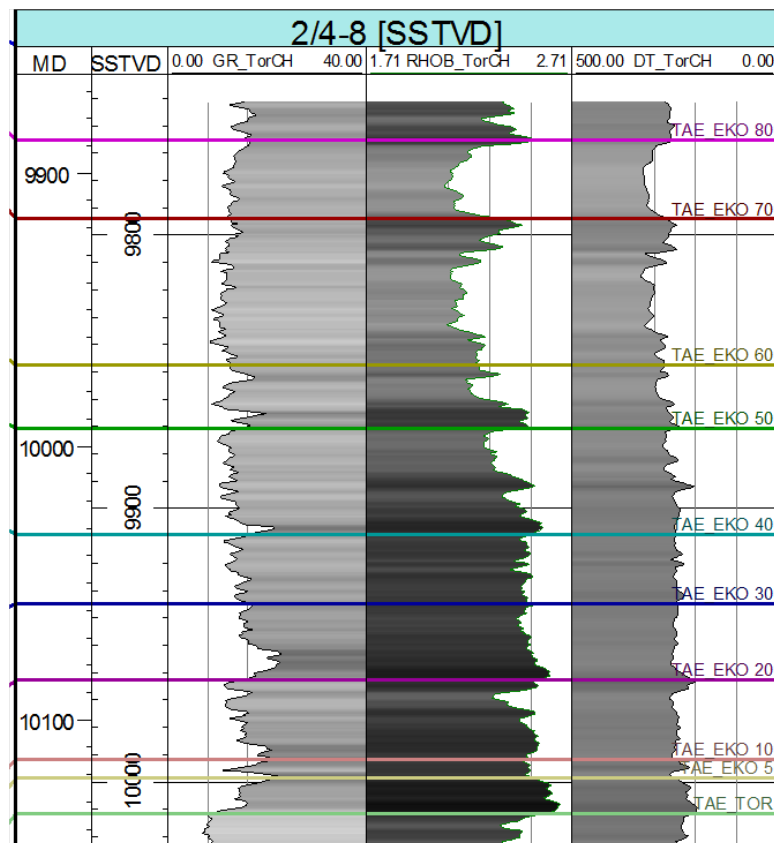


Figure 4.8: *Log signature at the Eko 80 marker (pink color) in well 2/4-8.*

New correlation

Throughout the Tor Field, the Eko 80 marker was placed at a density peak, consistent with the interpretation by (Gennaro et al., 2011). This density peak is just above an interval dominated by clean chalk with low density (Figure 4.3 and 4.8).

In the thickness map of the Eko 80 interval (Figure 4.9), a very low thickness can be observed in the middle of the field. The wells on the Western, Eastern and Southern flanks of the Tor Field, display slightly different log signatures in the Eko 80 to Eko 70 interval than the other wells, due to higher thickness.

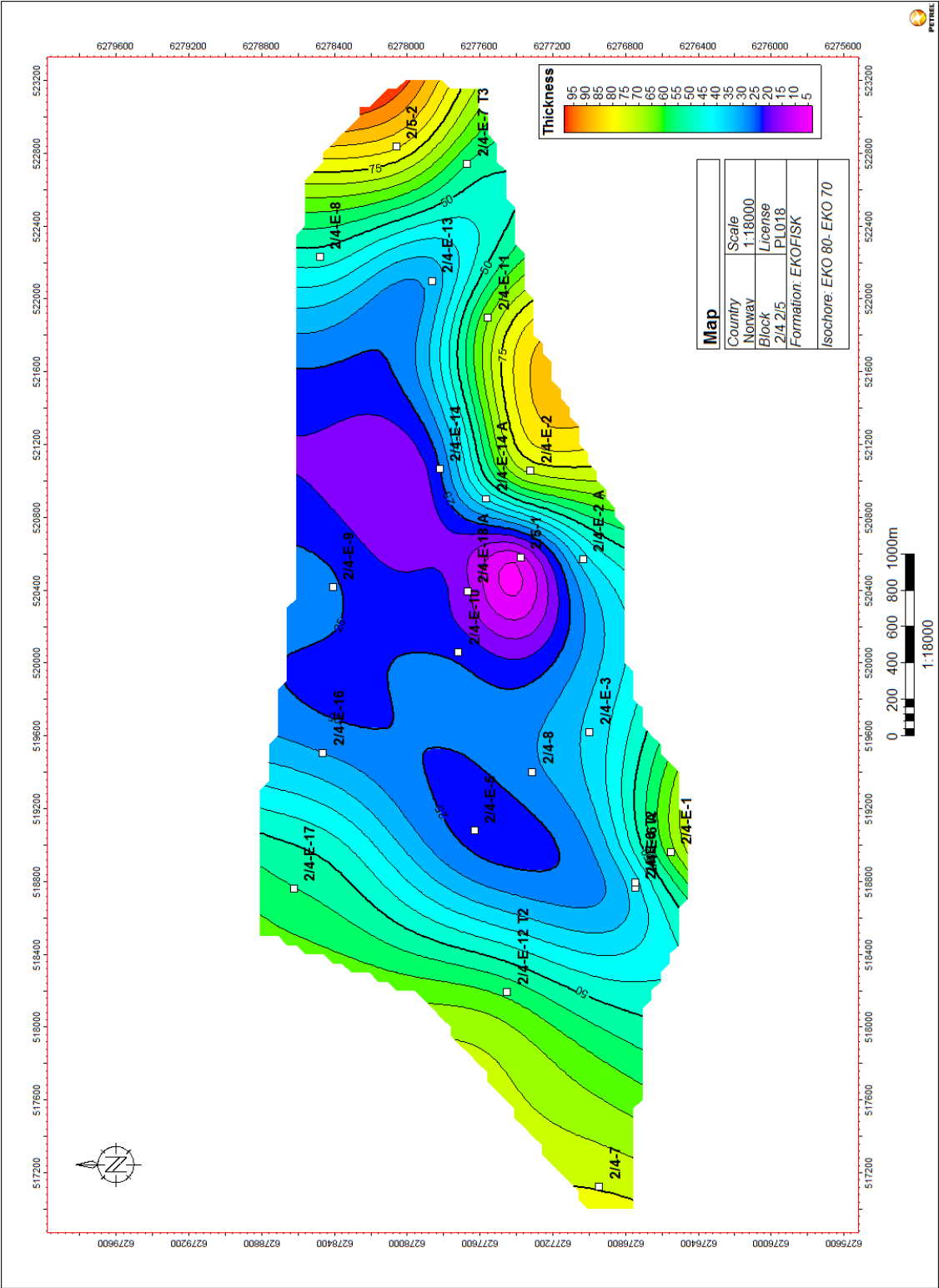


Figure 4.9: Isochore map of the Eko 80 interval

4.1.4 Eko 70

Observation and interpretation of the type wells (Gennaro et al., 2011)

The Eko 70 marker was placed on a increase in the RHOB and GR wireline logs, and a decrease in the DT log (Figure 4.10). Two exceptions are the type wells 2/4-7 and 2/4-8 (Figure 4.8 and 4.11), where the Eko 70 marker was not picked at a local maximum in the GR log. However, RHOB and DT signatures are consistent.

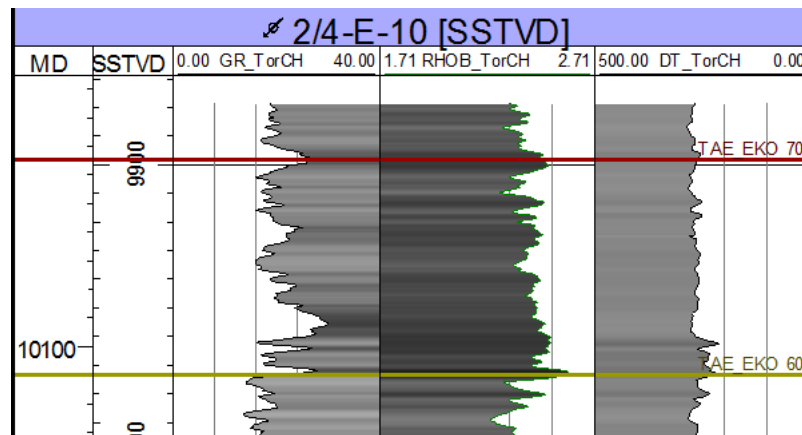


Figure 4.10: Log signature at the Eko 70 marker (red color) in well 2/4-E-10.

New correlation

The marker was easily recognizable by this log signature in most of the wells.

The thickness map of the interval between the Eko 70 and Eko 60 markers (Figure 4.12), displays a thinning trend towards the South-east and a thickening to the North.

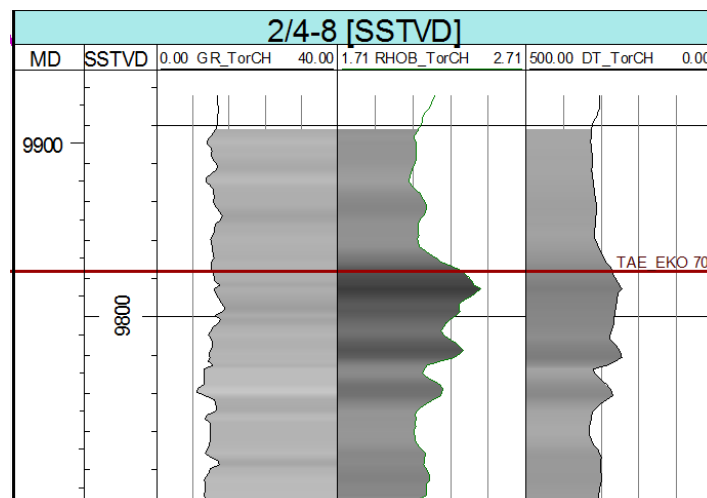


Figure 4.11: Log signature at the Eko 70 marker in well 2/4-8.

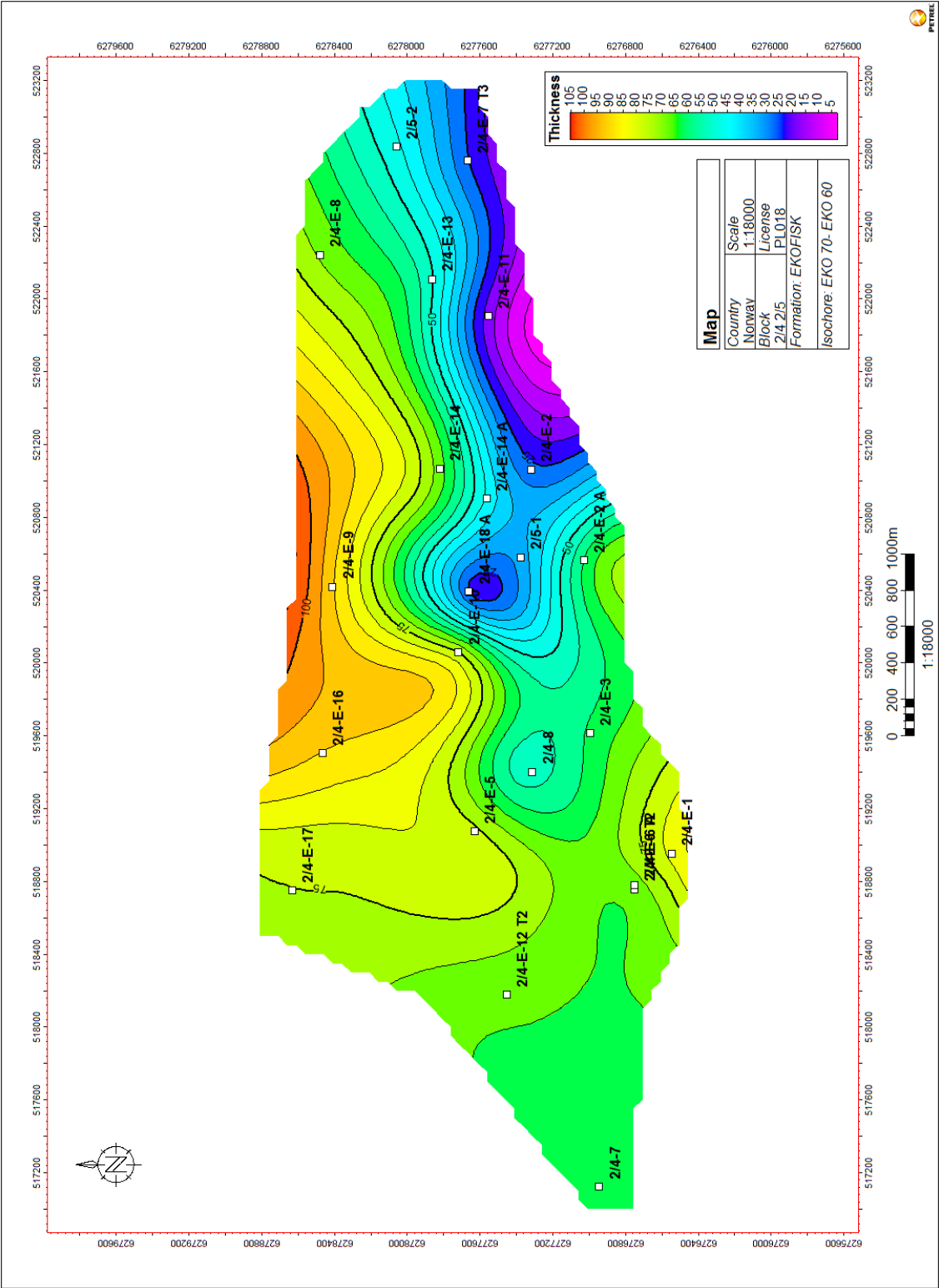


Figure 4.12: Isochore map of the Eko 70 interval

4.1.5 Eko 60

Observation and interpretation of the type wells (Gennaro et al., 2011)

The Eko 60 marker was placed on a peak or a high value in RHOB log, but the GR log in the type wells varied between local minimum and maximum (Figure 4.8 and 4.13).

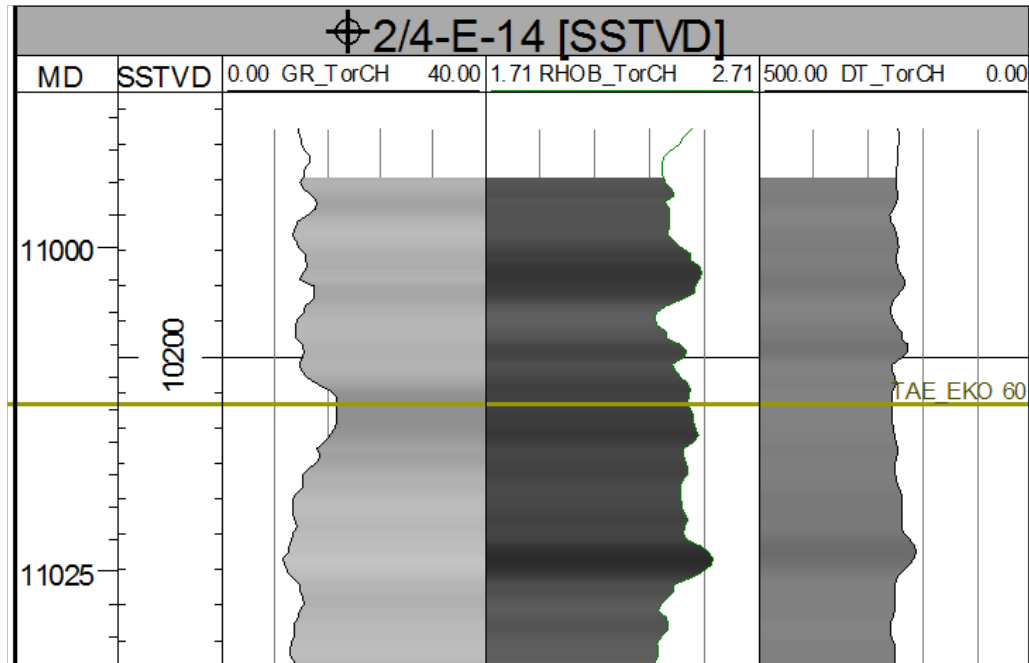


Figure 4.13: Log signature at the Eko 60 marker in well 2/4-E-14.

New correlation

In this correlation, the Eko 60 was placed on a high RHOB log value with a corresponding local maximum in the GR log.

The isochore map of the interval between the Eko 60 and Eko 50 markers (Figure 4.14), display iso-thicknesses along a South-west - North-east axis with a general thinning to the South-east.

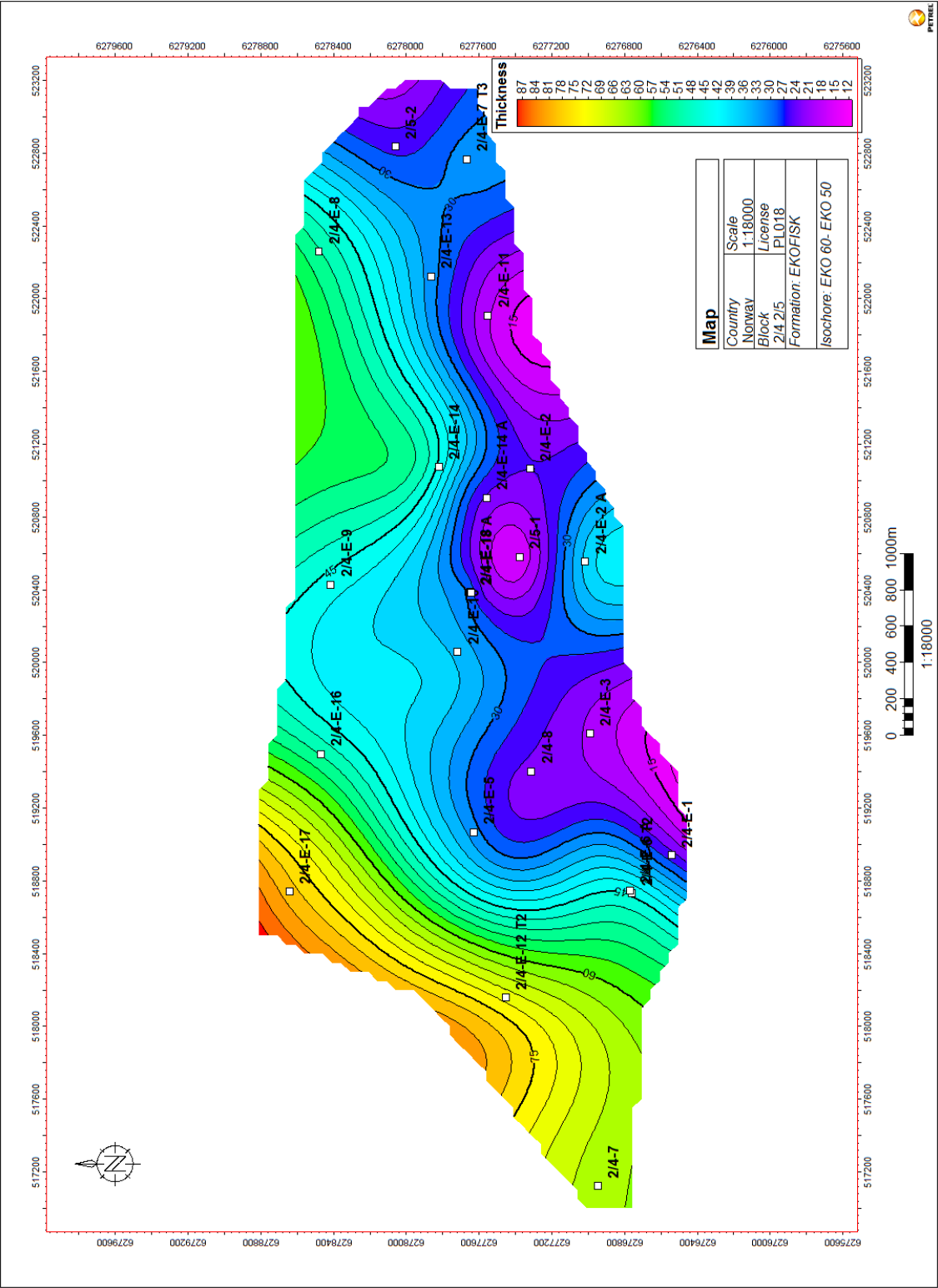


Figure 4.14: Isochore map of the Eko 60 interval

4.1.6 Eko 50

Observation and interpretation of the type wells (Gennaro et al., 2011)

The Eko 50 marker was placed at a peak in the GR, RHOB and DT logs, above a section of clean chalk (low GR), in the type wells (Figure 4.10 and 4.15). The Eko 50 interval is dominated by clean chalk and the next GR peak downhole is interpreted as the Eko 40 surface.

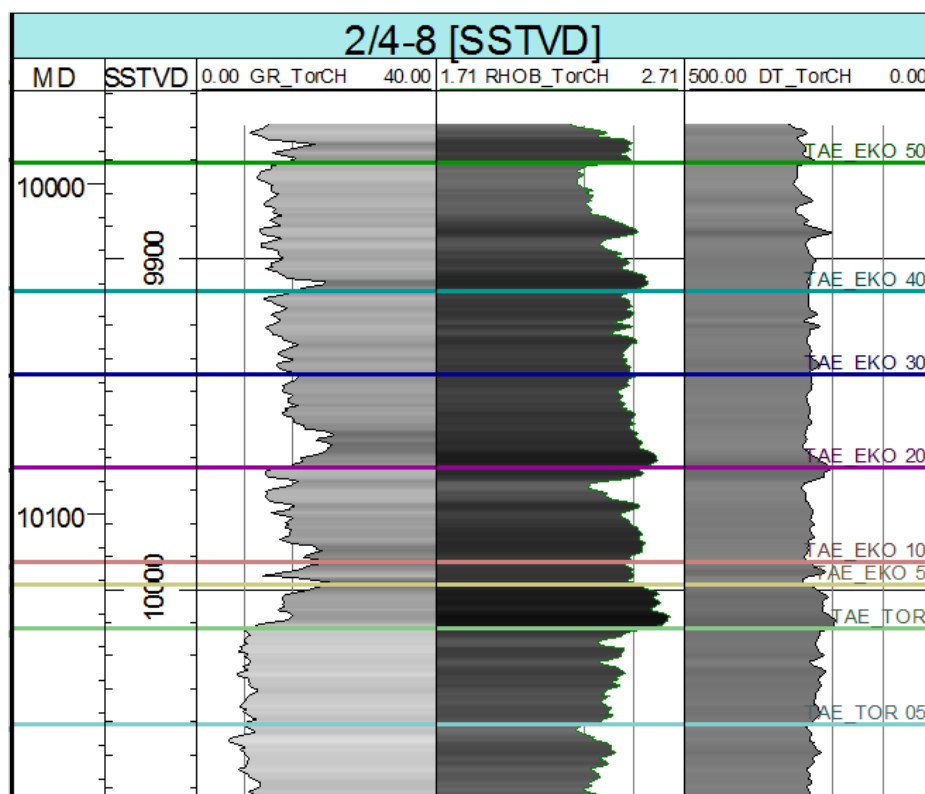


Figure 4.15: Log signature at the Eko 50 marker (green color) in well 2/4-8.

New correlation

The Eko 50 marker is positioned almost in the middle of the Ekofisk Formation and has a distinct log signature in all the wells on the Tor Field.

The thickness map of the Eko 50 interval shows an increasing thickness towards the North-east of the Tor Field (Figure 4.16).

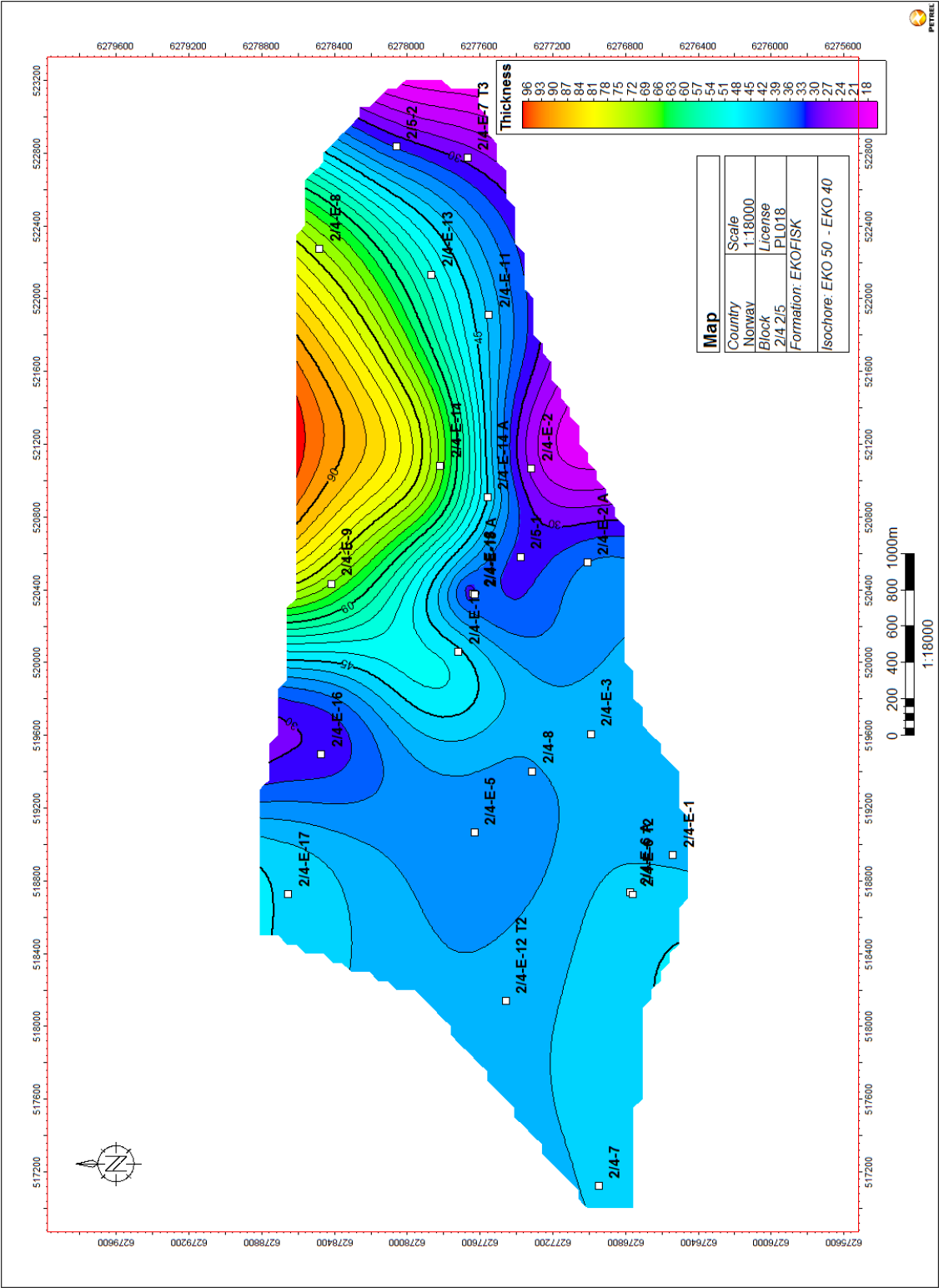


Figure 4.16: Isochore map of the Eko 50 interval

4.1.7 Eko 40

Observation and interpretation of the type wells (Gennaro et al., 2011)

The Eko 40 marker is placed on a peak in the GR log and a relatively high RHOB value (Figure 4.17). The interval from the Eko 40 marker and down to the Eko 30 marker, is characterized by a downhole rapid decrease in GR value (Figure 4.15).

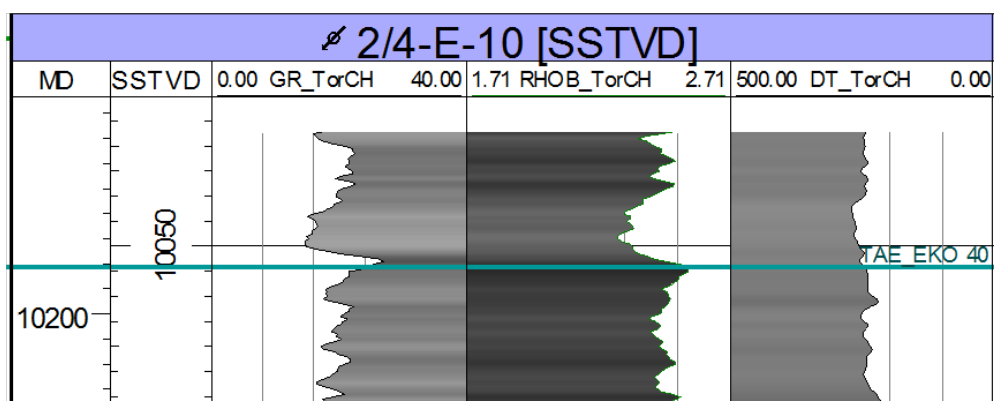


Figure 4.17: Log signature at the Eko 40 marker in well 2/4-E-10.

New correlation

The placement of the Eko 40 marker was difficult in the Southern wells of the Tor Field, with variations in log signatures. In some wells had a local maximum in GR value, but not a corresponding maximum in RHOB (Figure 4.18). The Eko 40 isochore map, display strong thickness variations (Figure 4.19). These thickness variations could indicate that the Eko 40 or Eko 30 markers are not correlated consistently throughout the Tor Field, especially in the Southern part, perhaps due to the variations in wireline log signatures.

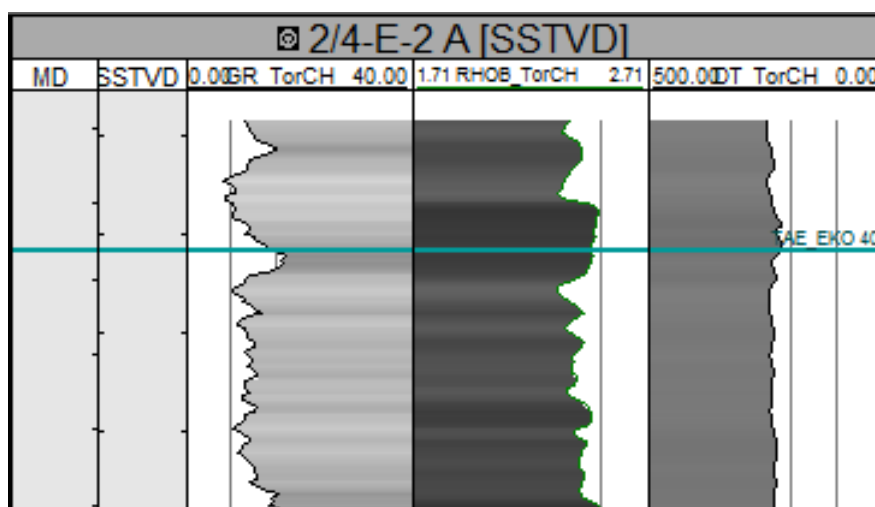


Figure 4.18: Log signature at the Eko 40 marker in well 2/4-E-2 A.

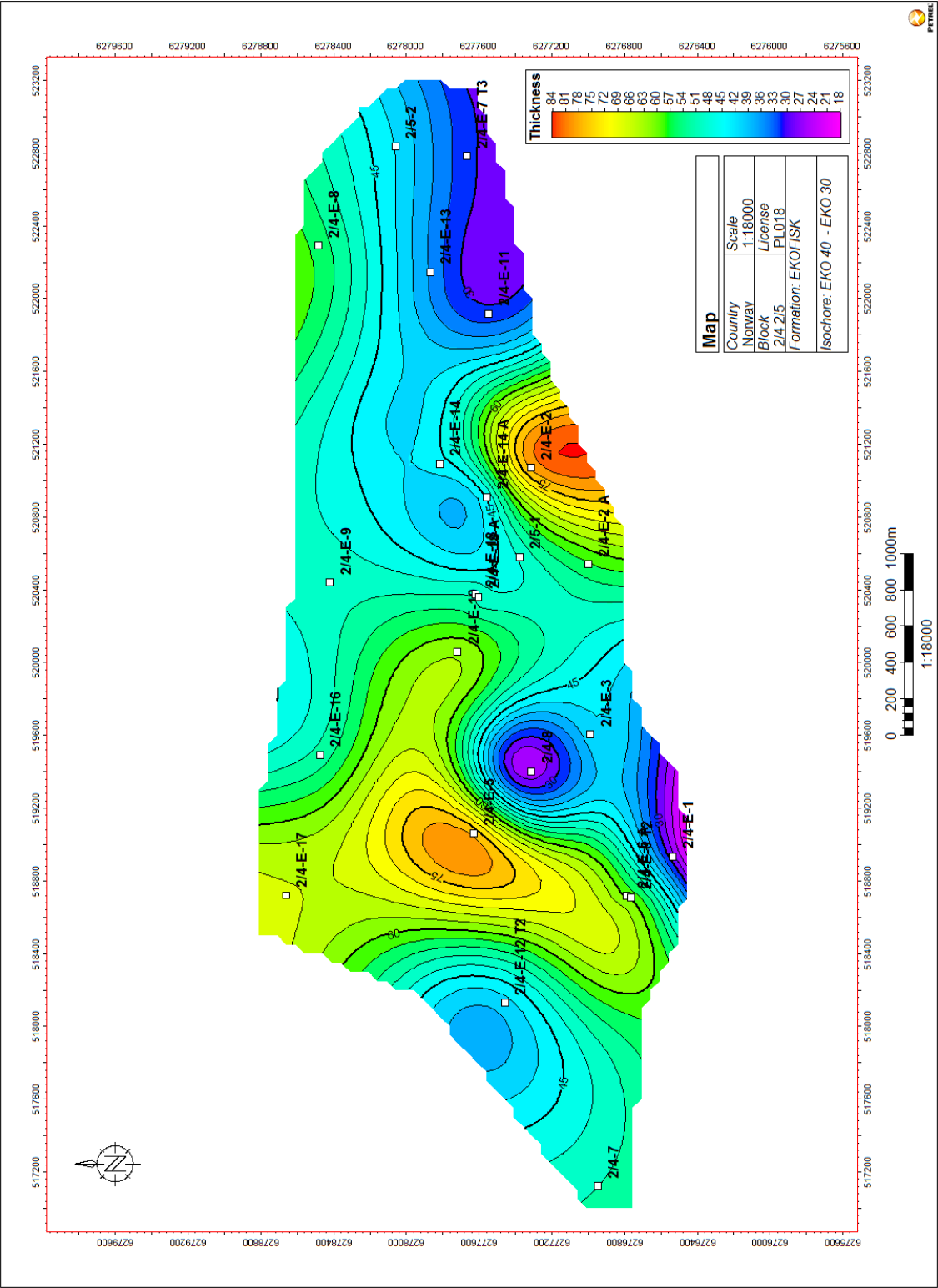


Figure 4.19: Isochore map of the Eko 40 interval

4.1.8 Eko 30

Observation and interpretation of the type wells (Gennaro et al., 2011)

In some of the type wells, the Eko 30 marker is placed at a peak in the GR log (Figure 4.20 and 4.21) and in other wells at a local peak (Figure 4.15). Below the marker, the RHOB log has a high value down to the Eko 20 marker below.

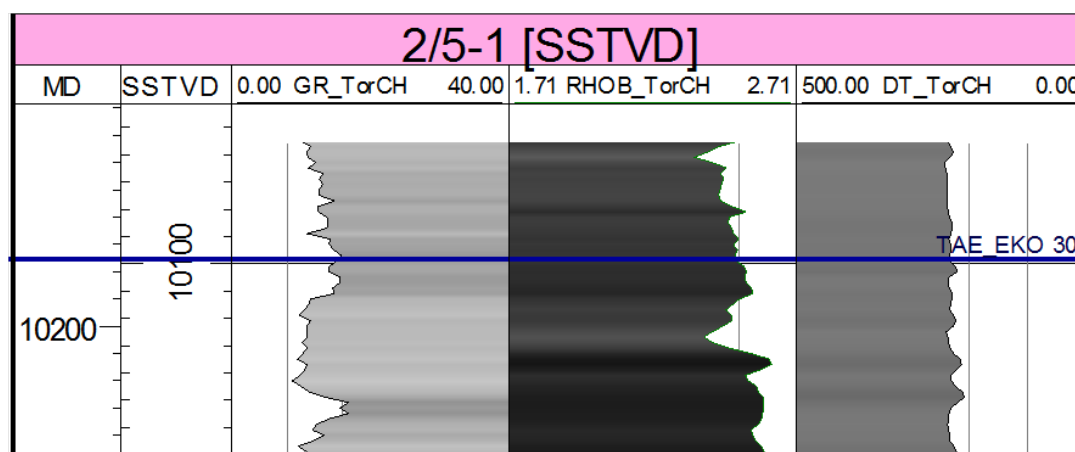


Figure 4.20: Log signature at the Eko 30 marker in well 2/5-1.

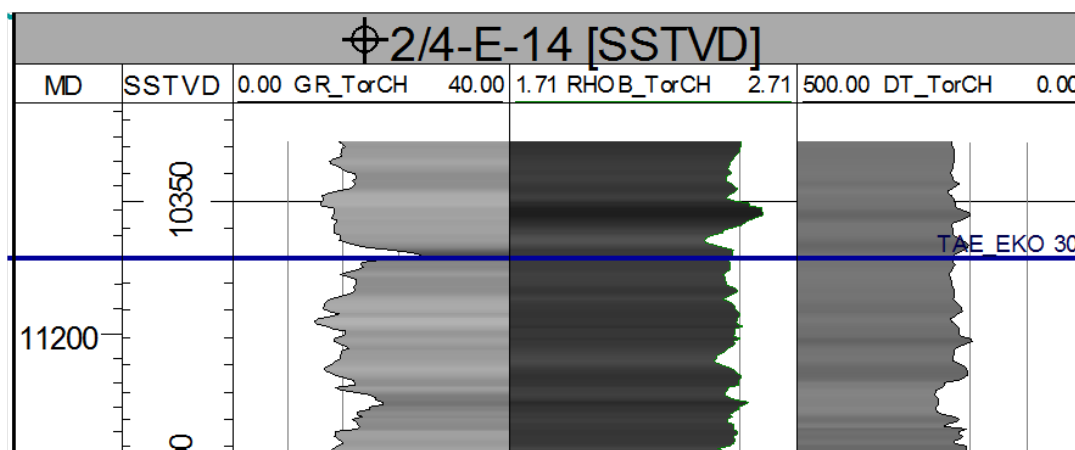


Figure 4.21: Log signature at the Eko 30 marker in well 2/4-E-14.

New correlation

Since the GR log signatures from the type wells varied, the Eko 30 marker was placed on a local GR maximum.

The isochore map of the Eko 30 interval shows higher interval thickness in wells 2/4-E-10 and 2/4-E-9 (Figure 4.22).

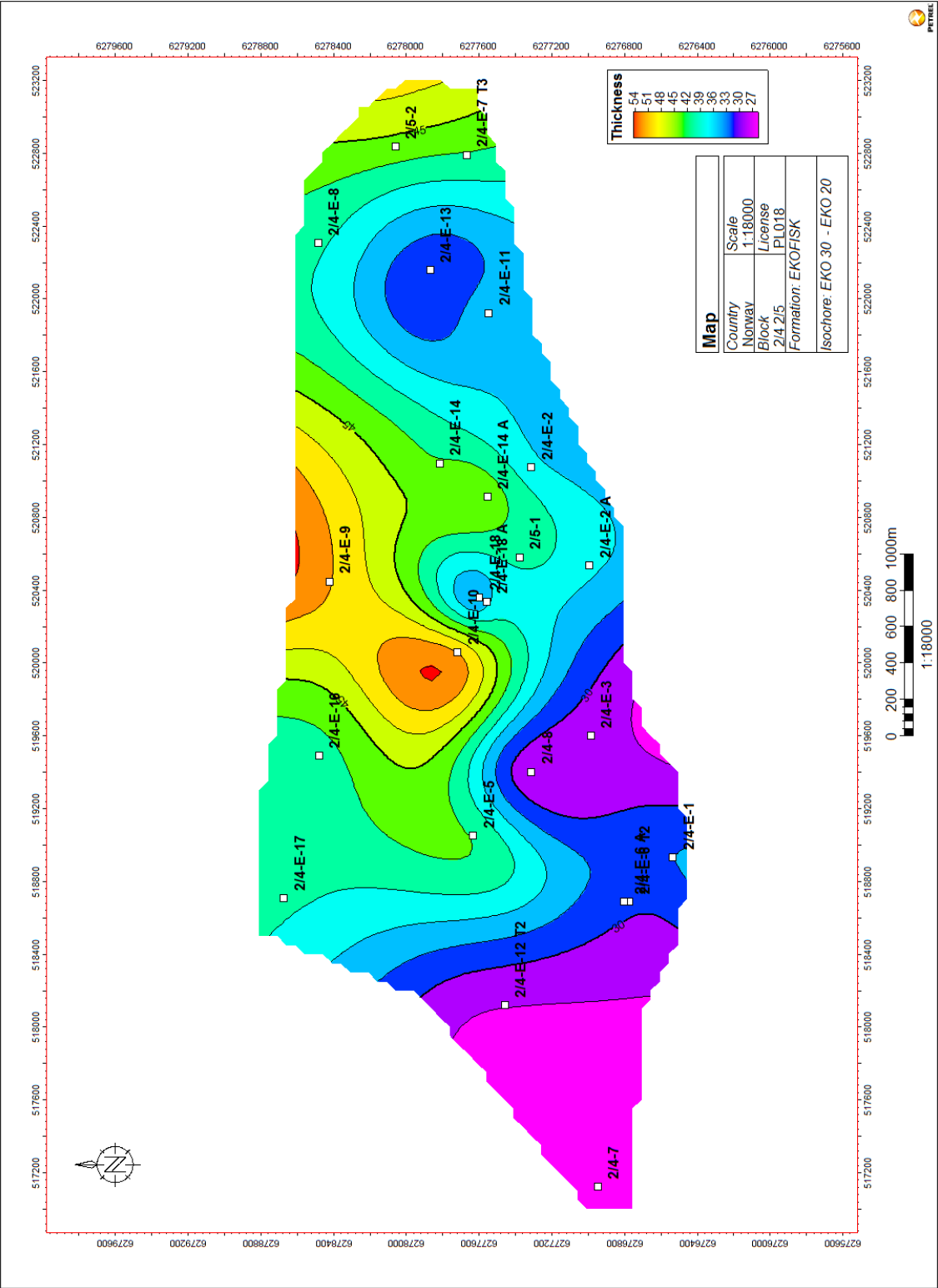


Figure 4.22: Isochore map of the Eko 30 interval

4.1.9 Eko 20

Observation and interpretation of the type wells (Gennaro et al., 2011)

The Eko 20 marker is interpreted at a GR minimum. Above the interpreted Eko 20 marker, the GR log increases sharply and reaches a local peak (Figure 4.23 and 4.24). The RHOB log shows a density peak, which also manifests itself as local minimum of the sonic log.

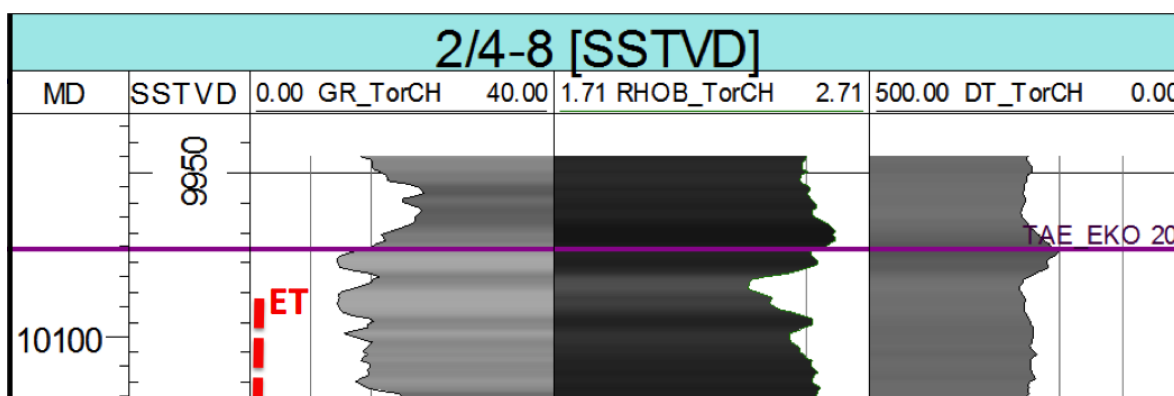


Figure 4.23: Log signature at the Eko 20 marker in well 2/4-8. The upper part of the Ekofisk Tight Zone (ET) is shown in the log display (red stippled line).

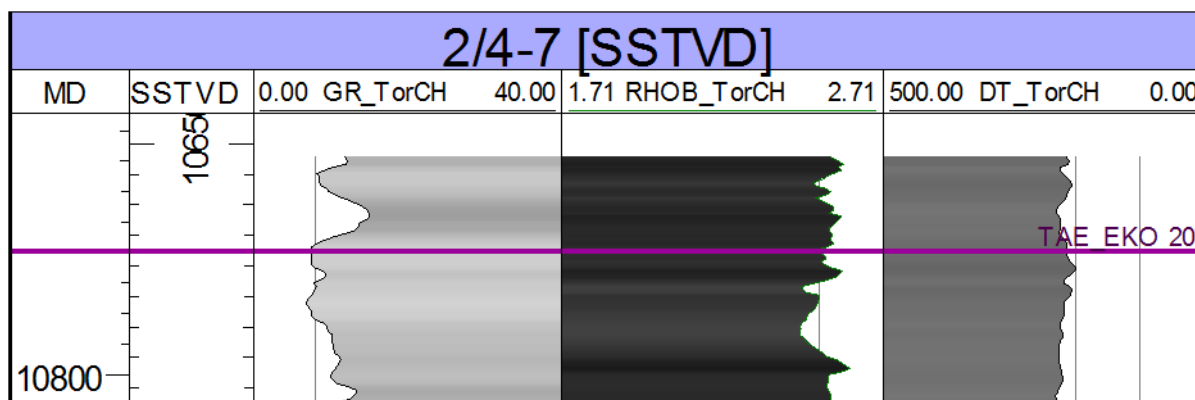


Figure 4.24: Log signature at the Eko 20 marker in well 2/4-7.

New correlation

Within the Eko 20 interval, the upper boundary of the Ekofisk Tight Zone is interpreted in the lithostratigraphic correlation (Figure 4.23). The Eko 20 marker is interpreted, throughout the Tor Field, on a local minimum in the GR log between the clay-rich tight zone below and a new local maximum above (Figure 4.15). The isochore map in Figure 4.25 shows that the type well 2/4-E-10 has a significantly higher Eko 20 interval thickness, than the rest of the wells.

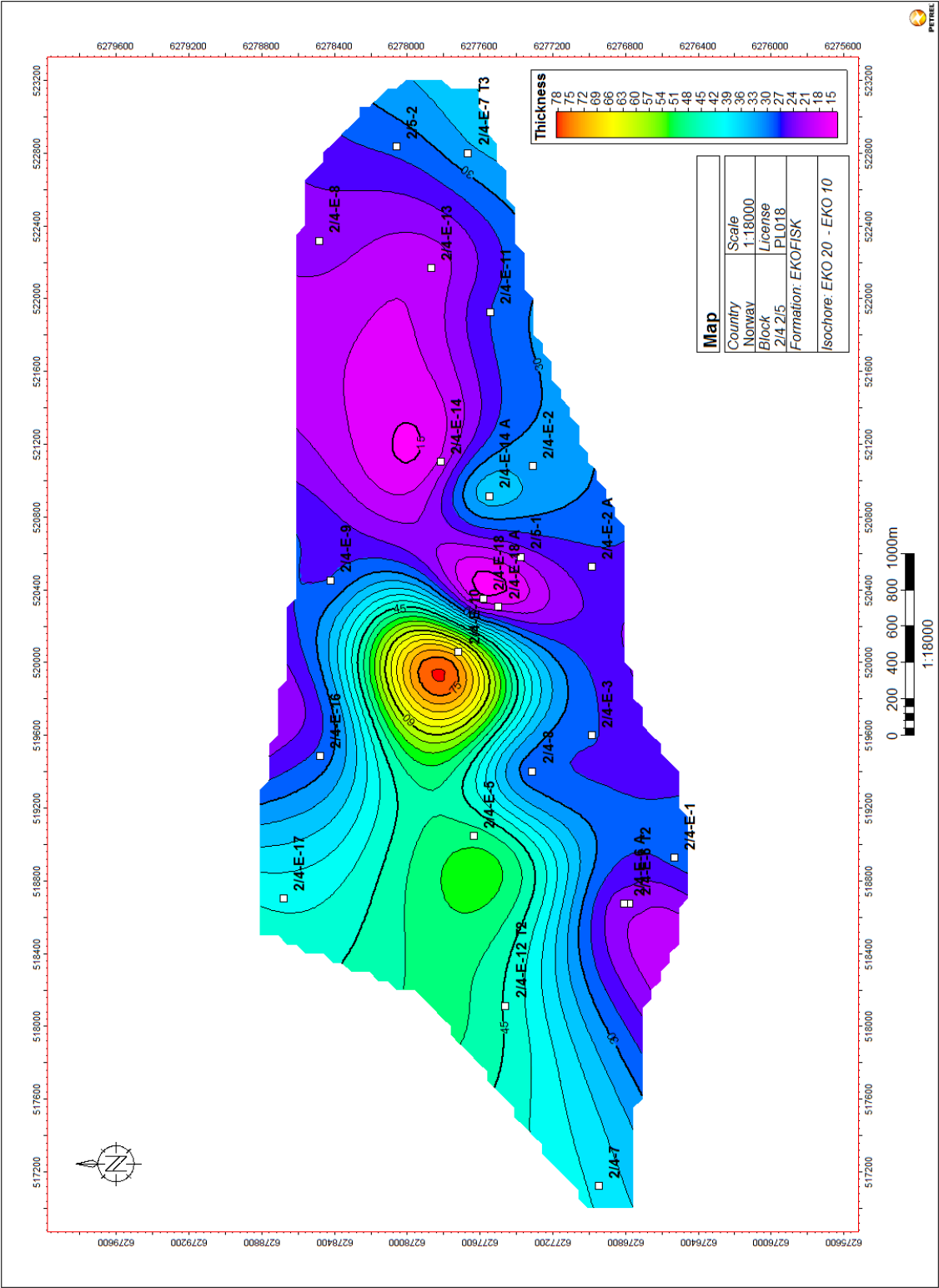


Figure 4.25: Isochore map of the Eko 20 interval

The Eko 10 marker is placed at the first GR peak downwards from the top of the tight zone (Figure 4.26). Above the Eko 10 marker there is a decrease in the GR log towards the Eko 20 marker (Figure 4.15).

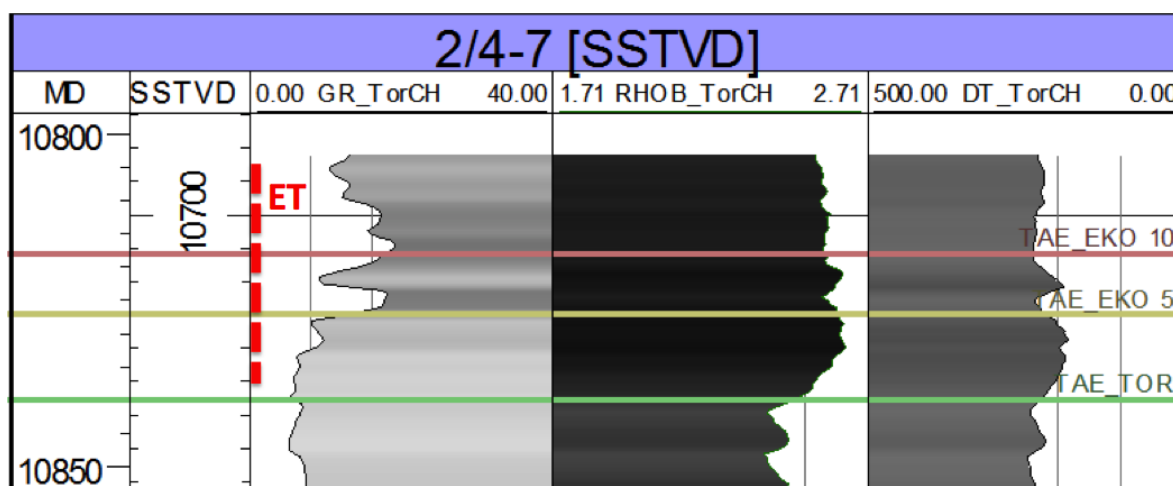


Figure 4.26: *Log signature at the Eko 10 marker (red color) in well 2/4-7. The Ekofisk Tight Zone (ET) is marked in the log display with a red stippled line.*

The Eko 10 marker is a key surface in this correlation, as it is placed close to the uppermost limit of the Tight Zone and it is easily recognized in the GR log (Figure 4.26). The Ekofisk Tight Zone was deposited at the Cretaceous - Tertiary (K-T) boundary, which represent an important sequence boundary separating the Ekofisk Formation from the Tor Formation. The zone contains high amounts of argillaceous material, as seen in the large increase in the GR readings. In addition, the zone is characterized by high density values (TorCh-project, 2007).

The Tight Zone represents a period of very low sedimentation rates, high degree of bioturbation and hardground development. At the K-T boundary, the sea level in the Central Graben area had a relative drop, which led to more clastic influx (TorCh-project, 2007).

The Eko 10 interval, includes the main part of the Tight Zone from the Eko 10 marker down to the Eko 5 marker. In all the wells on the Tor Field, the GR log between the two mentioned markers display one or more local minimums within the tight zone (Figure 4.26).

The Eko 10 interval is relatively thin with an average thickness of around 30 feet (Figure 4.27). The highest interval thickness can be observed in wells 2/4-E-2 and 2/4-E-8.

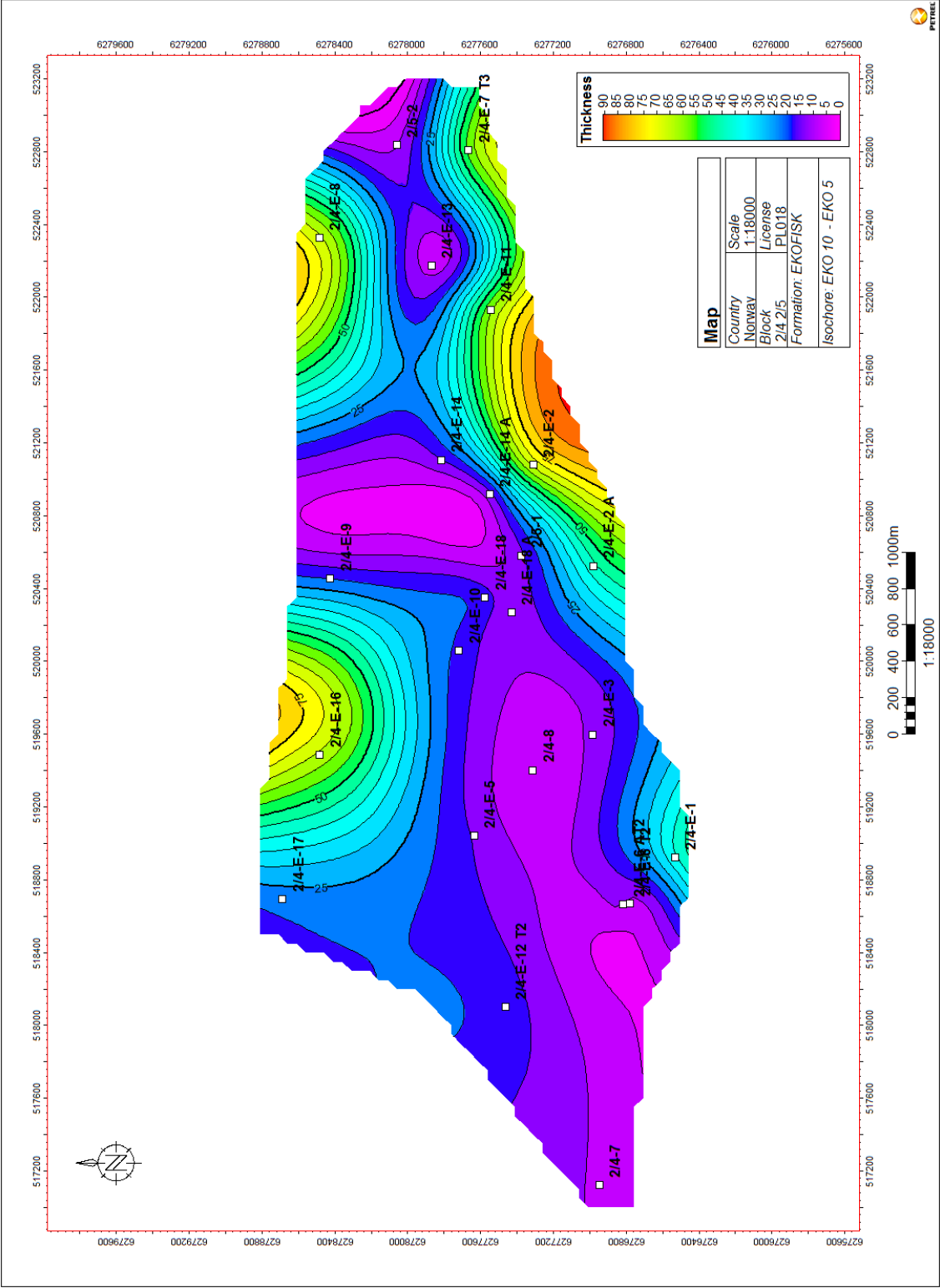


Figure 4.27: Isochore map of the Eko 10 interval

4.1.11 Eko 5

Observation and interpretation of the type wells (Gennaro et al., 2011)

The Eko 5 marker is placed at the lowermost local maximum on the GR log within the Tight Zone. Below the position of the marker, the GR log value decreases towards the top Tor marker (Figure 4.28). In some type wells the marker is not placed in the apex of the GR peak, but instead put at the sharp decrease in the GR log below the maximum peak (Figure 4.26).

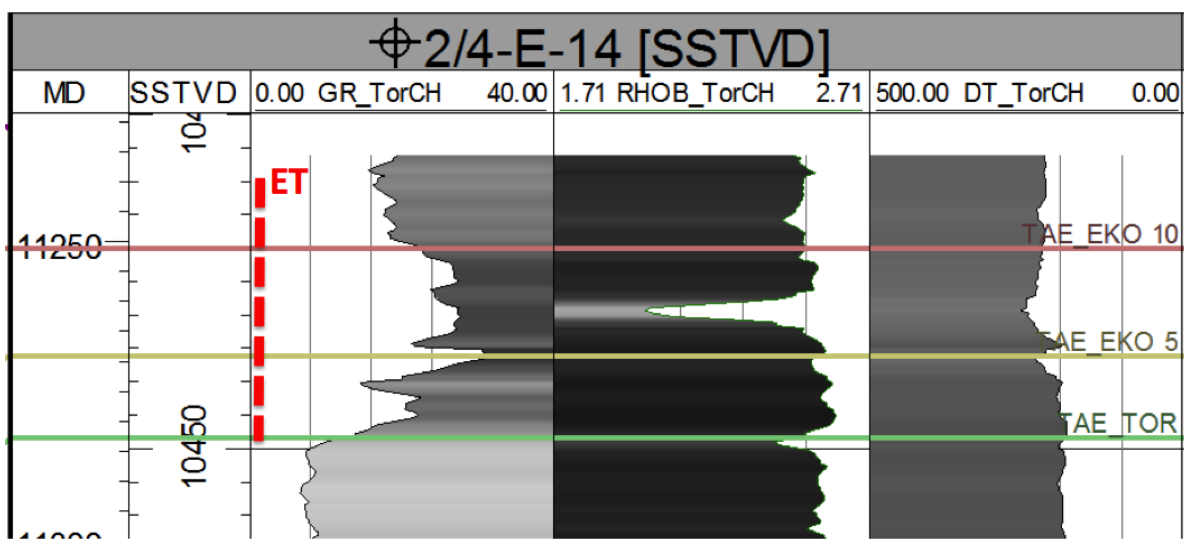


Figure 4.28: Log signature at the Eko 5 marker (yellow color) in well 2/4-E-14. The Ekofisk Tight Zone (ET) is marked in the log display with a red stippled line.

New correlation

The Eko 5 marker is another key surface within the Ekofisk Tight Zone, placed at a GR peak (Figure 4.28). The isochore map of the Eko 5 interval (Figure 4.29), shows a relatively uniform thickness distribution with an average thickness of around 10-15 feet. A thickness increase can be observed in well 2/5-2.

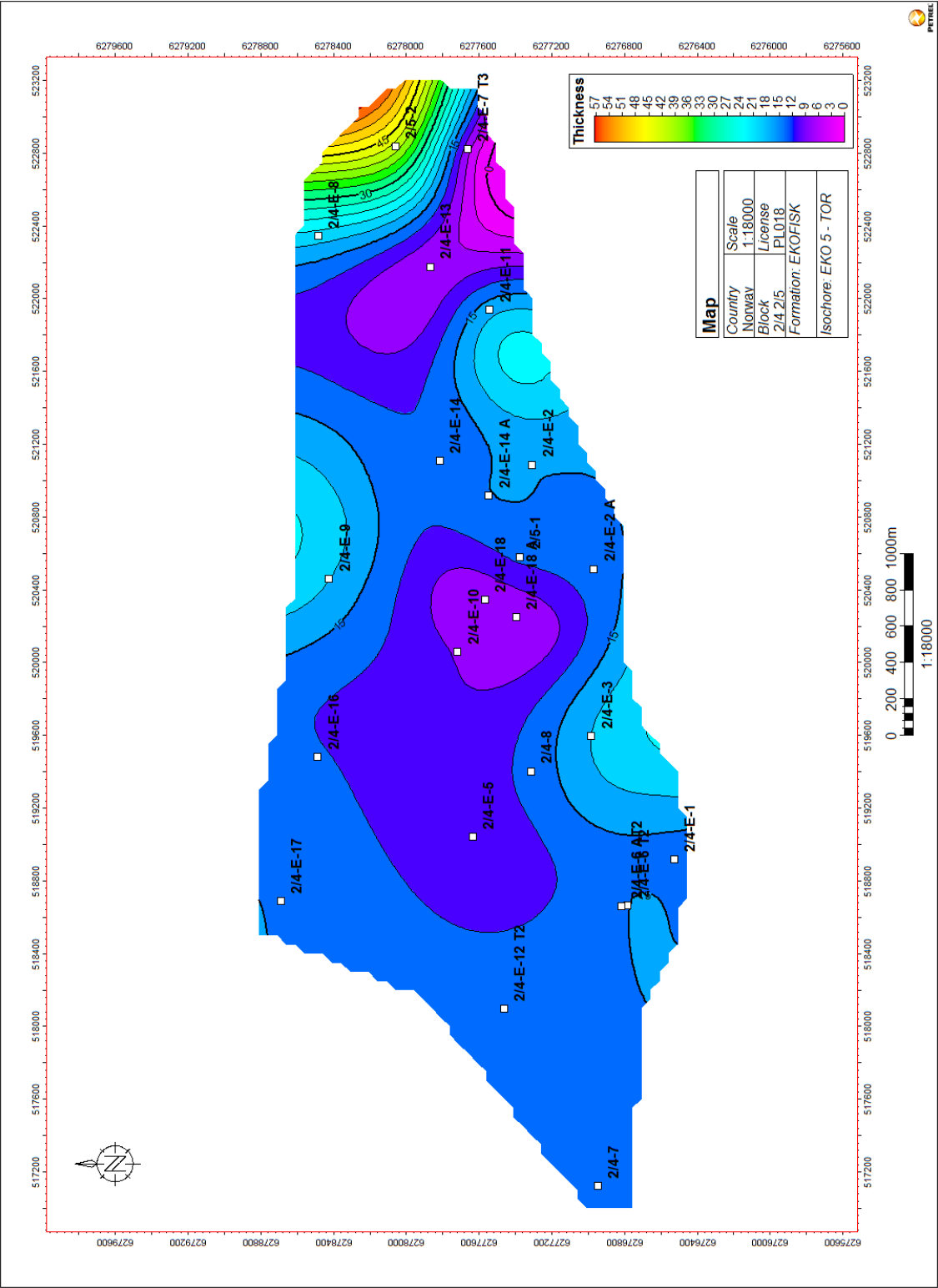


Figure 4.29: Isochore map of the Eko 5 interval

4.1.12 Top Tor

Observation and interpretation of the type wells (Gennaro et al., 2011)

The Top Tor marker is picked at the top of the clean, massive chalk below the Eko 5 marker (Figure 4.30 and 4.31).

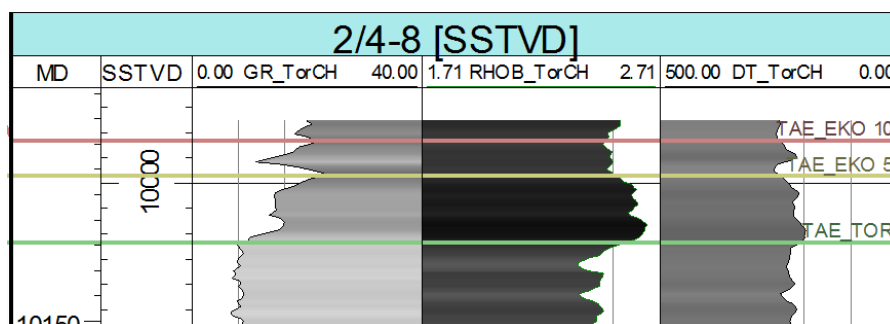


Figure 4.30: Log signature at the Tor marker (green color) in well 2/4-8.

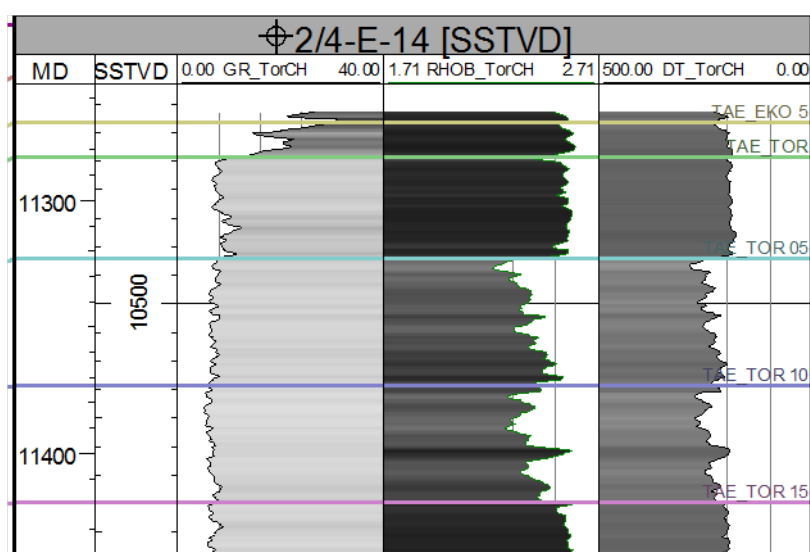


Figure 4.31: Log signature at the Tor marker (light green) in well 2/4-E-14.

New correlation

The Tor marker is a key surface in this correlation and it represents the boundary between the Tor and Ekofisk Formation. In all of the Tor Field wells, it is placed at the top of the clean massive chalk, which is consistent with the type wells. The chalk in the Tor Formation has a lower clay content than chalk in the Ekofisk Formation. The GR log shows very little variation within the entire Tor Formation. Wells 2/4-E-6 T2 and 2/4-E-6 AT2 displays the highest Top Tor interval thickness (Figure 4.32)

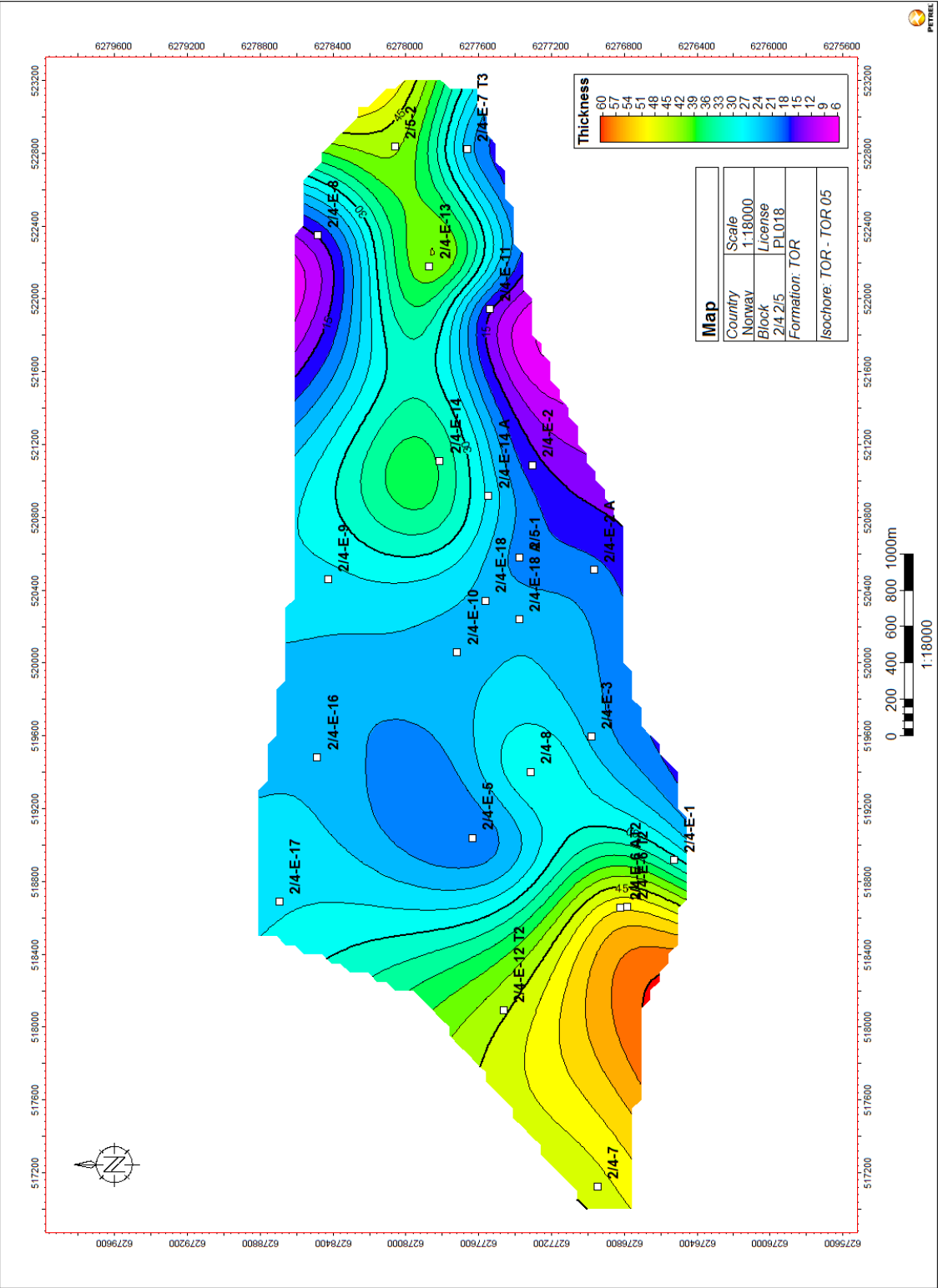


Figure 4.32: Isochore map of the Tor interval

4.1.13 Tor 05

Observation and interpretation of the type wells (Gennaro et al., 2011)

The Tor 05 marker is in most wells placed in the middle or at the base on a density peak in the RHOB log, with a sharp decrease just below the marker (Figure 4.33 and 4.34). The inverse pattern can be observed in the DT log. When correlating the Tor 05 marker, the GR was not used as a criteria, as it shows both small local minimums and maximum in the different wells (Figure 4.33 and 4.34).

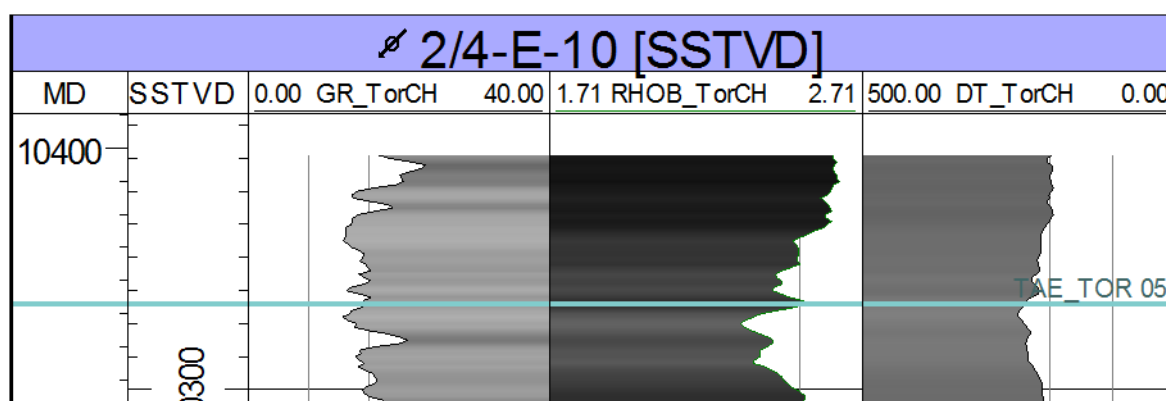


Figure 4.33: Log signature at the Tor 05 marker in well 2/4-E-10.

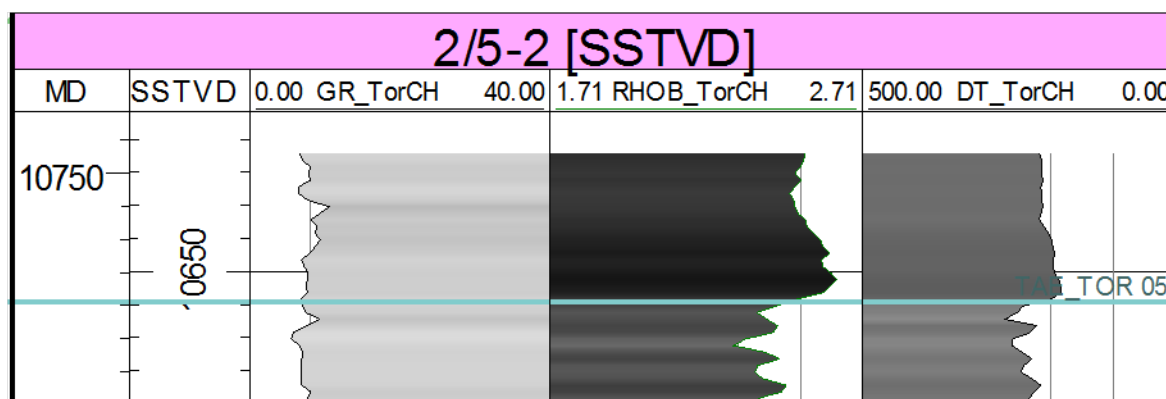


Figure 4.34: Log signature at the Tor 05 marker in well 2/5-2.

New correlation

The isochore map for the Tor 05 interval, have similar thickness along a West-East trend with thinning towards the North (Figure 4.35). Well 2/4-E-7 T3 has the highest Tor 05 interval thickness in the Tor Field.

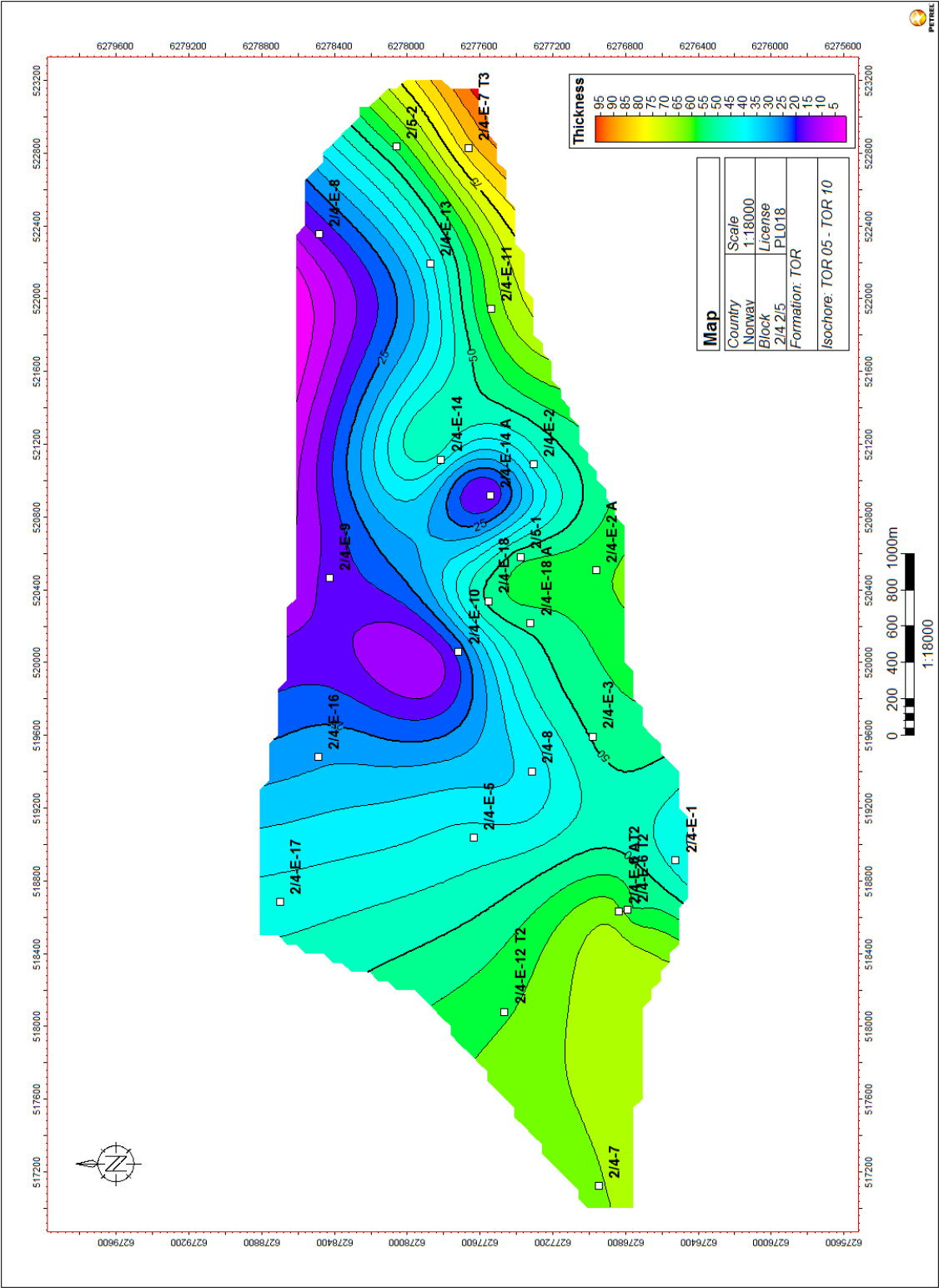


Figure 4.35: Isochore map of the Tor 05 interval

4.1.14 Tor 10

Observation and interpretation of the type wells (Gennaro et al., 2011)

The Tor 10 marker is normally placed on a sharp decrease in the RHOB log and an increase in DT (Figure 4.36 and 4.37).

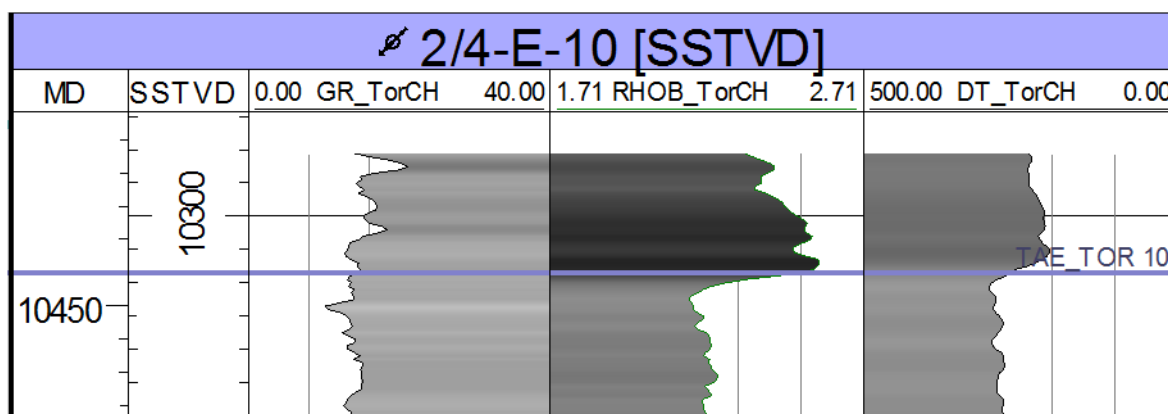


Figure 4.36: Log signature at the Tor 10 marker in well 2/4-E-10.

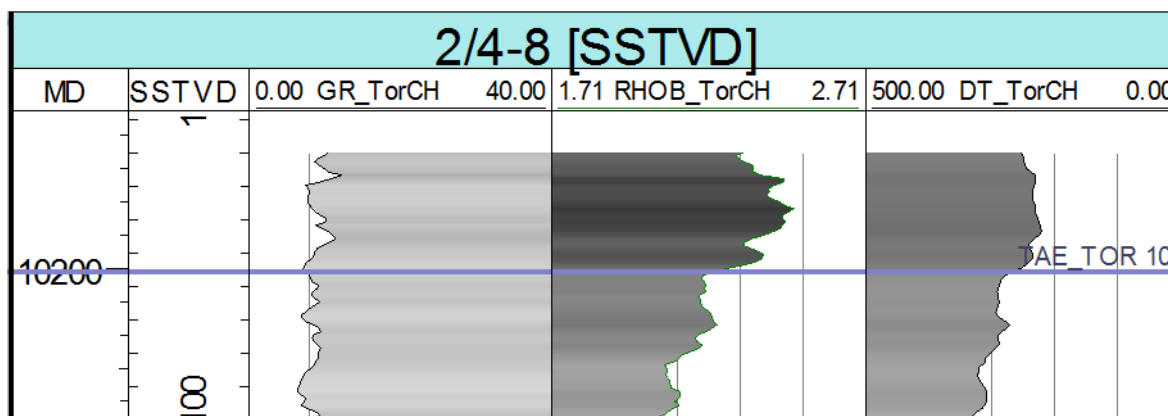


Figure 4.37: Log signature at the Tor 10 marker in well 2/4-8.

New correlation

The Tor 10 marker was correlated and placed in the remaining wells of the Tor Field, on the same log signature as displayed the type wells. The wireline logs from the Tor 10 interval generally displays an overall low, sometimes decreasing, density and a corresponding mirrored sonic log response (Figure 4.37). A West to East isochore trend, with thinning towards the North, can be seen in the thickness map (Figure 4.38).



4.1.15 Tor 15

Observation and interpretation of the type wells (Gennaro et al., 2011)

The wireline log response at the Tor 15 marker is interpreted, shows an abrupt downhole increase in RHOB and decrease in DT logs (Figure 4.39). The GR log shows typically very little variation in this interval and cannot be used for the purpose of correlation.

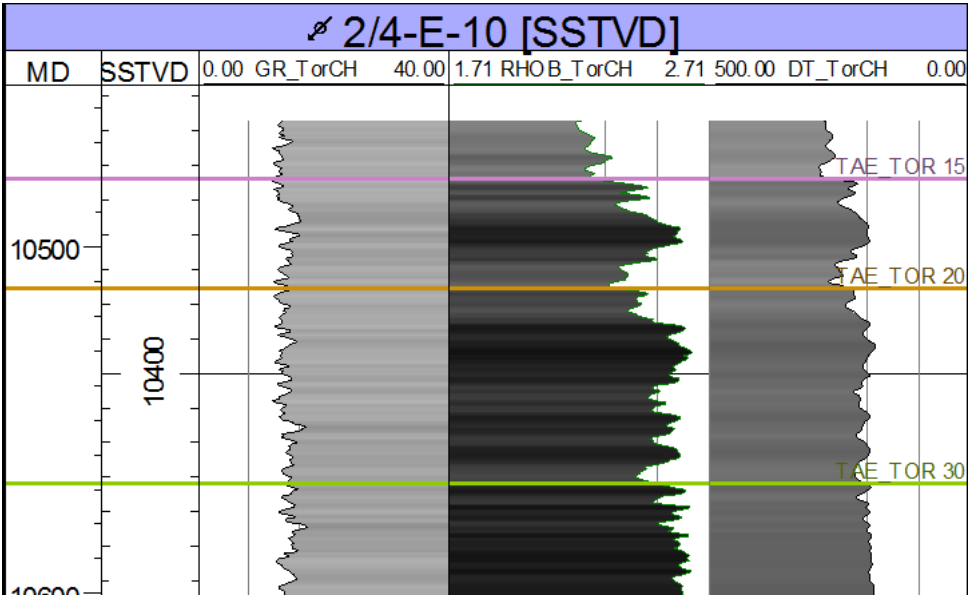


Figure 4.39: Log signature at the Tor 15 marker (pink color) in well 2/4-E-10.

New correlation

The Tor 15 marker is correlated in all wells, based on the same log signatures as in the type wells (Figure 4.40). However, the log signatures in the Tor 15 interval vary in different wells. The RHOB log in the interval displays little downhole variation, slightly increasing and slightly decreasing trend depending on the well. Some wells display a large maximum peak in RHOB log reading of this interval (Figure 4.39). The isochore map display many thickness anomalies and varying thickness throughout the Tor Field (Figure 4.41).

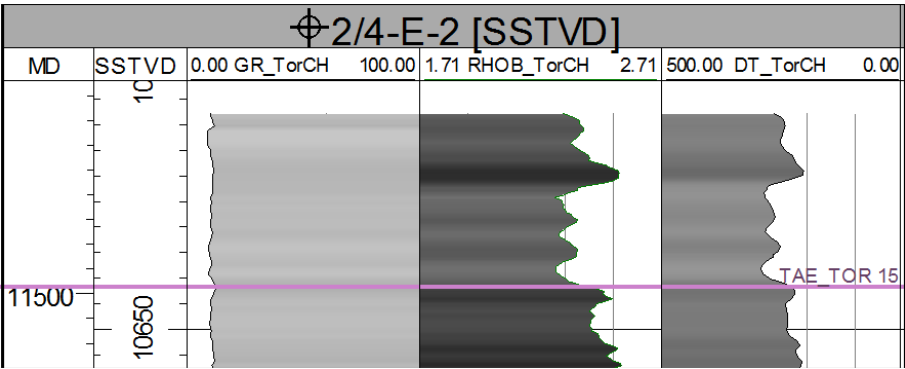


Figure 4.40: Log signature at the Tor 15 marker in well 2/4-E-2.

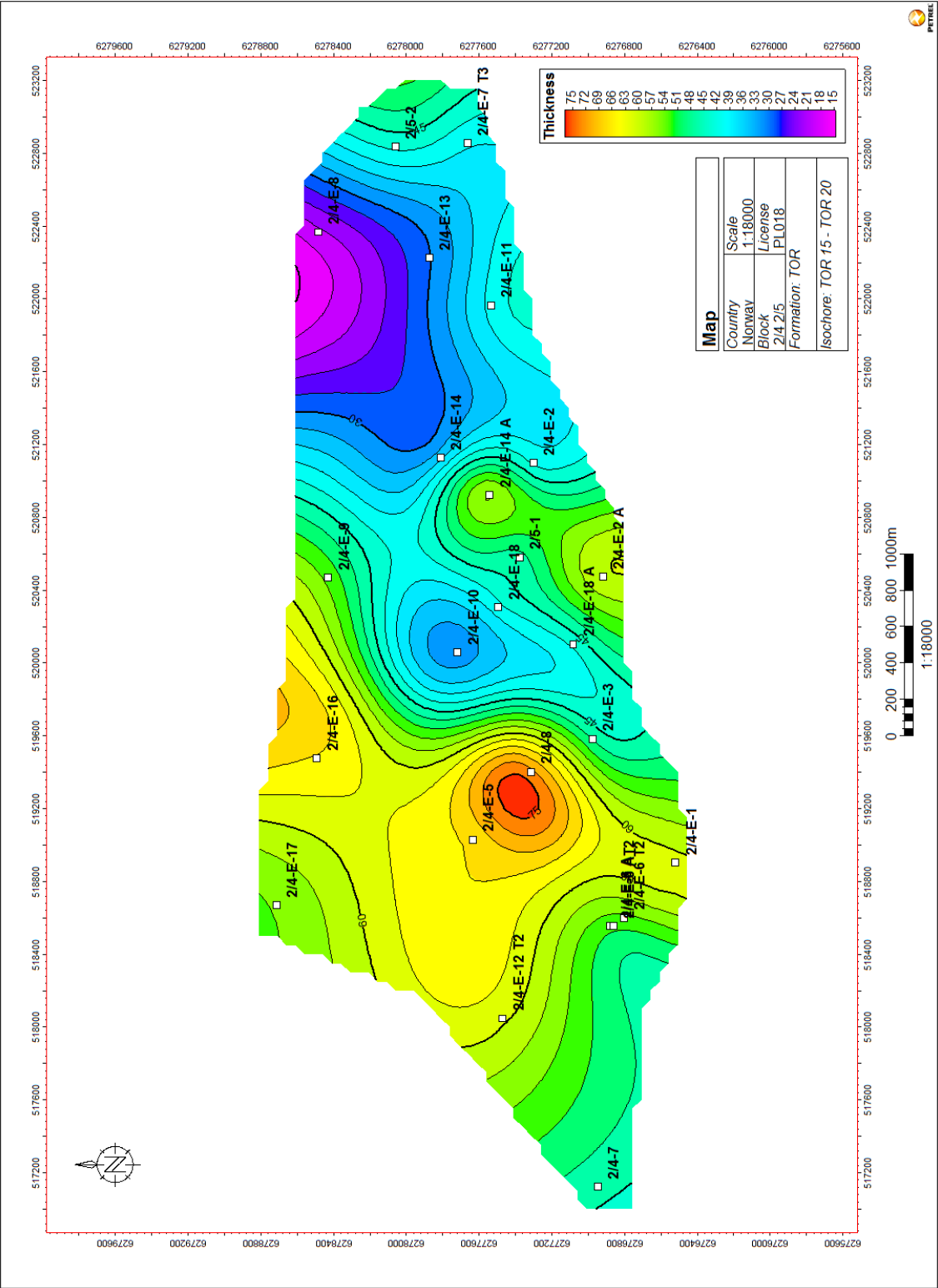


Figure 4.41: Isochore map of the Tor 15 interval

4.1.16 Tor 20

Observation and interpretation of the type wells (Gennaro et al., 2011)

The Tor 20 marker is normally placed on a density minimum just above a density peak (Figure 4.39 and 4.42). The DT log displays a corresponding local maximum at the position of the marker, where the DT log value decreases beneath the marker. The Tor 20 marker is normally placed just above a small local peak in the GR log, even though the GR log shows little variation in this interval.

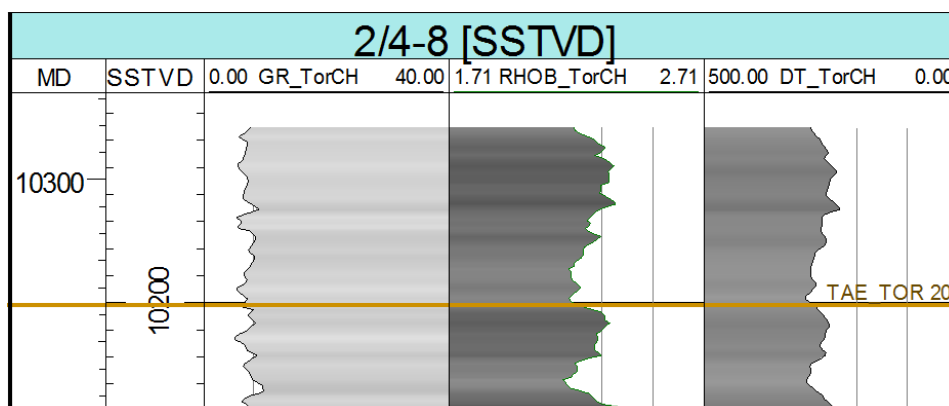


Figure 4.42: Log signature at the Tor 20 marker in well 2/4-8.

New correlation

The log signature where the Tor 20 marker was placed in this correlation, varies in some of the wells. Figure 4.43 displays the marker in well 2/4-E-2 with a slightly different log response for RHO and DT than in most wells. The marker is placed on a small maximum in the RHO rather than a minimum. The RHO log readings in most wells are increasing downwards in the Tor 20 interval, towards the Tor 30 marker. The thickness map of the interval displays a weak thickening trend towards the North-west, but the map also contains large thickness variations (Figure 4.44). The Tor 20 interval has the largest thickness in the new correlation of the wells 2/4-E-14 A, 2/4-E-12 T2 and 2/4-E-13.

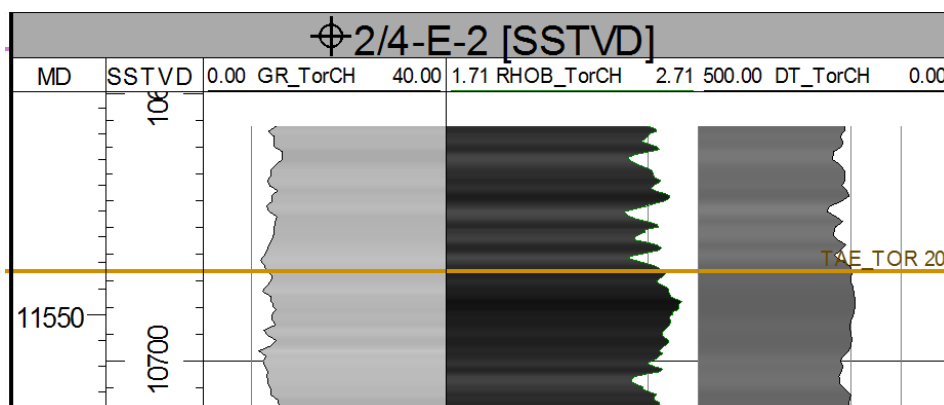


Figure 4.43: Log signature at the Tor 20 marker in well 2/4-E-2.

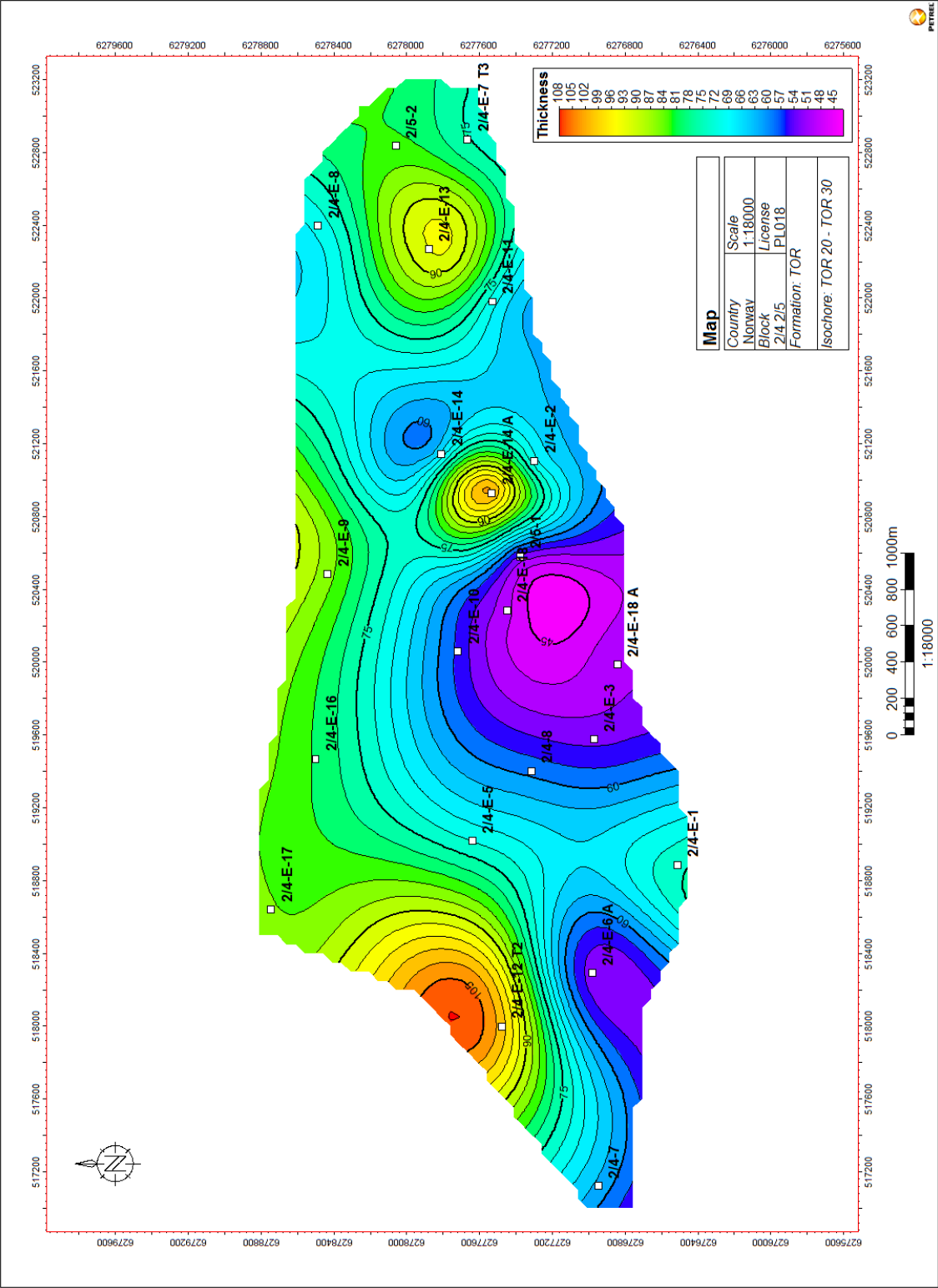


Figure 4.44: Isochore map of the Tor 20 interval

4.1.17 Tor 30

Observation and interpretation of the type wells (Gennaro et al., 2011)

The Tor 30 is placed on at a level where the RHOB log is at a local minimum value (Figure 4.45), and in some wells in a downwards decreasing trend (Figure 4.46). The corresponding DT log has the same log signatures only with a local maximum value or a downwards increasing trend. The GR log varies little.

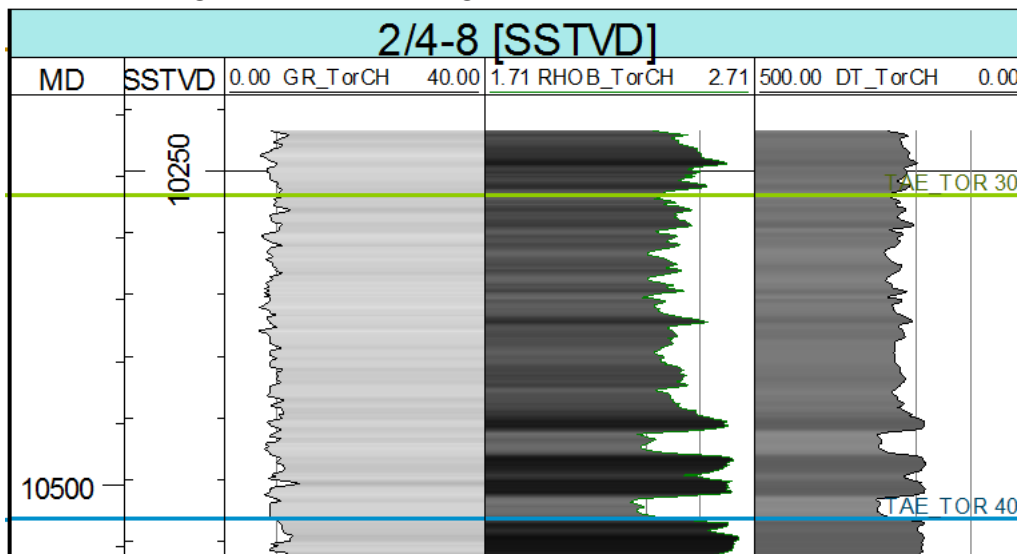


Figure 4.45: Log signature at the Tor 30 marker in well 2/4-8.

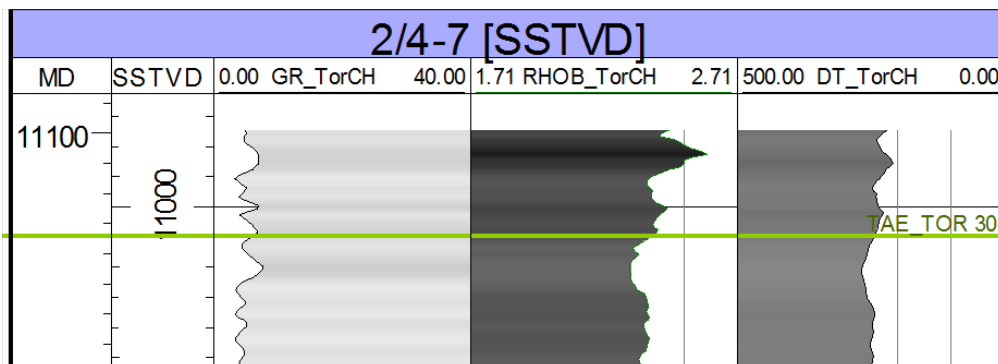


Figure 4.46: Log signature at the Tor 30 marker in well 2/4-7.

New correlation

The RHOB and DT log signatures corresponding to the Tor 30 interval is varying in different parts of the field. Generally the RHOB log readings tend to increase when it gets closer to the Tor 40 marker. In some wells the log responses between the Tor 30 and Tor 40 markers are not varying much (Figure 4.39). The thickness map of the Tor 30 interval displays a thinner interval at the crest of the Tor Field (Figure 4.47).

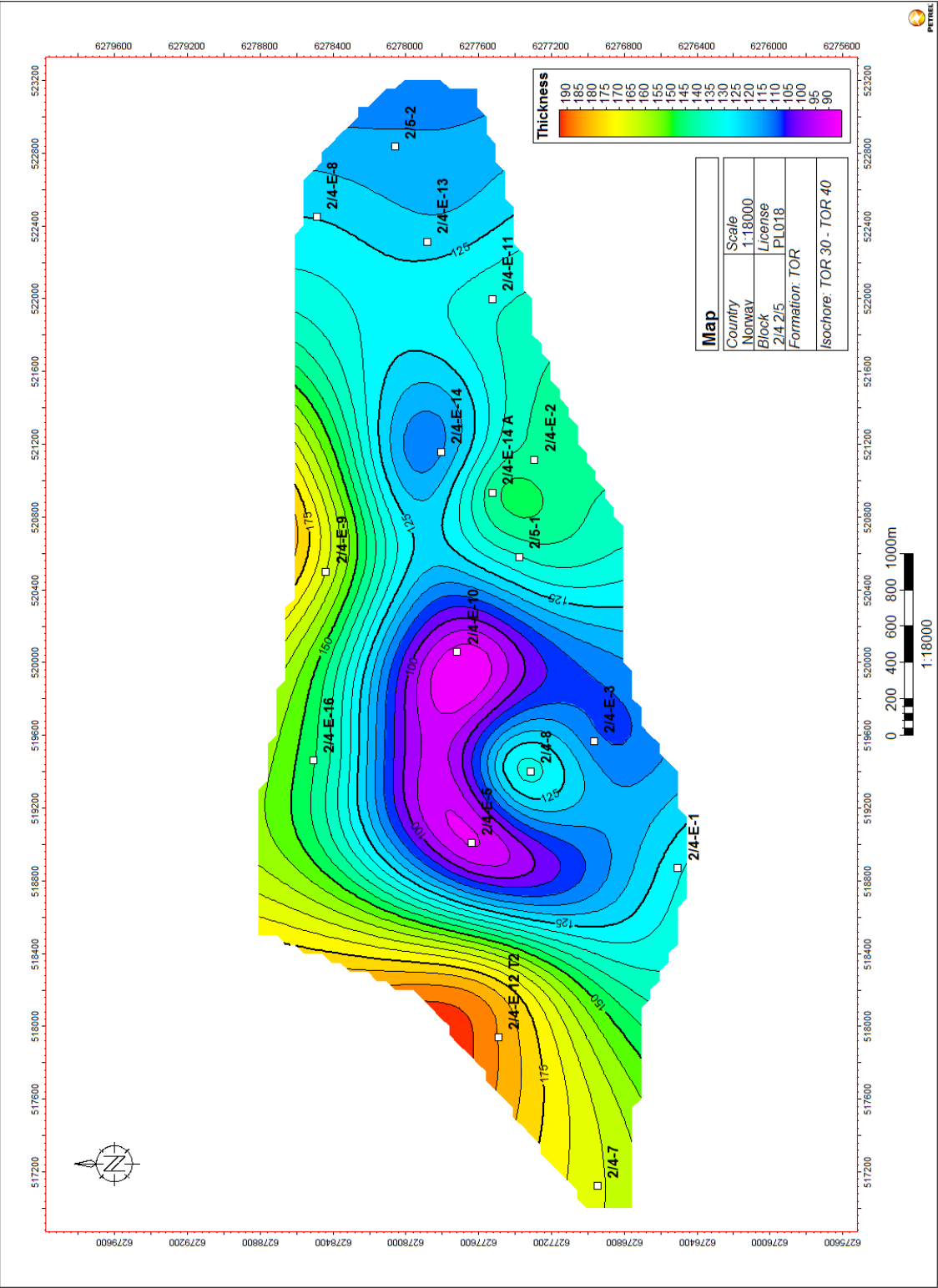


Figure 4.47: Isochore map of the Tor 30 interval

4.1.18 Tor 40

Observation and interpretation of the type wells (Gennaro et al., 2011)

The Tor 40 marker is placed on the lowermost part of the trough in the RHOB log and a sharp increase in the DT log (Figure 4.48).

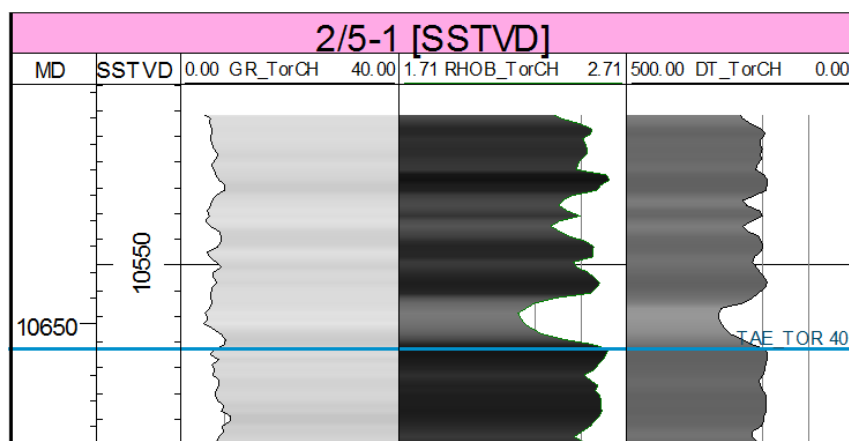


Figure 4.48: Log signature at the Tor 40 marker in well 2/5-1.

New correlation

The log signature for the Tor 40 marker is recognizable in most of the wells (Figure 4.49). In this correlation the marker is interpreted in 17 of the Tor Field wells, because the remaining wells did not penetrate down to the Tor 40 marker.

The thickness map for the Tor 40 interval is interpolated based on the thickness from 6 wells (Figure 4.50), due to a limited number of wells penetrating down to the Tor 50 marker. A reduction of Tor 40 interval thickness can be observed from South to North.

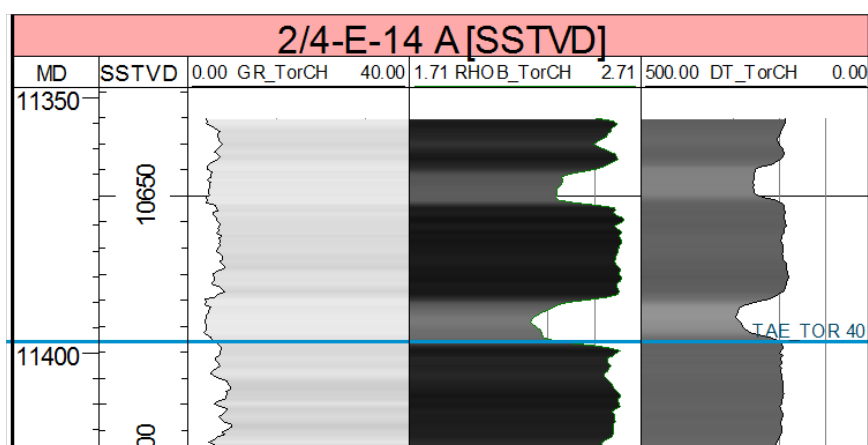


Figure 4.49: Log signature at the Tor 40 marker in well 2/4-E-14 A.

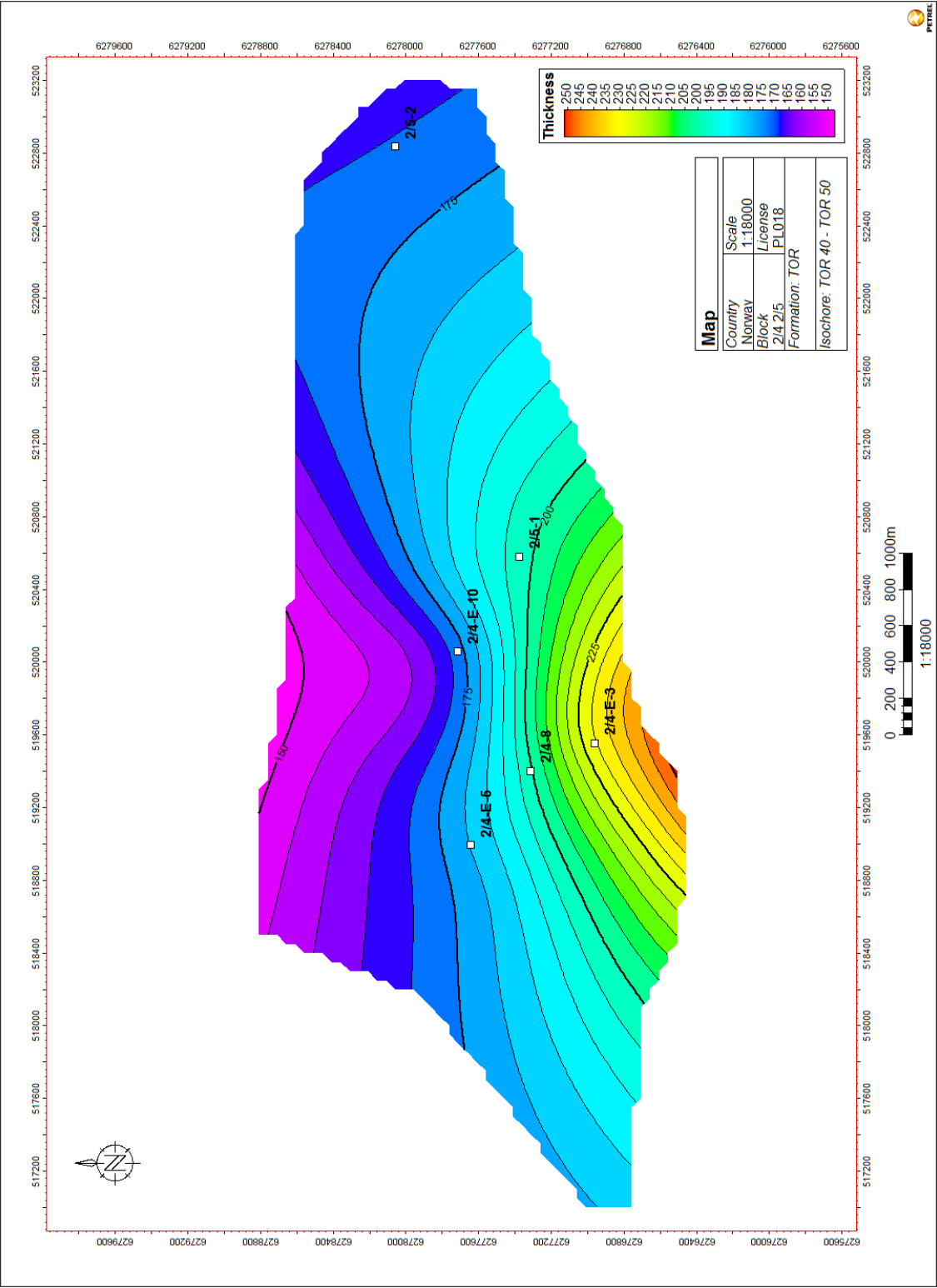


Figure 4.50: Isochore map of the Tor 40 interval

4.1.19 Tor 50

Observation and interpretation of the type wells (Gennaro et al., 2011)

The Tor 50 marker is placed at a trough in RHOB and an increase in DT, in an interval characterized by little variation in log signatures (Figure 4.51).

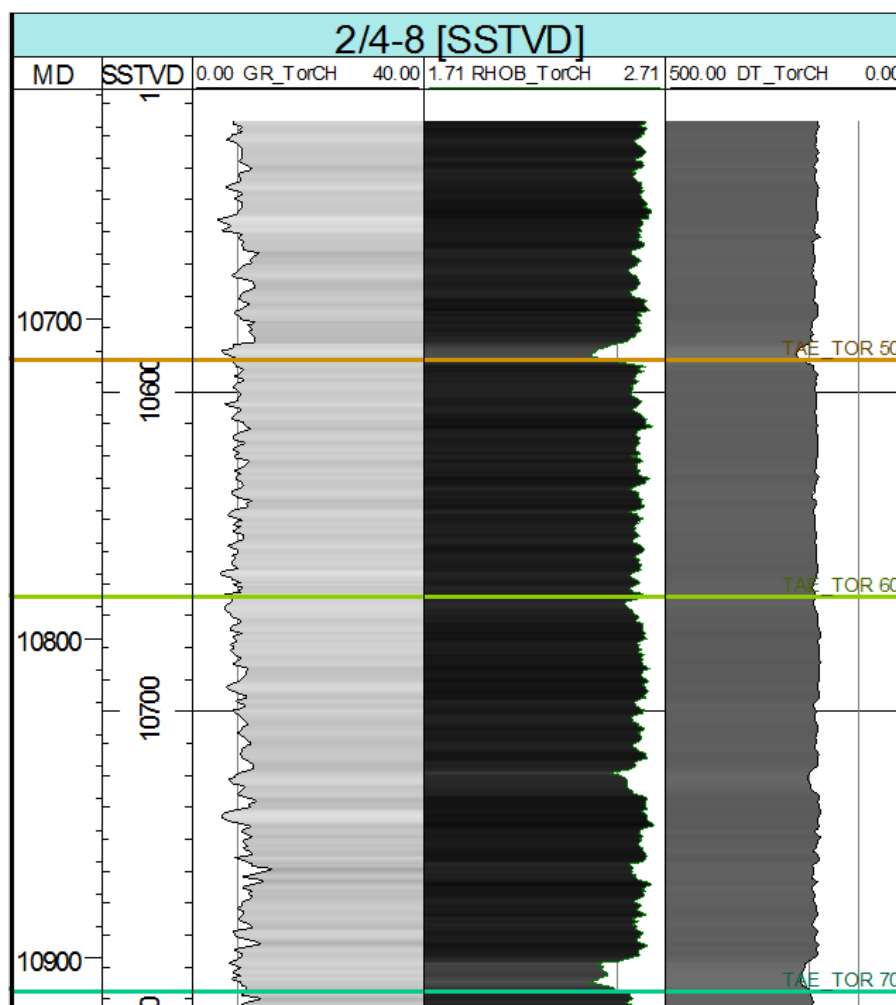


Figure 4.51: Log signature at the Tor 50 marker (orange color) in well 2/4-8.

New correlation

Only 4 wells penetrate this interval, which reduces the number of isochore points used for generating Figure 4.52. Interval thickness is reducing from East to West.

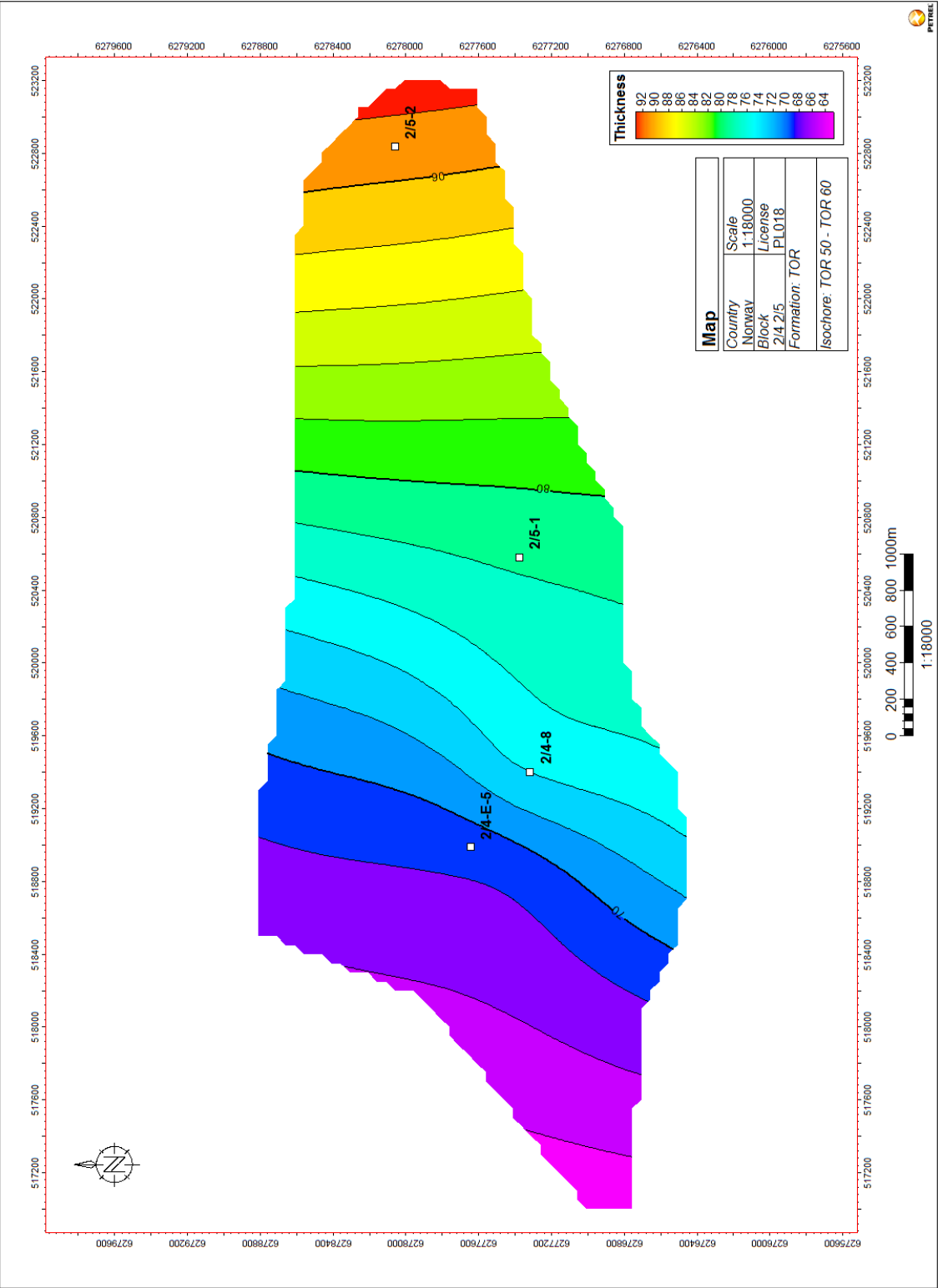


Figure 4.52: Isochore map of the Tor 50 interval

4.1.20 Tor 60

Observation and interpretation of the type wells (Gennaro et al., 2011)

The Tor 60 marker is placed on a small increase in the RHOB log (Figure 4.53 and 4.54). The GR and DT logs do not have a consistent response at the Tor 60 marker.

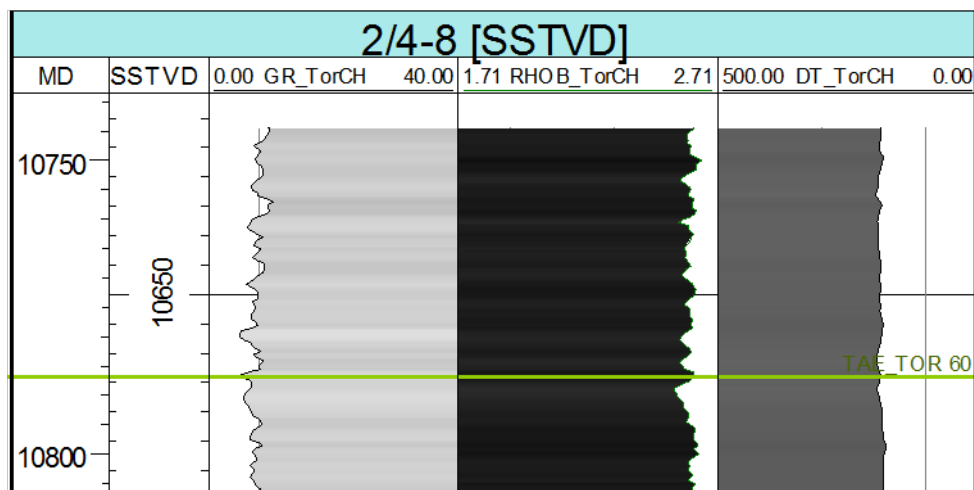


Figure 4.53: Log signature at the Tor 60 marker in well 2/4-8.

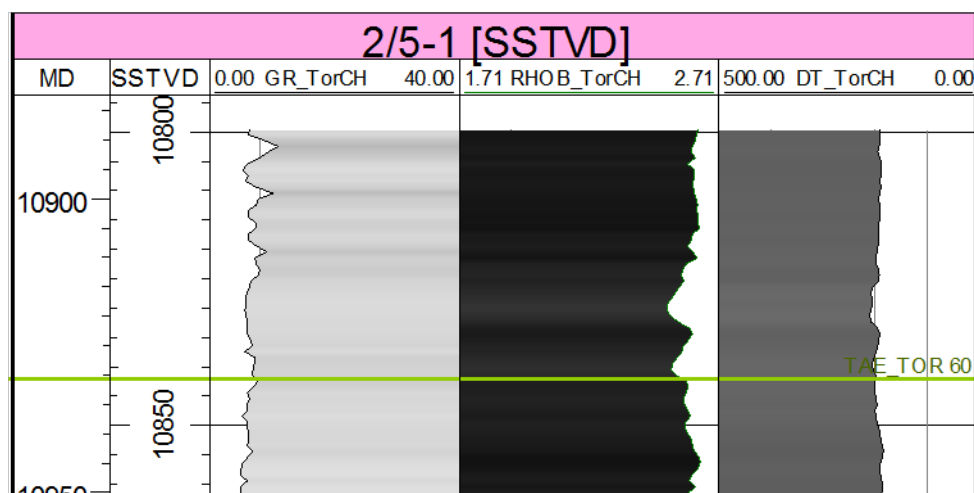


Figure 4.54: Log signature at the Tor 60 marker in well 2/5-1.

New correlation

Only 3 wells penetrate this interval, which reduces the number of isochore points used for generating the Tor 60 interval isochore (Figure 4.55). Interval thickness is decreasing from East to West, similar to the Eko 50 interval.

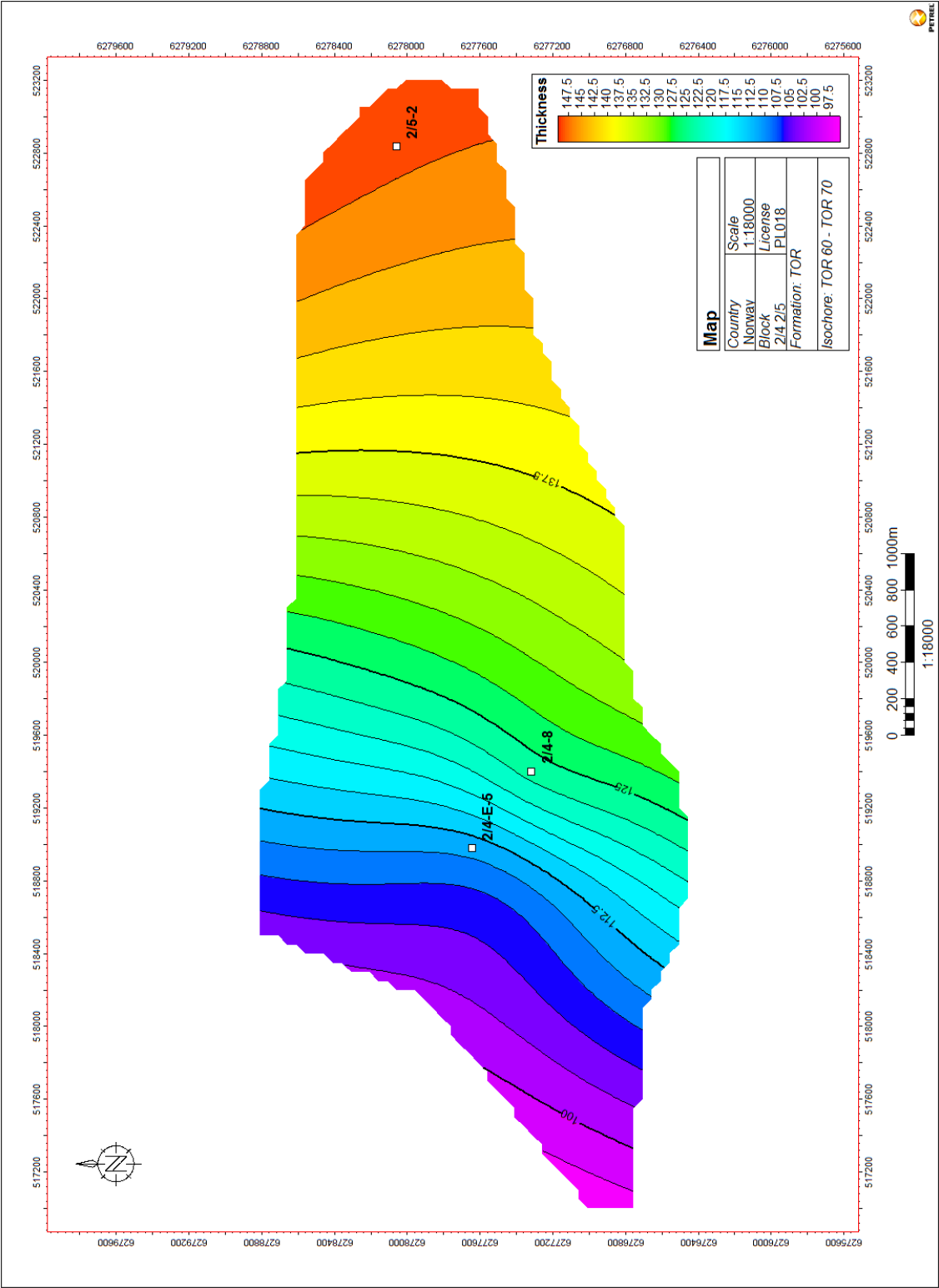


Figure 4.55: Isochore map of the Tor 60 interval

4.1.21 Tor 70

Observation and interpretation of the type wells (Gennaro et al., 2011)

The Tor 70 marker is placed at an sharp downhole increase of density (Figure 4.56). The same interval displays a minor downhole decrease in the DT log. The GR log response in the type wells is not showing any distinctive GR response, compared to the one observed at the Tor 70 marker in well 2/4-E-5.

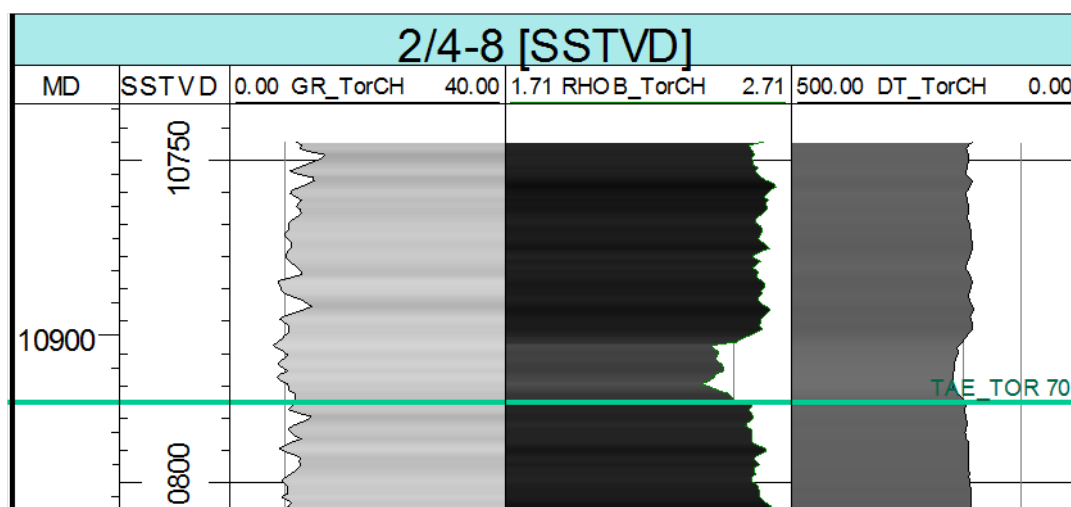


Figure 4.56: Log signature at the Tor 70 marker in well 2/4-8.

New correlation

Only 3 wells penetrate this marker. In well 2/4-E-5, the Tor 70 marker is placed at a peak in the GR log (Figure 4.57). No isochore map has been generated since this is the lower-most surface picked by Gennaro et al. (2011) and correlated in this study.

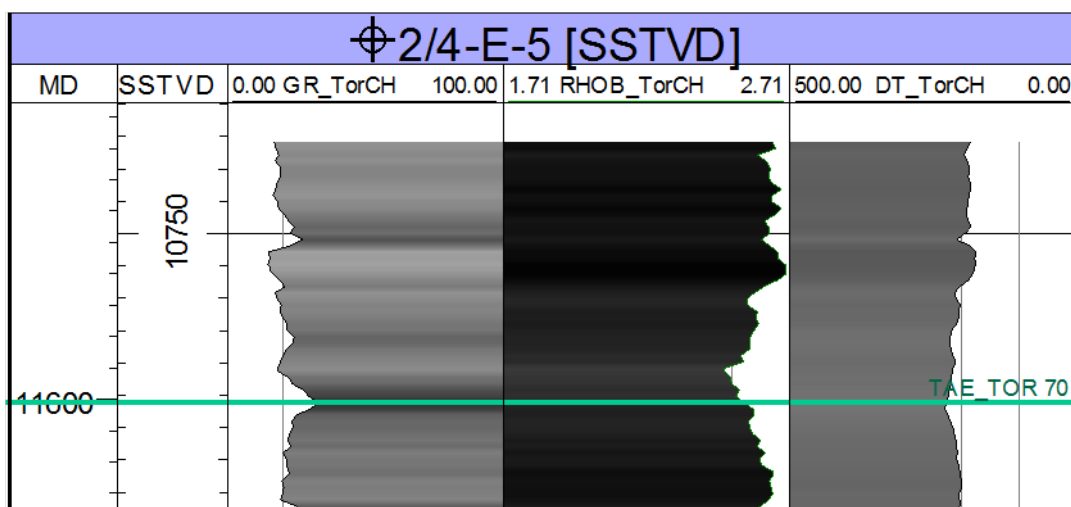


Figure 4.57: Log signature at the Tor 70 marker in well 2/4-E-5.

4.2 Well sections

4.2.1 Type wells, West - East well section

The well section displaying the correlation of all the type wells is included in the Appendix (Figure A.1). The map in Figure 4.58 displays the location of the type wells (marked with stars) and the path of the cross-section. All markers in the type wells are positioned as they were picked and correlated by Gennaro et al. (2011), except for the Eko 90 marker in well 2/4-E-14, and the Eko 90 to Eko 50 markers in well 2/5-2. This modification will be discussed in chapter 5.

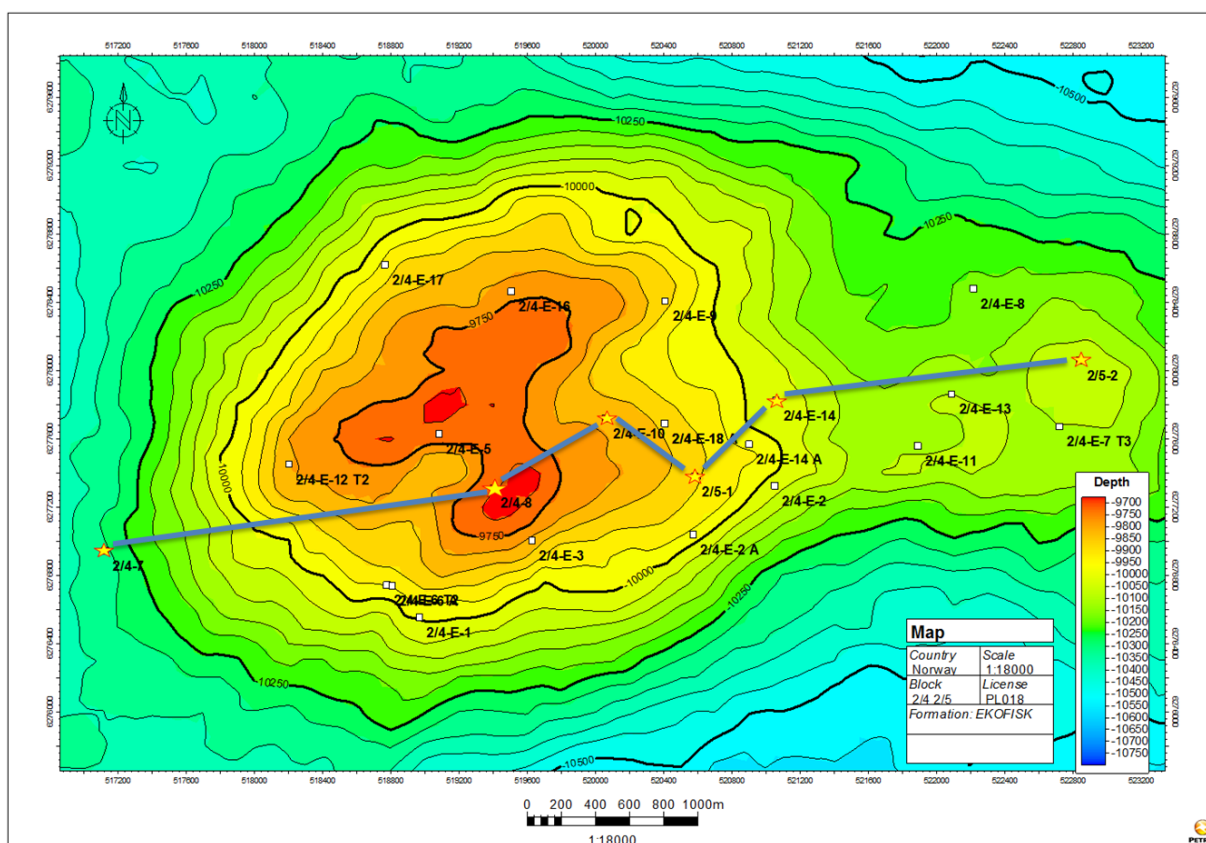


Figure 4.58: Map displaying the path of the well section with the "type wells".

The correlation of the type wells shows (Figure A.1), the largest thickness variations between the top Ekofisk and the Eko 50 markers. The entire Ekofisk Formation appears to be more condensed in well 2/4-8 and 2/5-1. The stratigraphic intervals in the Tor Formation show a more uniform thickness than the intervals in the Ekofisk Formation. However, both the Ekofisk and Tor formations contain thickness variations in different intervals.

4.2.2 Middle of the Tor Field, West - East well section

A foldout figure of the well section going from West to East across the middle part of the crest (Figure 4.59), can be found in the Appendix (**Figure A.2**). The well section includes the correlation of the wells 2/4-E-12 T2, 2/4-E-5 and 2/4-E-13, in addition to the type wells 2/4-7, 2/4-E-10, 2/4-E-14 and 2/5-2.

In the West to East well section across the middle of the Tor Field (Figure 4.59), the thickness of the interval between the top Ekofisk and Eko 70 markers are thicker in the wells 2/4-7 and 2/4-E-12 T2 (West) and the 2/5-2 well (East). The Eko 20 interval represents the upper part of the Ekofisk Tight Zone, and in well 2/4-E-10 it is thicker than in the rest of the wells in this cross section. Although the intervals in the Tor Formation have a more uniform thickness, some also show thickness variations, e.g. the Tor 20 interval in well 2/4-E-12 T2.

4.2.3 Southern part of the Tor Field, West - East well section

The West to East well section across the Southern part of the Tor Field (**Figure A.3**), display the correlation of the wells 2/4-E-6 T2, 2/4-E-6 A, (2/4-E-6 AT2), 2/4-E-1, 2/4-E-3, 2/4-E-2 A, 2/4-E-2, 2/4-E-11 and 2/4-E-7 T3. In figure 4.59, the path of the well section is shown. Wireline data was missing for well 2/4-E-6 AT2. The three 2/4-E-6 wells are situated very close and they display similar log signatures.

The Eko 10 interval, which correspond to the main part of the Ekofisk Tight Zone (Chapter 4.1.10), is generally thicker in the Eastern part of this well section than in most of the other parts, e.g. in well 2/4-E-2 A, 2/4-E-2 and 2/4-E-7 T3 (Figure A.3). The upper part of the Tor Formation displays relatively uniform thickness.

4.2.4 Northern part of the Tor Field, West - East well section

The well section from West to East, across the Northern part of the Tor Field, can be seen as a foldout figure in the Appendix (**Figure A.4**). It displays the wells 2/4-E-12 T2, 2/4-E-17, 2/4-E-16, 2/4-E-9 and 2/4-E-8. The path of the well section can be seen in the map in Figure 4.59.

Most of the intervals in this cross section show relatively uniform thickness. One exception is the Eko 10 interval in well 2/4-E-16 and 2/4-E-8, which are many times thicker than in the rest of the wells. The large thickness is due to the thick interval with high GR log values corresponding to the Ekofisk Tight Zone. Other exceptions are the top three intervals of the Ekofisk Formations (Ekofisk, Eko 90 and Eko 80), which increases in thickness both towards West and East from well 2/4-E-16.

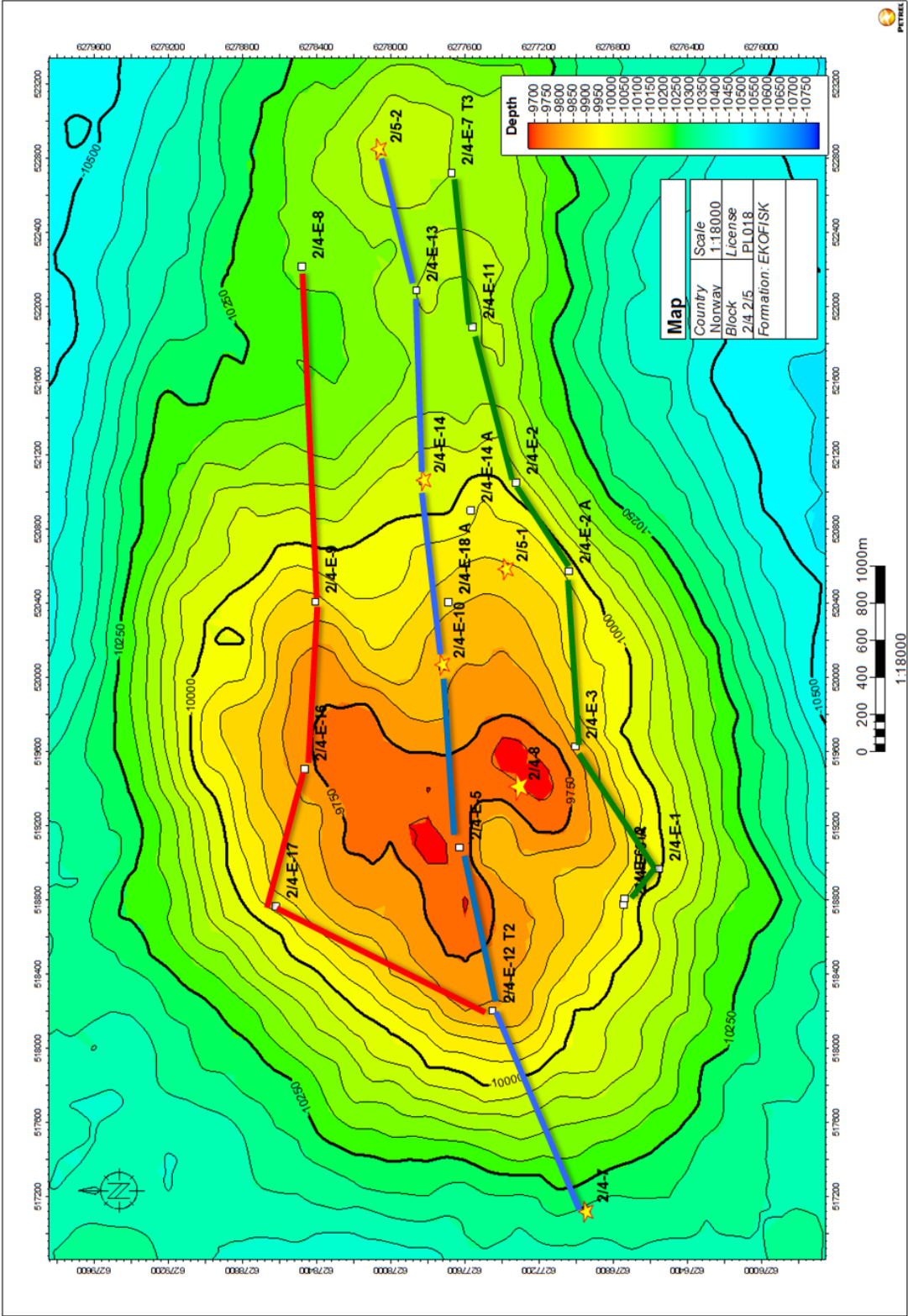


Figure 4.59: Map displaying the path of 3 well sections, crossing the Tor Field from West to East. The middle path (blue color, Figure A.2), Southern path (green color, Figure A.3) and the Northern path (red color, Figure A.4).

4.2.5 Western part of the Tor Field, North - South well section

The well section from North to South across the Western part of the Tor Field (**Figure A.5**), displays the wells 2/4-E-17, 2/4-E-12 T2 and 2/4-E-1. The path of the well section can be seen in the map in Figure 4.60.

In this well section, the Eko 60 and Eko 40 intervals are thinning towards the South. Most of the Tor intervals are relatively uniform in thickness, except for the Tor 10 interval, which is decreasing in thickness towards North.

4.2.6 Middle part of the Tor Field, North - South well section

The well section from North to South across the middle part of the Tor Field (**Figure A.6**), displays the wells 2/4-E-16, 2/4-E-5, 2/4-8 and 2/4-E-3. The path of the well section can be seen in the map in Figure 4.60.

In this North - South well section, the top Ekofisk interval displays an increasing thickness towards the South. The Eko 40 interval is thicker in well 2/4-E-5 than it is in the wells to the North and South of E-5. This thickness variation can also be seen in the isochore map in Chapter 4.1.7. However, the Eko 40 interval shows a more constant thickness towards the East, in the intersecting West to East well section (Figure A.2) The Tor formation is characterized by relatively uniform interval thickness.

4.2.7 Central-Eastern part of the Tor Field, North - South well section

The well section from North to South across the Central-Eastern part of the Tor Field (**Figure A.7**), displays the wells 2/4-E-9, 2/4-E-18, 2/4-E-18 A, 2/4-E-14 A and 2/4-E-2. The path of the well section can be seen in the map in Figure 4.60.

In the two 2/4-E-18 wells, the GR log was the only available wireline log for this correlation. The Ekofisk Formation in the two wells is condensed compared to the other wells, while the intervals in the Tor Formation are of similar or greater thickness compared with the other wells. The Eko 80 interval is thinning towards the North.

4.2.8 Eastern part of the Tor Field, North - South well section

The well section from North to South across the wells furthest to the East on the Tor Field (**Figure A.8**), displays wells 2/4-E-8, 2/5-2, and 2/4-E-7 T3. The path of the well section is shown in the map in Figure 4.60.

The upper part of the Ekofisk Formation, in the type well 2/5-2, has been modified in this correlation and will be discussed in Chapter 5. Well 2/4-E-7 T3, to the South-east of the Tor Field, displays the thinnest interval in the Ekofisk Formation compared to the two other wells in this well section.

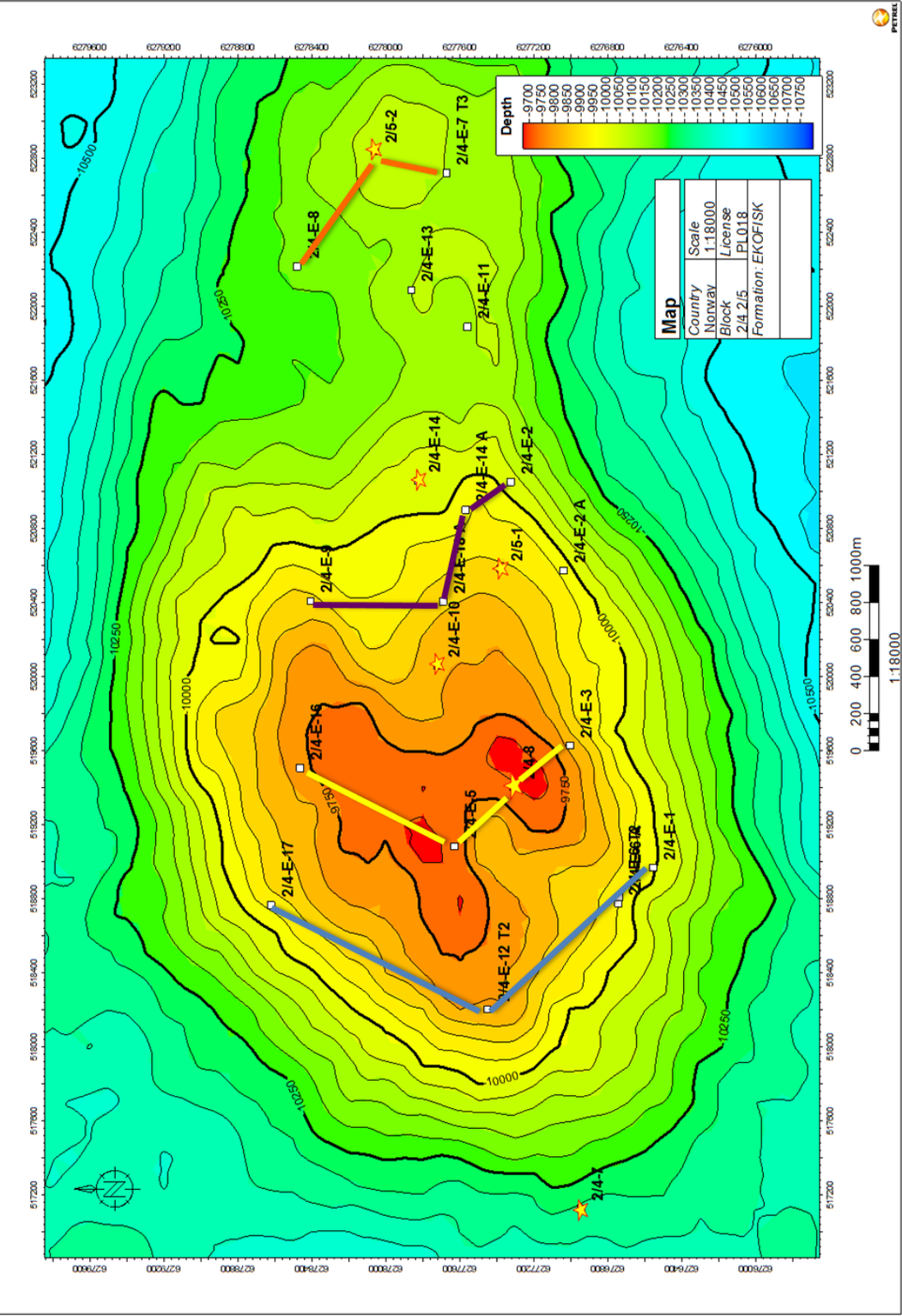


Figure 4.60: Map displaying the path of the 4 well sections, crossing the Tor Field from North to South. Displayed from the left, the Western path (blue color, Figure A.5), middle path (yellow color, Figure A.6), Central-Eastern path (purple color, Figure A.7) and the Eastern-most path (orange color, Figure A.8).

5 Discussion

New correlation compared to the regional correlation by Gennaro et al. (2011)

The new correlation of the Tor Field is based on the stratigraphic markers from six type wells at the Tor Field, which Gennaro et al. (2011) integrated in a regional correlation. The definition of markers by Gennaro et al. (2011) was applied to the remaining 20 wells of the Tor Field. The original markers were left as they were originally defined. Changes were only made to some of the markers in two wells, following discussions with M. Gennaro.

The Eko 90 marker in well 2/4-E-14 has been moved down by approximately 8 feet (Figure 5.1). The reason for this change, was the difference in log signature compared to other type wells (Figure 4.5 & 4.6).

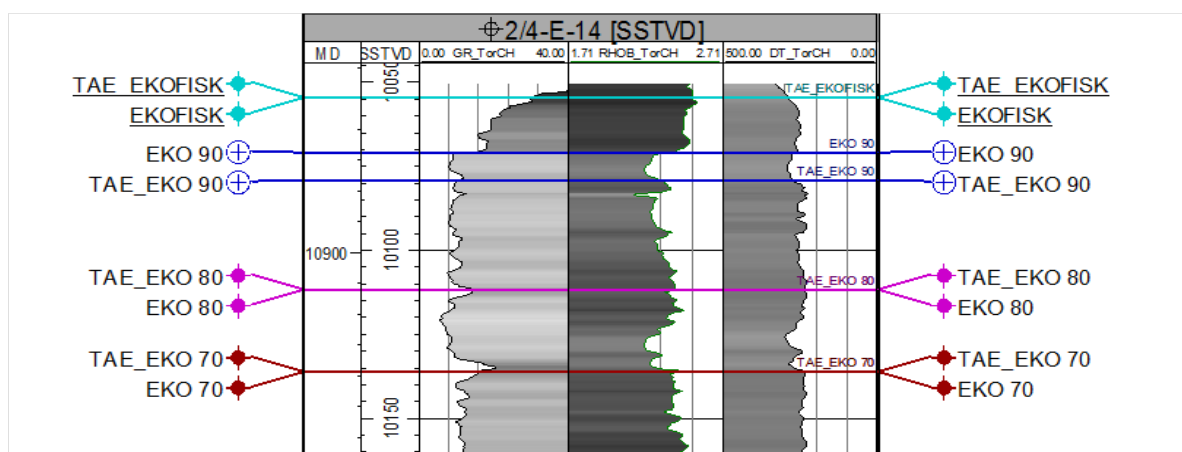


Figure 5.1: Log display of Type Well 2/4-E-14, before and after Eko 90 marker was moved. EKO 90 is the original marker by Gennaro et al. (2011), while the TAE_EKO 90 is the modified marker.

In well 2/5-2, the Eko 80, Eko 70, Eko 60 and Eko 50 markers were moved down by 62, 105, 48 and 25 feet, and the Eko 90 marker was removed. The reasons for changing these markers in this type well were:

- a significantly higher thickness of the upper Ekofisk Formation compared to other wells (Figure A.8)
- a biostratigraphic analysis by Lottaroli and Catrullo (2000) suggests a repeated section (Figure 5.2)

On the right side of Figure 5.2, a zone log with bio-zones derived from the nannofossil data of Lottaroli and Catrullo (2000) is displayed. The bio-zones that are shown in the figure have an age range between oldest (D4 C.Asymmetricus, yellow color), younger (D5-D6 C.Danicus, blue color) and youngest (D9-S1-S2, green color). The black intervals represent parts without classifiable nannofossil data. The interpretation by Lottaroli and Catrullo (2000) suggest that a repeated section of chalk strata occurs from somewhere

between the green bio-zone and the overlying yellow bio-zone, to the top Ekofisk marker (Figure 5.2).

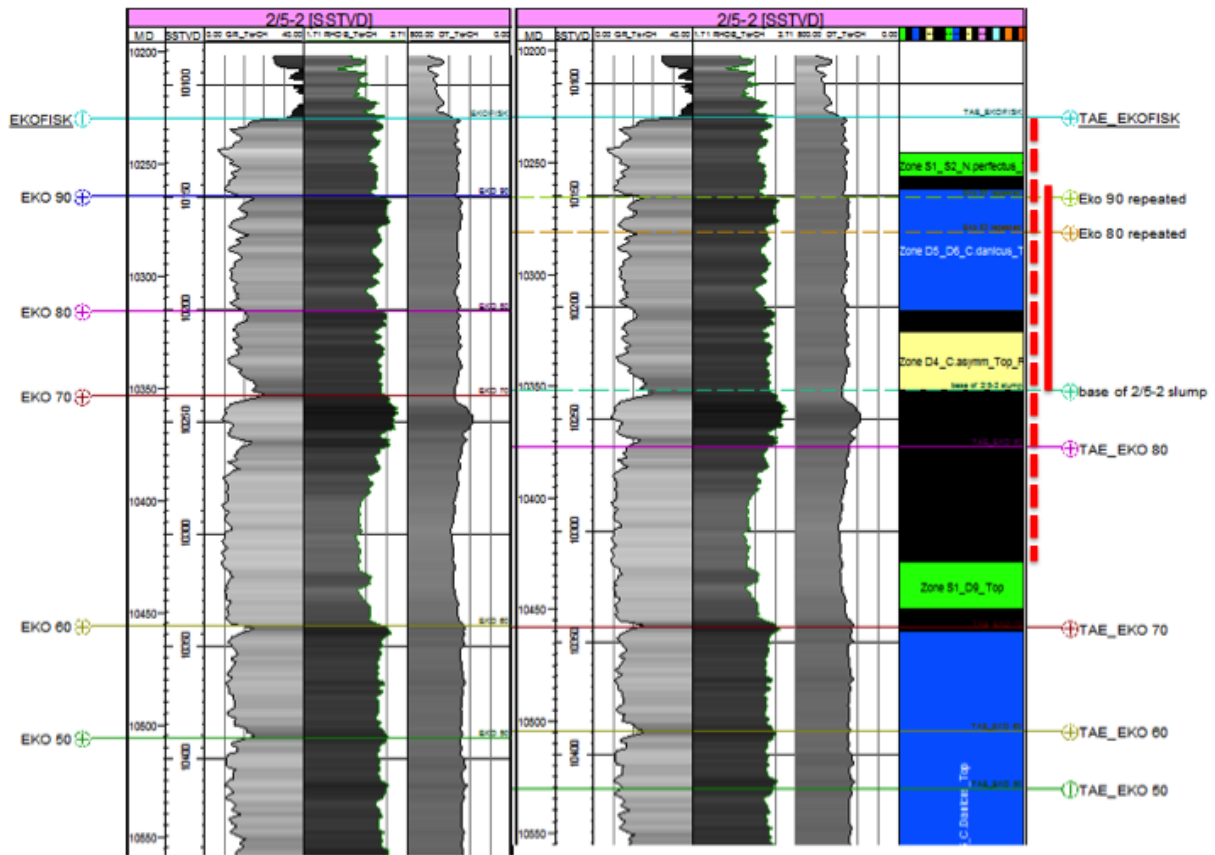


Figure 5.2: Log display of Type Well 2/5-2, before and after re-interpretation of the Upper Ekofisk Formation. To the left are the original markers by Gennaro et al. (2011) and to the right the same interval with re-interpreted markers. The well section to the right includes the nannofossil data from Lottaroli and Catrullo (2000), with bio-zones after Heck and Prins (1987), which show a repeated section of strata from around the TAE_EKO 80 marker and up to the TAE_EKOFISK. The minimum thickness of the repeated section according to the bio stratigraphy is shown with the whole red line and the maximum with the stippled red line.

The repeated section could have been explained by either:

- compressional tectonics and faulting
- massive downslope redeposition of chalk with preserved internal structure by a slide.

None of the faults visible and interpreted from seismic in the Tor Field intersect the path of well 2/5-2. If the repeated section in well 2/5-2 is not created by post depositional tectonics in the chalk, then it could have been caused by redeposition of a thick section

of chalk sliding downslope. The measured thicknesses of the repeated section in the well, based on the nannofossil data, range between a minimum of approximately 92 feet (28 meter) to a maximum of approximately 200 feet (61 meter) . If this repeated unit is caused by a massive slide, is it likely to only be present in well 2/5-2 in the Tor Field (Figure A.8).

The regional interpretation of depositional mechanisms in the Lower Ekofisk Member by Kennedy (1987) , suggest that the Tor area was subjected to extensive redeposition (Figure 2.9). The thickness of the repeated section, might suggest that it should have a wider distribution than just well 2/5-2. The chronological correct continuity of nannofossils inside the repeated section, suggest a depositional process with little internal deformation like a slide.

If the original marker placements in 2/5-2 (Figure 5.2) were correct and it exists a repeated section of strata at the top of the Ekofisk Formation, this would have meant that the repeated section also is present in all the other wells containing the Eko 90 and Eko 80 markers. This cannot be supported by the biostratigraphy in well 2/4-8, and is one of the reasons for changing the interpretation in well 2/5-2 compared to Gennaro et al. (2011). Another reason is the significantly higher thickness of the upper Ekofisk Formation, as mentioned earlier.

In the correlation study conducted by Total E&P Geosciences Technologies in 2005, the nomenclature of the markers was almost identical to the one in the correlation by Gennaro et al. (2011). The big difference is the position of the markers and in particular the Eko 90 and Eko 80. Of the six type wells, which all had the Eko 90 and Eko 80 markers included in the correlation by Gennaro et al. (2011), only some of the wells contained the Eko 90 (3 wells) and Eko 80 (4 wells) markers in the 2005 study. This can support a theory about the presence of the repeated section in more wells than well 2/5-2, were the log signature for the Eko 90 and Eko 80 correspond to the thick allochthonous section. However, the markers from the correlation conducted by Gennaro et al. (2011) are tied in a regional correlation, and it is beneficial to describe the Tor Field with regionally valid markers. All the markers from the type wells (except 2/5-2) have therefore been used to describe the rest of the Tor Field wells.

New correlation compared to the lithostratigraphic correlation currently used by the Tor Field operator ConocoPhillips for reservoir characterization.

The lithostratigraphic correlation currently used for reservoir characterization (Chapter 3.1), has been criticized by Total E&P Norge (G. Sambet) in 2005 for the following reasons:

1. the correlation of the reservoir units is only based on the porosity derived from wireline logs (monothetic correlation).
2. the correlation displays random thickness variation, which cannot be explained with faults visible on seismic.

In Figure 5.3, two log displays of well 2/4-8 are shown next to each other with the

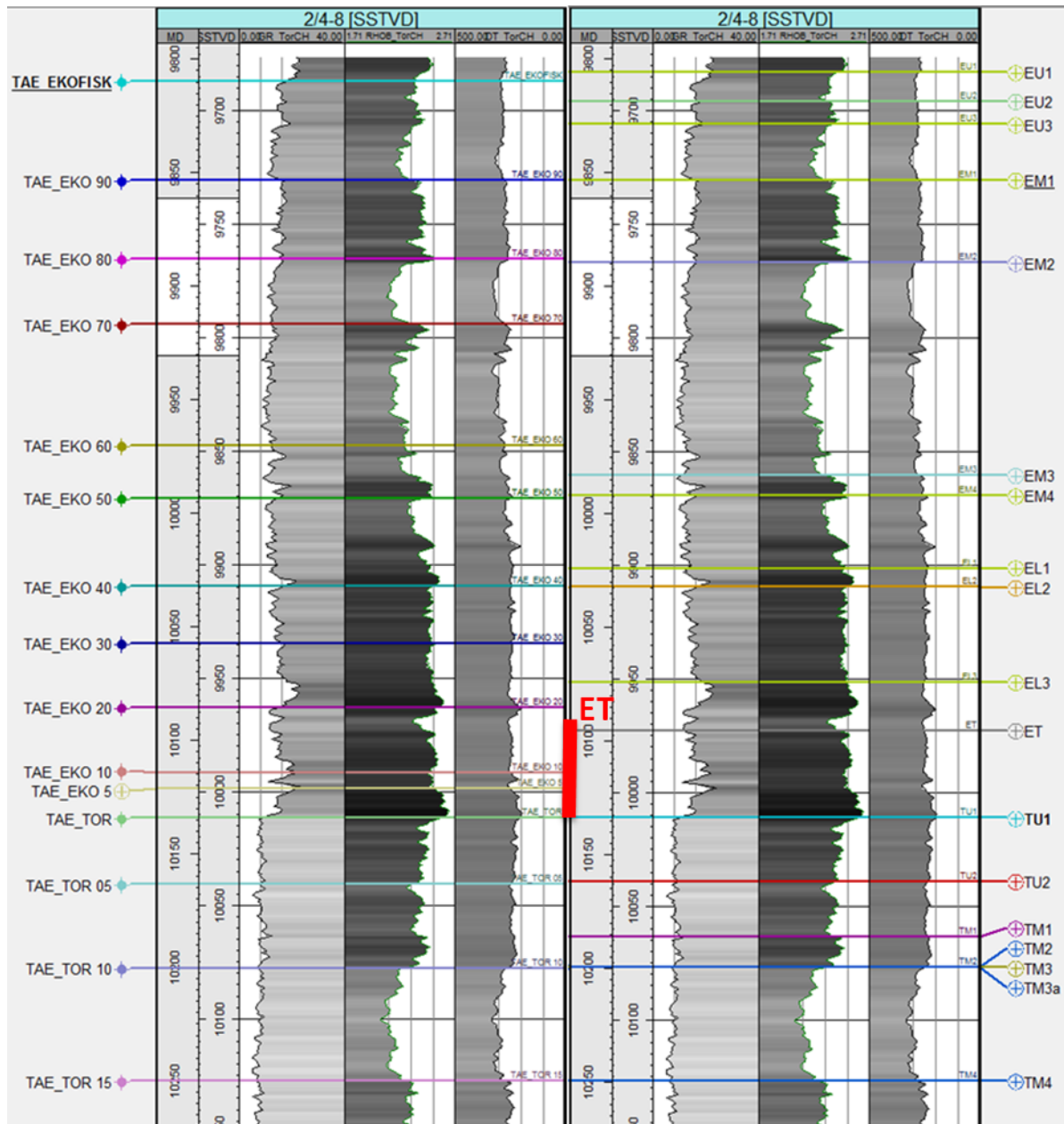


Figure 5.3: Log display including GR, RHOB and DT logs of well 2/4-8, with stratigraphic markers from both the new correlation (left) and the lithostratigraphic correlation currently used by Tor Field operator ConocoPhillips (right). The Ekofisk Tight Zone (ET) is marked with a vertical red line.

markers from both the new sequence stratigraphic correlation and the lithostratigraphic correlation of the Tor Field. Some of the stratigraphic markers are interpreted at similar depth in both correlations, e.g. the EKO 90 and EM1, EKO 80 and EM2, EKO 50 and EM4. However, other markers are significantly different in the new correlation due to the different approach used. Moreover, the new correlation is consistent with the regional correlation by Gennaro et al. (2011).

The stratigraphically very important Ekofisk tight zone, has a different subdivision in the two correlations (Figure 5.3). The lithostratigraphical correlation marks the upper and lower boundary of the Tight Zone with the ET and TU1 markers, while the new sequence stratigraphical correlation uses four markers to divide the Tight Zone into three intervals.

In order to compare the new correlation with the lithostratigraphic correlation, isochore maps of corresponding marker intervals were generated. In well 2/4-8, the Eko 50 and Eko 40 markers had similar placement as the EM4 and EL2 markers (Figure 5.4). The isochore maps of the two intervals are shown in Figure 5.5(a) and Figure 5.5(b). The thickness distribution of the EM4 - EL2 interval, shows higher variations than the thickness map of the Eko 50 - Eko 40 interval. In the Eko 50 interval there is seemingly more uniform thickness distribution and a faint West to East isochore trend.

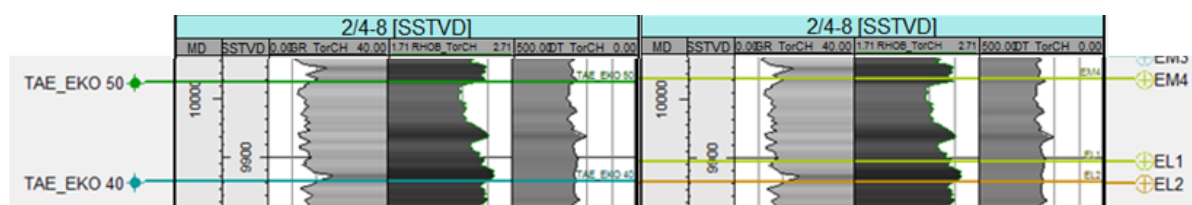


Figure 5.4: Log display of the Eko 50 (equivalent of EM4-EL2) interval in well 2/4-8, with stratigraphic markers from both the new correlation (left) and the lithostratigraphic correlation (right).

The thickness of the Eko 50 interval in type well 2/5-2, was modified due to the doubled section in the upper part of the Ekofisk Formation (Figure 5.2). This depth shift of the upper markers in this well, has made the interpolated thickness around well 2/5-2 fit the general thickness trend for the Eko 50 interval (Figure 5.5.a). The lithostratigraphic correlation has not taken the repeated section into account.

A similar thickness comparison for an interval in the Tor Formation, is displayed in Figure 5.6 and 5.7. The first of the two compared intervals are the Tor 10 (Figure 5.7.a), which in well 2/4-E-10 corresponds to the interval from TM3a to TM4 (Figure 5.7.b). By observing the isochore maps, it is evident that the Tor 10 interval has much smoother thickness distribution and a clear West - East isochore trend across the Tor Field. The interval between the TM3a - TM4 displays a random thickness variation. The red area in the middle of the isochore map in Figure 5.7.b, is an artifact of the interpolation technique and does not in any way represent the real thickness in the area between the wells.

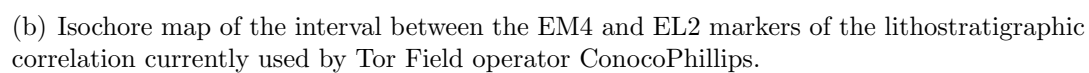
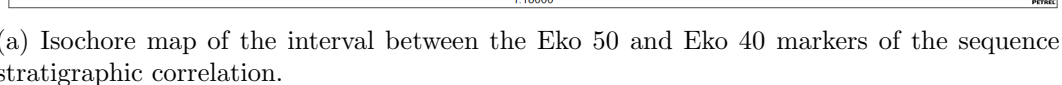


Figure 5.5: Comparison of isochore maps (example from the Ekofisk Formation).

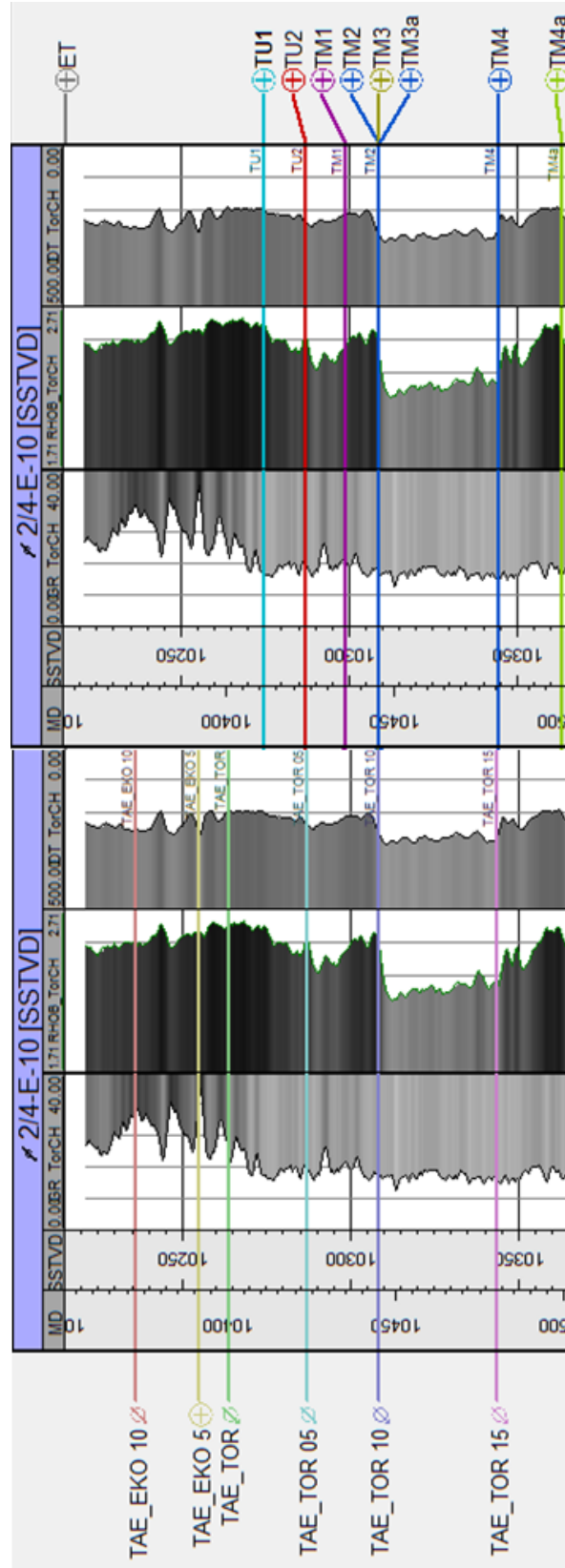


Figure 5.6: Log display of the Tor 10 (equivalent of TM3a-TM4) interval in well 2/4-E-10, with stratigraphic markers from both the new correlation (left) and the lithostratigraphic correlation (right).

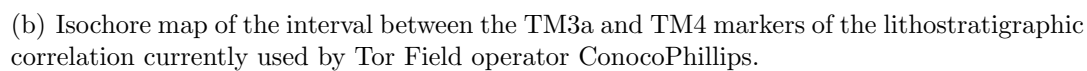


Figure 5.7: Comparison of isochore maps (example from the Tor Formation).

6 Conclusion

In this thesis, a sequence stratigraphic correlation of all the wells in the Tor Field has been carried out. The correlation was based on the interpretation of six Tor Field wells with markers from a regional correlation by Gennaro et al. (2011). It was considered a clear advantage for the correlation that the interpreted markers were part of time-boundaries on a regional scale.

The depositional setting and mechanisms of the chalk are highly complex. Conventional sequence stratigraphic principles in wireline interpretation, could not always be used on this deep marine carbonate environment. Many times, it was not obvious which criteria had been used in the "type wells" when interpreting the markers. The correlation presented in this MSc thesis could be further improved.

1. One result from the new correlation is that the distribution of strata is more uniform in terms of interval thickness, compared to the current lithostratigraphic correlation. Describing the reservoir units without the frequent thickness variations, as in the currently used subdivision in the reservoir model, could strongly improve reservoir simulation and production strategy. The simulation model, as well as the simulation results, will be more accurate so a better production strategy can be made.
2. The biostratigraphy from Lottaroli and Catrullo (2000) helped identifying the repeated section in well 2/5-2. However, the nannofossil data did not prove to be as useful as initially hoped, due to limited data. Data from only two wells (2/4-8 and 2/5-2) from the Tor Field was included in the publication by Lottaroli and Catrullo (2000). These two type wells did not display much nannofossil chrono-coherency for the different marker intervals in the Ekofisk Formation.
3. No core interpretations of the Tor Field wells were conducted during the presented thesis. Two core facies descriptions of well 2/4-7 by Kennedy (1985) and Caldwell and Siemers (1993), were utilized in order to test if vertical facies distribution could aid the correlation. However, the use of a core facies interpretation of only one well is of limited use for the correlation work. The use of a more systematic core facies interpretation of all available core data would be recommended. For future work on the correlation of the Tor Field, the recommendation is to implement existing or new cores facies interpretations from the eight cored Tor Field wells and see if this can improve the correlation.

This new correlation will be tested by Total E&P Norge in a revision of the reservoir characterization model and dynamic simulation model.

References

- Bailey, H., L. Gallagher, M. Hampton, H. Krabbe, B. Jones, D. Jutson, A. Moe, E. B. Nielsen, N. W. Petersen, F. Riis, D. Sawyer, B. Sellwood, T. Strand, P. E. Øverli, and I. Øknevad (1999). A Joint Chalk Stratigraphic Framework. In A. Fritsen (Ed.), *Joint Chalk Research Phase V*. Norwegian Petroleum Directorate (NPD).
- Bergfjord, E. (2007). Tor field - extreme workover of a veteran. In *The 12th Conference on FIELD RESERVOIR MANAGEMENT*. NPF.
- Boggs, J. S. (1995). *Principles of sedimentology and stratigraphy* (2nd ed.). Prentice-Hall, Inc.
- Bramwell, N. P., G. Caillet, L. Meciani, N. Judge, M. Green, and P. Adam (1999). Chalk exploration, the search for a subtle trap. In A. J. Fleet and S. A. R. Boldy (Eds.), *Petroleum Geology of Northwest Europe: Proceedings of the 5th Conference*, pp. 911–937. Geological Society, London.
- Brekke, H. and S. Olaussen (2006). Høyt hav og lave horisonter. In A. Nøttvedt, I. B. Ramberg, and I. Bryhni (Eds.), *Landet blir til - Norges geologi*, Chapter 13. Norsk Geologisk Forening.
- Brewster, J. and J. A. Dangerfield (1984). Chalk fields along the Lindesnes Ridge, Eldfisk. *Marine and Petroleum Geology* 1, 239–278.
- Caillet, G., N. C. Judge, N. P. Bramwell, M. Green, P. Adam, and L. Meciani (1996). Structural history of the chalk fields in the Norwegian Central Graben. In *Fifth North Sea Chalk symposium*. Joint Chalk Research.
- Caldwell, C. D. and W. T. Siemers (1993). Phillips 2/4 7X core, Tor Field, North Sea, Norway. Lithostratigraphy, sedimentology and reservoir character of the Maastrichtian and Danian chalk section. Research and services report 14905, Phillips Petroleum Company.
- Deegan, C. E. and B. J. Scull (1977). A standard lithostratigraphic nomenclature for the central and northern North Sea. *Institute of Geological Sciences Report, NPD Bulletin* (1), 35.
- D’Heur, M. (1984). Porosity and hydrocarbon distribution in the North Sea chalk reservoirs. *Marine and Petroleum Geology* 1, 211–238.
- D’Heur, M. (1987). Tor. In A. M. Spencer (Ed.), *Geology of the Norwegian Oil and Gas fields.*, pp. 129–142. Norwegian Petroleum Society, Graham and Trotman, London.
- Elind, T. A. (2011, December). Literature Review on depositional environments and structural processes that have affected the reservoir quality of the Chalk in the Norwegian North Sea. Technical report, Department of Geology and Mineral Resources Engineering, NTNU.

- Friedman, G. M. (1996). Chalk reservoirs. In *Carbonate Reservoir Characterization - A Geologic-Engineering Analysis, Part II*, Chapter 8. Elsevier.
- Gale, A. (2011). The Petroleum Geology of the Wessex Oilfield, and an introduction to the chalk. Field-guide Petrox.
- Gennaro, M., J. P. Wonham, R. Gawthorpe, and G. Sælen (2011). *3D seismic stratigraphy and reservoir characterization of the Chalk Group in the Norwegian Central Graben, North Sea*. Ph. D. thesis, Department of Earth Science, University of Bergen.
- Gowers, M. B. and A. Sæbøe (1985). On the structural evolution of the Central Trough in the Norwegian and Danish sectors of the North Sea. *Marine and Petroleum Geology* 2, 298–318.
- Hatton, I. R. (1986). Geometry of allochthonous Chalk Group members, Central Trough, North Sea. *Marine and Petroleum Geology* 3.
- Heck, S. E. V. and B. Prins (1987). A refined nannoplankton zonation for the Danian of the Central North Sea. *Abh. Geol. B. -A.* 39, 285–303.
- Isaksen, D. and K. Tonstad (1989). A revised Cretaceous and Tertiary lithostratigraphic nomenclature for the Norwegian North Sea. *NPD Bulletin* (5), 59.
- Johnsen, S. O. (2010). Lecture notes, TGB4165 Sedimentology and Stratigraphy, NTNU.
- Kennedy, W. J. (1980). Aspects of chalk sedimentation in the Southern Norwegian Offshore. In *The Sedimentation of the North Sea Reservoir Rocks*. Norsk Petroleumsforening, Geilo.
- Kennedy, W. J. (1985). Sedimentology of the Late Cretaceous and Early Paleocene Chalk Group, North Sea Central Graben. In *North Sea Chalk Symposium*, Number 1.
- Kennedy, W. J. (1987). Sedimentology of Late Cretaceous - Paleocene Chalk Group, North Sea Central Graben. In J. Brooks and K. Glennie (Eds.), *Petroleum Geology of Northwest Europe.*, pp. 469–481. Graham & Trotman, London.
- Knott, S. D., M. T. Burchell, E. J. Jolley, and A. J. Fraser (1993). Mesozoic to Cenozoic plate reconstruction of the North Atlantic and hydrocarbon plays of the Atlantic margins. In J. R. Parker (Ed.), *Petroleum Geology of Northwest Europe.*, pp. 953–974. Geological Society London.
- Larsen, B. T., S. Olaussen, B. Sundvoll, and M. Heeremans (2006). Vulkaner, forkastinger og ørkenklima, osloriften og nordsjøen i karbon og perm. In A. Nøttvedt, I. B. Ramberg, and I. Bryhni (Eds.), *Landet blir til - Norges geologi*, pp. 286–327. Norsk Geologisk Forening.
- Lottaroli, F. and D. Catrullo (2000). The calcareous nannofossil biostratigraphic framework of the Late Maastrichtian - Danian North Sea chalk. *Marine Micropaleontology* (39), 239–263.

- Lucia, F. J. (1995). Rock-Fabric/Petrophysical Classification of Carbonate Pore Space for Reservoir Characterization. *AAPG Bulletin* 79(9), 1275–1300.
- Mabesoone, J. M. and V. Neumann (2005). *Cyclic Development of Sedimentary Basins*. Number 57 in Developments in Sedimentology. Elsevier.
- Moore, C. H. (2001). Carbonate Reservoirs, Porosity evolution and diagenesis in a sequence stratigraphic framework. In *Developments in sedimentology*, Number 55. Elsevier.
- NPD (2012). Norwegian Petroleum Directorate, npd.no - Fact Pages.
- Ofstad, K. (1980). Lithology Well 2/4-1, 2/4-2, 2/4-3, 2/4-4 and 2/4-5. *Norwegian Petroleum Directorate (NPD) Paper* (25), 1–37.
- Schatzinger, R. A., C. T. Feazel, and W. E. Henry (1985). Evidence of resedimentation in Chalk from the Central Graben, North Sea. In *North Sea Chalk Symposium, Book III*.
- Spencer, A. M., G. G. Leckie, and K. J. Chew (1996). North Sea hydrocarbon plays and their resources. *First Break* 14.
- Surlyk, F., T. Dons, C. K. Clausen, and J. Higham (2003). Upper cretaceous. In D. Evans, C. Graham, A. Armour, and P. Bathurst (Eds.), *The Millenium Atlas: Petroleum Geology of the Central and Northern North Sea*, Chapter 13, pp. 213–233. The Geological Society of London.
- TorCh-project (2007). Tor Field, Geomodel. Tor Reservoir Characterization Team: Erling Bergfjord, Kjersti Flaatt, Salem Zekkri, Vincent Lelarge, Basil Al Shamma, Matthew Reppert and Harald Bratli.
- Varol, O. (1998). Palaeogene. In P. R. Brown (Ed.), *Calcareous Nannofossil Biostratigraphy*, pp. 200–218. Kluwer Academic Publishers.
- Wagoner, J. C. V., R. M. Mitchum, K. M. Campion, and V. D. Rahmanian (1990). Siliciclastic sequence stratigraphy in well logs, cores, and outcrops: concepts for high-resolution correlation of time and facies. In *AAPG Methods in Exploration Series*, Number 7. AAPG.
- Wray, D. S. and A. S. Gale (2006). The paleoenvironment and stratigraphy of Late Cretaceous Chalks. *Proceedings of the Geologists' Association* (117), 145–162.

A Appendices

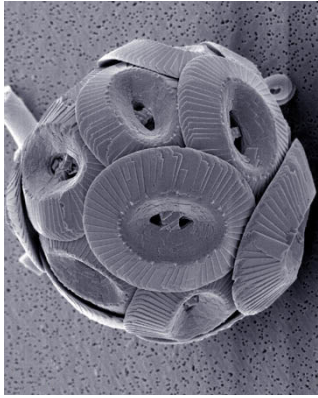


Figure A.1: *Well section, West-East, with correlation of the Type Wells. Included in the .zip file.*

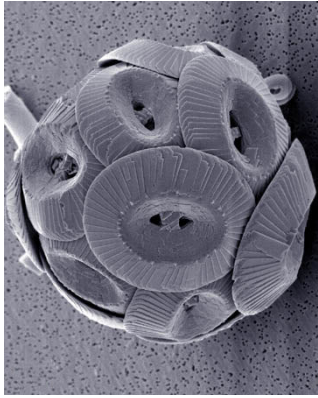


Figure A.2: Well section, West-East across the Middle of the Tor Field, with correlation of the wells. Included in the .zip file.

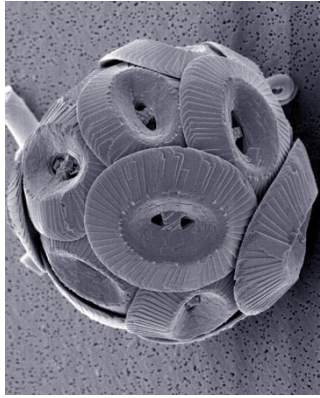


Figure A.3: Well section, West-East across the Southern part of the Tor Field, with correlation of the wells. Included in the .zip file.

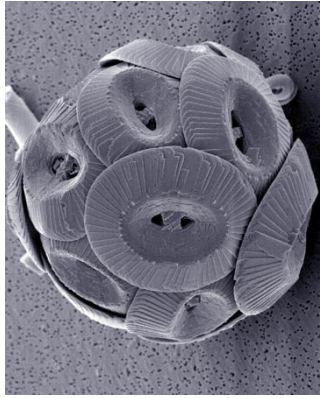


Figure A.4: *Well section, West-East across the Northern part of the Tor Field, with correlation of the wells. Included in the .zip file.*

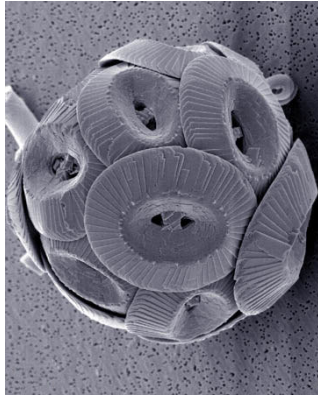


Figure A.5: Well section, North-South across the Western part of the Tor Field, with correlation of the wells. Included in the .zip file.

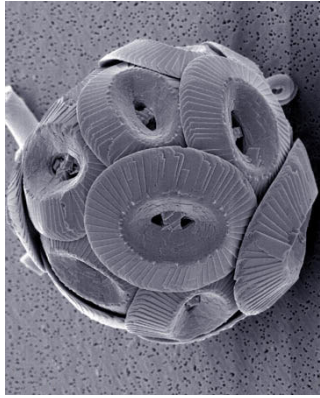


Figure A.6: Well section, North-South across the middle part of the Tor Field, with correlation of the wells. Included in the *.zip file*.

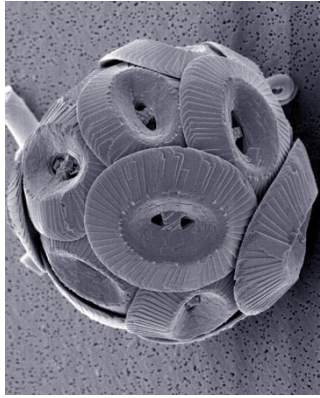


Figure A.7: Well section, North-South across the Eastern part of the central Tor Field, with correlation of the wells. Included in the .zip file.

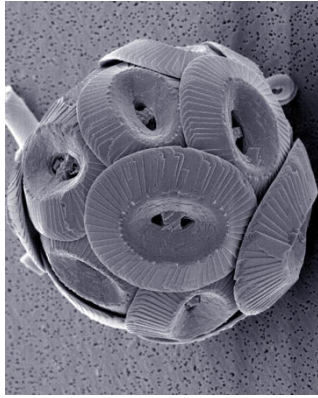


Figure A.8: Well section, North-South across the Eastern-most part of the Tor Field, with correlation of the wells. Included in the .zip file.